INFORMATION TO USERS

This manuscript has been reproduced from the microfilm master. UMI films the text directly from the original or copy submitted. Thus, some thesis and dissertation copies are in typewriter face, while others may be from any type of computer printer.

The quality of this reproduction is dependent upon the quality of the copy submitted. Broken or indistinct print, colored or poor quality illustrations and photographs, print bleedthrough, substandard margins, and improper alignment can adversely affect reproduction.

In the unlikely event that the author did not send UMI a complete manuscript and there are missing pages, these will be noted. Also, if unauthorized copyright material had to be removed, a note will indicate the deletion.

Oversize materials (e.g., maps, drawings, charts) are reproduced by sectioning the original, beginning at the upper left-hand corner and continuing from left to right in equal sections with small overlaps.

Photographs included in the original manuscript have been reproduced xerographically in this copy. Higher quality 6" x 9" black and white photographic prints are available for any photographs or illustrations appearing in this copy for an additional charge. Contact UMI directly to order.

ProQuest Information and Learning
300 North Zeeb Road, Ann Arbor, MI 48106-1346 USA
800-521-0600

Modeling and Robust Adaptive Control of Metal Cutting via Application of Piezoactuator

Jingchuan Pan

A Thesis

in

The Department of

Mechanical Engineering

Presented in Partial Fulfillment of the Requirement
For the Degree of Master of Applied Science at
Concordia University
Montreal, Quebec, Canada

March 2001

Abstract

Modeling and Robust Adaptive Control of Metal Cutting via Application of Piezoactuator

Jingchuan Pan

Self-excited vibration, so called chatter, is known to cause detrimental effects on the machined surface finish and to decrease the machining efficiency. Because of the small amplitude, high frequency properties of chatter, it requires active vibration control providing a force to the cutting system to overcome the chatter effect. To provide such a force, the piezoactuator has been introduced into the cutting system as an important controllable positioning device for ultra-precision machining. With the application of piezoactuator, a much more accurate model is required for achieving the ultra-precision control. In this thesis, rather than using the commonly accepted linear Merchant model, the relationship of cutting force and chip thickness variations is explored as a nonlinear hysteresis model. Furthermore, the piezoactuator itself also exhibits hysteretic behavior. Thereafter, the turning system investigated in this thesis is described as a class of uncertain systems with hysteresis and time delay. The novelty of this thesis is that the hysteresis model is for the first time incorporated into the chatter suppression design for metal cutting systems, but notoriously, it severely complicates the task of controller design and analysis. In this thesis, in order for ultra-precision machining, several robust adaptive control schemes are proposed in different circumstances with such complicated turning systems. The simulation results show significant reduction of chatter by the proposed adaptive controllers in all the circumstances.

Acknowledgments

The author wishes to express his indebtedness to his thesis supervisor Dr. Chun-Yi Su for his invaluable guidance, financial support and encouragement throughout the development of this thesis and all the relevant papers.

I would like to thank Dr. Henry Hong, Dr. Jaroslav Svoboda, Ms. Leslie Hosein, and the former colleague Mr. Michael Bole for their encouragement, and their selfless help.

I would also like to thank my wife, Mrs. Ran Chen, for her encouragement, moral and emotional support. We had been far apart in two different countries during most of the period of study, but her patience and understanding has become an indispensable support in my life.

I would like to thank my parents, for all that they have done for a son whom they love so much, for all that they have taught to a son whom they believe to be excellent.

The financial support provided by the Concordia University during my program is gratefully acknowledged.

Table of Contents

List of Figures viii

Nomenclature xiii

Chapter 1 Introduction 1

1.1 An Industrial Problem in Metal Cutting – Chatter 1

1.2 Chatter Mechanism in Turning 7

1.2.1 Relationship of Cutting Force and Chip Thickness 7

1.2.2 Relationship of Contact Force and Tool Displacement 13

1.3 Cutting Dynamics in Turning 19

1.4 Chatter Suppression in Turning 23

1.5 Contributions of the Thesis 24

1.6 Organization of the Thesis 26

Chapter 2 Modeling of Dynamic Cutting Process 29

2.1 Hysteresis – A Cause for Chatter Occurrence 29

2.2 Hysteresis Models in Dynamic Metal Cutting 33

2.2.1 Cutting/Thrust Force Models 33

2.2.2 Contact/Frictional Force Models 36

2.3 Mathematical Hysteresis Models of Dynamic Cutting Process 39

2.4 Simulation Results 42

2.5 Summary 47

Chapter 3 Modeling of Linear Cutting Dynamics with Piezoactuator **48**

3.1 Cutting Tool Dynamics 48

3.2 Piezoactuator Dynamics 52

3.3 System Dynamics without Independent Tool Holder Dynamics 54

3.4 System Dynamics with Independent Tool Holder Dynamics 54

3.5 Summary 56

Chapter 4 Chatter Suppression via Linear Piezo-actuation

Adaptive Controller Design – 1 **57**

4.1 Dynamic Turning System Model 57

4.2 Adaptive Controller Design 60

4.2.1 Adaptive Controller for Backlash-like Hysteresis Model 64

4.2.2 Adaptive Controller for Backlash Hysteresis Model 71

4.3 Simulation Results 77

4.4 Summary 83

Chapter 5 Chatter Suppression via Nonlinear Piezo-actuation

Adaptive Controller Design – 2 **84**

5.1 Turning System Model with Hysteresis 84

5.2 Adaptive Controller Design 90

5.3 Simulation Results 97

5.4 Summary 100

Chapter 6 Chatter Suppression of Turning System with Tool Holder Dynamics Adaptive Controller Design – 3 **101**

6.1 Turning System with Tool Holder Dynamics 101

6.2 Adaptive Controller Design 104

6.3 Simulation Results 113

6.4 Summary 117

Chapter 7 Chatter Suppression of Cutting System with 2-DOF via Piezoactuator Adaptive Controller Design – 4 **118**

7.1 Turning System of 2-DOF 118

7.2 Adaptive Controller Design 124

7.3 Simulation Results 131

7.4 Summary 134

Chapter 8 Conclusions and Future Work **135**

8.1 Conclusions 135

8.2 Future Work 136

References **138**

Publications Relevant to This Thesis **148**

List of Figures

Figure 1.1	Mode coupling chatter	1
Figure 1.2	Type A and type B chatter	3
Figure 1.3	Primary chatter	4
Figure 1.4	Regenerative chatter	5
Figure 1.5	Chip thickness definition of Ota and Kono (1974)	6
Figure 1.6	Multi-regenerative chatter	6
Figure 1.7	Relationship of cutting force and surface slope	9
Figure 1.8	Relationship of cutting force and workpiece displacement	12
Figure 1.9	Hysteresis relationship of $F_{\Delta} - v(t)$ in metal cutting	13
Figure 1.10	Machine Tool Cutting on the Wavy Surface	14
Figure 1.11	Cutting Edge with Rounded sharpness	15
Figure 1.12	Schematic diagram of simplified displaced volume	16
Figure 1.13	Resultant contact force under free vibration	17
Figure 1.14	Relationship between contact force and cutting tool deflection	18
Figure 1.15	Schematic model of turning metal cutting system	20
Figure 1.16	Transfer function between a tool and workpiece on the machine tools	21
Figure 1.17	Non-linear characteristic of stiffness	22
Figure 2.1	Hysteresis relationship between cutting force and chip thickness	30
Figure 2.2	Hysteresis relationship between cutting force and workpiece displacement	31

Figure 2.3	Type A and type B Chatter	31
Figure 2.4	Relationship between contact force and cutting tool deflection	32
Figure 2.5	Hysteresis relationship between cutting/thrust force fluctuations and chip thickness fluctuation	35
Figure 2.6	Chatter mark configuration	36
Figure 2.7	Deflection of cutting tool tip	37
Figure 2.8	Rounded tool nose model	38
Figure 2.9	Hysteresis relationship between contact force and cutting tool deflection	39
Figure 2.10	Backlash hysteresis model	40
Figure 2.11	Triangular hysteresis model	41
Figure 2.12	Force free response of turning system	43
Figure 2.13	Response of turning system with active hysteresis	44
Figure 2.14	Response of turning system with passive hysteresis	45
Figure 2.15	Regenerative chatter in turning	46
Figure 2.16	Multi-regenerative chatter in turning	47
Figure 3.1	Cutting system with two degrees of freedom	49
Figure 3.2	Transfer function between a tool and workpiece on the machine tools	51
Figure 3.3	Turning metal cutting	52
Figure 3.4	Section view of piezoactuator	53
Figure 3.5	Dynamic model 1 for cutting tool with piezoactuator	54
Figure 3.6	Dynamic model 2 for cutting tool with piezoactuator	55
Figure 4.1	Schematic model of turning system	58

Figure 4.2	Block diagram of turning system with piezoactuator	60
Figure 4.3	Relationship between $k^* sat\left(\frac{s}{\varepsilon}\right)$ and s	68
Figure 4.4	Backlash-like hysteresis of metal cutting system	78
Figure 4.5	Turning system without control (chattering)	79
Figure 4.6	Turning system with proposed adaptive controller	79
Figure 4.7	Turning cutting system without control (chattering)	81
Figure 4.8	Turning cutting system with proposed adaptive controller	82
Figure 4.9	Controlled displacement of piezoactuator	82
Figure 5.1	Dynamic model of turning process	85
Figure 5.2	Backlash hysteresis model	86
Figure 5.3	Hysteresis curves of a piezoactuator	87
Figure 5.4	Block diagram of turning metal cutting system with piezoactuator	89
Figure 5.5	Hysteretic relationship between piezo expansion and applied voltage	98
Figure 5.6	Turning cutting system without control (chattering)	99
Figure 5.7	Turning cutting system with proposed adaptive controller	99
Figure 6.1	Dynamic model of turning cutting system with piezoactuator	102
Figure 6.2	Block diagram of turning metal cutting system with piezoactuator	104
Figure 6.3	Backlash hysteresis model	105
Figure 6.4	Hysteresis curves of a piezoactuator	106
Figure 6.5	Hysteresis relationship between piezo expansion and applied voltage	115
Figure 6.6	Turning cutting system without piezoactuation	115
Figure 6.7	Turning cutting system with proposed adaptive controller	116
Figure 7.1	Cutting system with 2 degrees of freedom	119

Figure 7.2	Backlash hysteresis model	120
Figure 7.3	Triangular hysteresis model	121
Figure 7.4	Hysteretic relationship between expansion and applied voltage	122
Figure 7.5	Block Diagram of turning metal cutting system of 2-DOF with piezoactuator	123
Figure 7.6	Turning cutting system without control	133
Figure 7.7	Turning system with proposed adaptive controller	134

Nomenclature

F_{Δ}	force variance/fluctuation
$F_{c\Delta}$	cutting force variance
$F_{t\Delta}$	thrust force variance
$F_{i\Delta}$	contact force variance
F_{nt}	frictional force due to contact force
$v(t)$	chip thickness variance
x_{τ}	$x(t-\tau)$
h	hysteresis slope
B	hysteresis distance

Chapter 1

Introduction

Introduction – A brief introduction and a literature survey regarding chatter vibration in metal cutting are given in this chapter; contributions and organization of this thesis are also presented.

1.1 An industrial problem in Metal Cutting – Chatter

Chatter, which in itself is a sufficient and independent source of chatter vibration energy, is known to cause detrimental effects on the machined surface finish and to decrease the machining efficiency. In order to improve the surface quality of the workpiece and the production efficiency by overcoming the chatter oscillations in the process of metal cutting, the dynamic models of metal cutting have been investigated and different chatter models have been proposed.

In the cutting process, there are many identified types of self-vibrations excited by different mechanism. Three basic principles of chatter in metal cutting are given by Koenigsberger and Tlusty (1970). *1. Regenerative Chatter*. It is excited due to the tool

tip difference between the current cut and the previous cut, and it can be found in the simplest single DOF system. *2. Mode Coupling.* It can be found within vibratory systems with at least two degrees-of-freedom. Gasparetto (1998) presents a theoretical analysis of mode coupling chatter without damping.

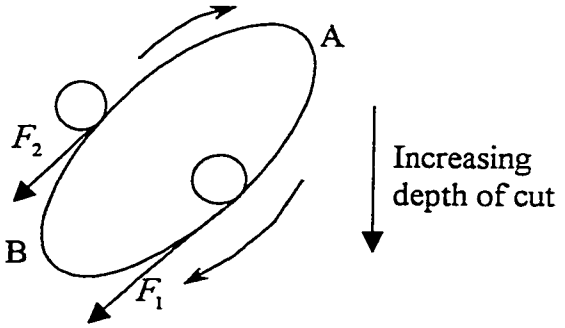

Figure 1.1 Mode Coupling Chatter

In Figure 1.1, the counter-clock-wise ellipse describes the track of the cutting tool. When mode-coupling chatter is present, if the tool rotates counterclockwise, the unstable mode corresponds to an ellipse run clockwise. The force F is in phase with the velocity of the tool between point A and point B, whereas F is 180 degrees out of phase with the velocity between point B and point A. The positive work by force F between point A and B is greater than the negative work done between point B and A, increasing the amplitude of the ellipse, thus giving rise to mode-coupling chatter. *3. Velocity Component.* It is excited due to the existence of a phase shift between the change of the chip thickness and the change of the cutting force. It is fully understood on the basis of vibration theory, that a time lag of the force behind the vibration would create energy, which would cause self-excitation of vibration. The name of this principle means that the cutting force contains a variable component in phase with the velocity of vibration.

Focusing on the chatter directions, Tobias and Fishwick (1958), Tobias (1965) distinguish that there are two types of chatter based on different chatter directions. *Type A* chatter occurs when the amplitudes lie in the plane perpendicular to the cutting direction. *Type B* chatter occurs when the chatter amplitudes have a component co-directional with the cutting speed, regardless whether the amplitudes are co-directional with the feed or perpendicular to it. And furthermore it is shown in Tobias (1965) that type A chatter is a special case of type B chatter.

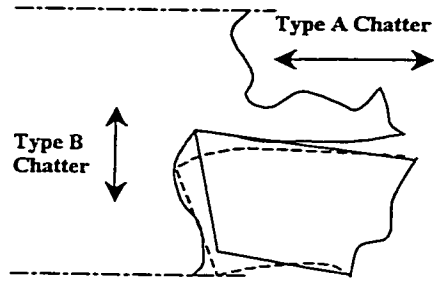

Figure 1.2 *Type A* and *type B* chatter

As type A chatter involves chip thickness variation, it can be classified, according to different as *primary effect* [Merrit (1965)], *regenerative effect* [Koenigsberger and Tlusty (1970)] and *multi-regenerative effect* [Tlusty and Ismail (1981)].

Primary effect accounts for the fact that the cutting tool is cutting on a "fresh" workpiece with smooth surface. For turning metal cutting, primary effect can only dominate in the first cutting revolution and it strongly depends on the pre-condition that the workpiece

has a smooth surface when it is "fresh", which has made it a negligible problem in turning metal cutting, comparing to the regenerative or multi-regenerative effect.

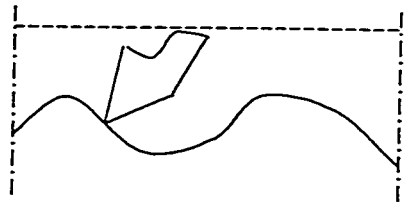

Figure 1.3 Primary chatter

Regenerative effect occurs when the tool subsequently cuts a surface that it has already cut during the previous revolution. Therefore, if there was a vibration between tool and workpiece during the *i*th cut and the produced surface has become undulated, the chip of the (*i*+1)th cut is removed from that undulated surface. Regenerative effect is the unavoidable factor for chatter occurrence in turning, it occurs after the first revolution of cutting subjected to the effect of wavy surface produced during the preceding revolution, and it is a combination of both wave-producing and wave-removing processes. In fact, primary chatter is always being called as "wave producing" chatter while regenerative chatter as "wave removing" chatter [Merrit (1965)]. For orthogonal cutting, it is generally considered that the regenerative effect can be described as the follows, [Chiou and Liang (1998, 1999), Kondo, *et al* (1997)]

$$v(t) = x(t) - x(t - T)$$

where $v(t)$ is the chip thickness variation and T is the time interval during one revolution of cutting.

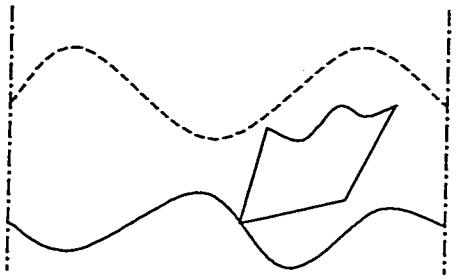

Figure 1.4 Regenerative chatter

In order to describe the chip thickness variation due to the different effect, Merritt (1965) provides an equation for uncut chip thickness, defining the primary chatter and regenerative chatter by use of the overlap factor μ,

$$v(t) = x(t) + \mu x(t - T)$$

$$\begin{cases} \mu = 0 & \text{Primary Chatter} \\ \mu \neq 0 & \text{Regenerative Chatter} \end{cases}$$

where $v(t)$ is the instantaneous chip thickness variation at time t, x is the relative displacement between tool and work piece normal to machined surface, and μ is the overlap factor and $0 \leq \mu \leq 1$. The overlap factor may also be used to account for the geometrical effects of rounding at the tool cutting edge and of tool clearance angle.

Considering the geometrical relations of shear angle, it was proposed in Ota and Kono (1974) that the chip thickness variation is

$$v(t) = x(t + H') - \mu x(t - T + H')$$

where the previous cut is precedent to the cutting edge by a time value H', as shown in the following figure.

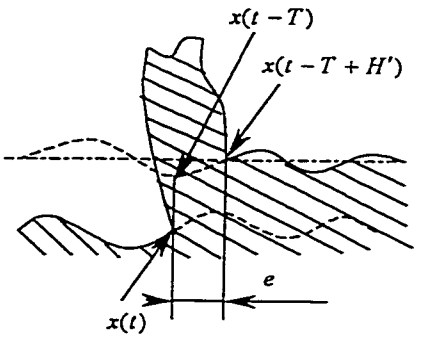

Figure 1.5 Chip thickness definition of Ota and Kono (1974)

The chatter due to the *regenerative effect* can grow as the metal cutting system stays in the oscillating state. During the cutting process, the amplitude of the chatter does not grow indefinitely but stabilizes at finite amplitude of vibration. It was first proposed by Tlusty and Ismail (1981) that this phenomenon of non-linearity is caused by the so-called *Multi-Regenerative Effect*. With the increase of vibration, the tool starts to move outside of the cut for an interval in a cutting revolution. It has been experimentally verified [Kondo, *et al* (1981)] that the tool separates from the work surface periodically due to the multiple regenerative effect during chatter. And the cutting force reduces to zero during the separation. So, the multi-regenerative effect limits the amplitude of the chatter. However, the re-contact of the work and the tool will cause unpredictable collapse and force generation.

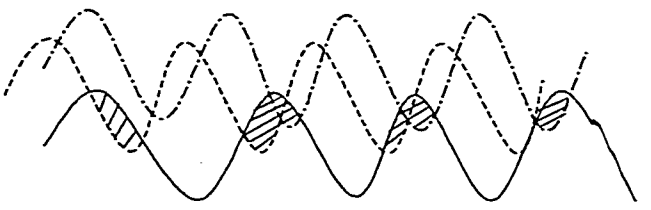

Figure 1.6 Multi-regenerative chatter

To account for the multi-regenerative effect, Kondo, *et al* (1981) and Kaneko, *et al* (1984) proposed that due to the multi-regenerative effect, the uncut chip thickness variation depends on the previous cutting revolutions.

$$v(t) = \min\{x(t-T),\ f_0 + x(t-2T),\ 2f_0 + x(t-3T),\ \cdots,\ (n-1)f_0 + x(t-nT)\} - x(t)$$

where f_0 is the steady feed of cutting tool.

1.2 Chatter Mechanism in Turning

The study on chatter occurrence requires a thorough investigation over the dynamic cutting process, i.e., the relationship of cutting force, contact force, chip thickness and tool displacement.

1.2.1 Relationship of Cutting Force and Chip Thickness

Consider a machine tool operating under nominal feed and cutting speed, which is regarded as a dynamic system in a condition of steady-state motion. If the steady-state cutting operation is disturbed, the cutting force variation F_Δ will be generated, superimposed on the static cutting force F_0. It may happen that the F_Δ is of such a form that it increases the original disturbance, so that a still larger F_Δ is built up and this in turn leads to an even more severe disturbance, and so on. Consequently the machine begins to vibrate, and so does the chatter occur. This explanation is given by

Tobias(1965) for the physical causes of chatter, and it reveals the fact that the chatter occurrence is related to the cutting force variance.

Many researches have been devoted to find out the relationship of the force and the chip thickness during the dynamic cutting process. For the cutting system in steady state, Merchant (1945 II) proposed the famous linear relationship between the force and the geometry of chip formation that the force is in proportion to the undeformed chip thickness.

$$F_0 = k \cdot v(t)$$

where k is a constant and $v(t)$ corresponds to the chip thickness. Obtained based on the principle of minimum energy, this cutting force model treats the chip as a "separate" body in stable mechanical equilibrium under the action of two equal, opposite resultant forces. Merchant model is proved to be a very good approximation for the actual cutting force in steady state, which leads to the fact that it has been accepted as the basic model for the analysis of dynamic cutting process in the research of chatter occurrence. Ever since the linear Merchant model was first proposed, it has become dominant in the modeling of metal cutting. Most of the existing theories on the dynamics of metal cutting employ the linear model [Merrit (1965), Kondo, *et al* (1981), Kaneko, *et al* (1984), Marui *et al* (1988), Olgac and Hosek (1998), Rao and Shin (1999), Chiou and Liang (1999)]. There are also many theories which are transformations of the linear Merchant model. It is indicated in Kaneko, *et al* (1984), Marui, *et al* (1988) that the cutting resistance may be influenced by the dynamic variations of the relative velocity between the tool and the work $\dot{x}$, and the resistance is inversely proportional to the cutting speed and proportional

to horizontal relative velocity between the tool and the work, however independent on the projected area of the uncut chip. Kaneko, et al (1984) considers the penetrating force to be

$$F_{x\Delta} = K_0 v(t) - k_\alpha \left(\frac{\dot{x}}{V_0 - \dot{x}} \right)$$

Marui, et al (1988) introduces variation of cutting speed as one more effect that influences the cutting resistance, and it is proposed that the cutting force gain can be described as the follows,

$$K = K_0 - k_v \dot{y} - k_\alpha \tan^{-1} \left(\frac{\dot{x}}{V_0 - \dot{y}} \right)$$

where $\dot{y}$ represents the relative velocity between the cutting tool and the work, which is proportional to the cutting speed.

Sarnicola and Boothroyel (1974) presents experiments to develop the equations for the effect of surface slope on machine forces and it is proposed that the force variation due to chip surface slope is in negative proportion to sectional area A_c and the slope angle β.

$$\Delta F_c = -k_s A_c \beta$$

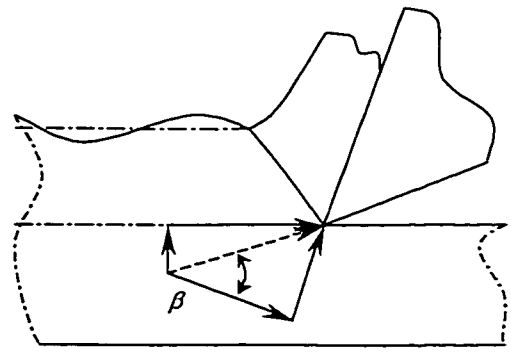

Figure 1.7 Relationship of cutting force and surface slope

Linear Merchant model is derived in steady state for metal cutting system, however, it should be noticed that many conditions are absolutely different in steady and dynamic state, i.e., the chip in chattering state can no longer remain the stable mechanical equilibrium, which results in a different description of the cutting process mechanics. Merchant model has been successfully introduced to describe the cutting system in steady state, however, Szakovits and D'Souza (1976) indicates that the assumption of modeling the dynamic cutting process with steady-state state data is invalid, and there are experimental results showing that the dynamic cutting process is a nonlinear model rather than a linear model [Albrecht (1965)].

Smith and Tobias (1961) suggested that the direction of cutting force in the vibrating state is different from that in the steady state. As a matter of fact, Merchant Model cannot explain the phase difference occurring between force and the chip thickness, which has been verified by Smith and Tobias (1961).

In order to account for the phase difference leading to non-linearity, Albrecht (1965) suggested hysteresis relationship between tool face force and uncut chip thickness, by analyzing a small phase lag of the force to the thickness. And Doi and Kato (1956), Marui *et al* (1988), Kato and Marui (1974), Ota and Kono (1974) present a model by introducing a time lag τ between force and chip thickness.

$$F = kv(t-\tau)$$

where v denotes the uncut chip thickness.

There is phase difference between the cutting force and the vibration wave, and it is verified that in some cases force lags behind the geometry vibration [Smith and Tobias (1961)]. With the linear Merchant model, Doi and Kato (1956) gives $F_{\Delta} = Kx(t-h)$ for the primary chatter, Kato and Marui (1974), Ota and Kono (1974) gives $F_{\Delta} = K[\mu x(t+\tau-h) - x(t-h)]$, Marui *et al* (1988) gives $F_{\Delta} = K(t)\cdot[\mu x(t+\tau-h) - x(t-h)]$, where h is the time lag of the cutting force and τ is the revolution period.

However, Shumsheruddin (1964), Szakovits and D'Souza (1976) found that the dynamic cutting force lags the chip thickness variation at low frequencies, and leads at high frequencies, and in Szakovits and D'Souza (1976), it is indicated that the phase angles between the fluctuating forces and undeformed chip thickness depend on cutting conditions and are definitely frequency dependent. Shumsheruddin (1964) explain this phenomenon by including the torsion characteristics of the tool, and Szakovits and D'Souza (1976) model the dynamic process of phase lead and phase lag with the introduction of hysteresis model.

It is not enough to describe the nonlinearity only with the introduction of phase difference, thus, in order to account for the non-linearity, Hanna and Tobias (1974) proposed a nonlinear relationship between cutting force and chip thickness variation.

$$F_{\Delta} = c_1 \Delta s + c_1 (\Delta s)^2 + c_2 (\Delta s)^3$$

where Δs represents the chip thickness variation. But, it is indicated in Szakovits and D'Souza (1976) the above equation does not accurately represent the dynamic cutting

process. Shi and Tobias (1984) considered the dynamic force variation with additional penetration factor other than the chip thickness variation,

$$F_{\Delta} = c_1 \Delta s + c_1 (\Delta s)^2 + c_2 (\Delta s)^3 + c_4 \dot{x}$$

where $\dot{x}$ corresponds to the penetration rate.

Pandit, *et al* (1975) considers the chatter as self-excited random vibration with white noise excitation,

$$F_{\Delta} = \frac{d^{2n}x}{dt^n} + a_{2n-1}\frac{d^{2n-1}x}{dt^{2n-1}} + \cdots + a_0 x,$$

Doi and Kato (1956), Kato and Marui (1974), Kaneko et al (1984), Marui et al (1988) showed by employing the experimental data that the relationship between the cutting force and the displacement of workpiece has got the characteristic of hysteresis.

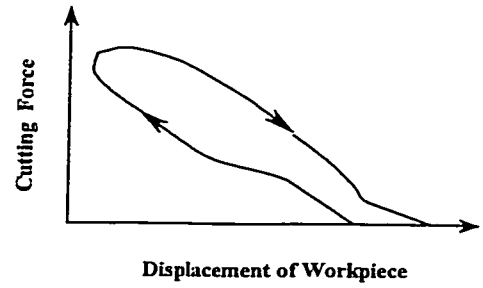

Figure 1.8 Relationship of cutting force and workpiece displacement

Fabris and D'Souza (1974), Szakovits and D'Souza (1976) proved by employing experimental data that in the dynamic cutting process, the relationship between cutting force *variation* F_{Δ} and chip thickness *variation* $v(t)$ exhibits hysteresis.

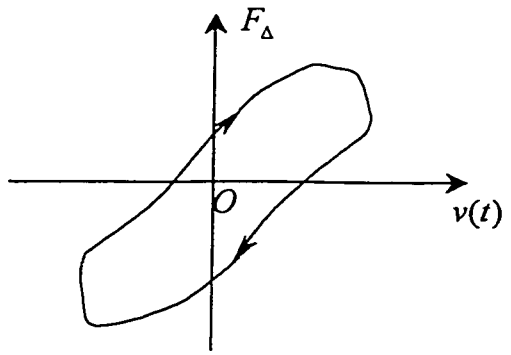

Figure 1.9 Hysteresis relationship of $F_\Delta - v(t)$ in metal cutting

The mechanism of energy excitation for chatter has been successfully explained in Doi and Kato (1956), Kato and Marui (1974), Kaneko et al (1984), Marui et al (1988), and it is concluded that chatter is the self-excited vibration caused by the hysteresis relationship between force and workpiece deflection, which ensures the system to gain energy necessary to maintain the vibration.

1.2.2 Relationship of Contact Force and Tool Displacement

A number of analyses of the contact force deflection due to the tool wear have been undertaken over the years. Koren and Lenz (1972) proposes that the tool wear occurrence involves thermally activated mechanism and mechanically activated mechanism. The following section will focus on mechanical mechanism.

In the metal cutting, the fluctuation of the clearance angle has the strongest effect on the contact force exerted on the flank face.

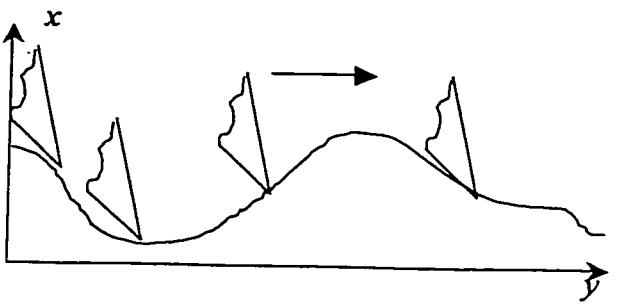

Figure 1.10 Machine Tool Cutting on the Wavy Surface

It is clear from the figure 1.10, that the flank face will come into contact with the workpiece when the tool is cutting on the "down" slope, which will cause extremely violent interference between the flank face of the tool and the workpiece. Sisson and Kegg (1969), Mauri, *et al* (1983 I), Jemieniak and Widota (1989), Tarng *et al* (1994) consider that clearance angle varies due to the relative vibration between turning tool and workpiece.

$$\gamma = \gamma_0 + \gamma_1 = \gamma_0 + \arctan\frac{\dot{x}}{V}$$

where γ_0 is the normal clearance angle and V is the cutting speed. The decreasing of clearance angle while cutting on a wavy work surface causes a additional damping force, and due to the increase of damping, the system stability at low cutting speed is greatly increased, which is known a the *Low Speed Stability*(LSS) [Kegg(1969)]. Furthermore, Mauri, *et al* (1983 I) proposed the clearance angle also varies due to the deflection of turning tool, which could be characterized as chatter B vibration of the tool (refer to Figure 1.2). Due to the elasticity of the machine tool, there is a deflection that contributes to the changing of the clearance angle.

$$\gamma = \gamma_0 + \gamma_1 + \gamma_2$$
$$= \gamma_0 + \arctan\frac{\dot{x}}{V - \dot{y}} + \frac{1.3784y}{l}$$

where l is the length of turning tool

Sisson and Kegg (1969) developed a physical explanation of the contact force between tool flank face and workpiece, in terms of tool edge roundness and tool clearance angle.

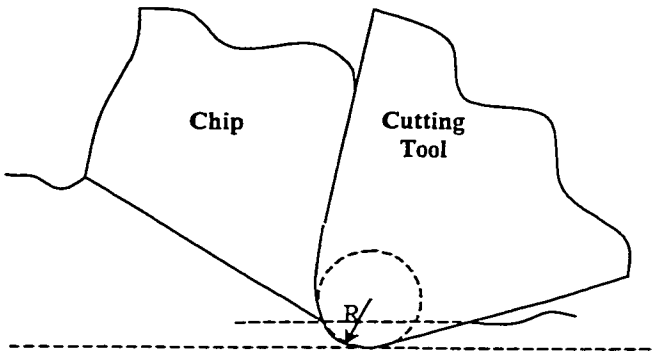

Figure 1.11 Cutting Edge with Rounded sharpness

According to the rounded tool nose model proposed by Sisson and Kegg (1969), Marui *et al* (1983 I/II), Chiou and Liang(1998) that, a very large negative rake angle at the rounded part of the cutting edge causes the separating action of chip and work material, the material at the lower part of the cutting edge is compressed under the tool nose and thereafter reacts elastically. Thus, contact force is exerted between the workpiece surface and the flank face of the turning tool. It is proposed by Sisson and Kegg (1969), Marui *et al* (1983 1/2) that the contact force is proportional to the contact area,

$$F_t = k_w w l$$

where w is the width of contact area, l is the length of contact area, and k_w is the constant proportional gain.

Furthermore, based on theoretical analysis for indention of a smooth spherical indenter on a plane, Shaw and DeSalvo (1970) proposed that the contact force is proportional to the volume of displaced material by the flank face of the cutting tool. Based on this idea, Chiou and Liang (1998) proposed a cutting system model with a simplified approximation of the displaced volume, which results in the proportionality of contact force and vibration velocity.

$$F_t = K_{sp}\hat{V} = -k_f \dot{x}$$

where K_{sp} and k_f are the constant coefficients, and $\hat{V}$ is the displaced volume of the chip.

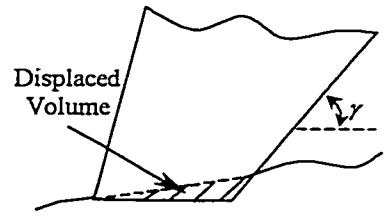

Figure 1.12 Schematic diagram of simplified displaced volume

However, because the cutting tool is not a sphere object but with differently shaped profile, it is clear that the obtained results of Chiou and Liang (1998) are simplified approximation. For the contact force related to vibration velocity, Jemielniak and Widota (1989), Tarng, *et al* (1994), Chiou and Liang (1998) consider the directionality of the vibration velocity. Because the contact force is always compressive and non-negative,

the contact force becomes zero when the vibration velocity is positive. The following figure illustrates the free vibration and the area in gray represents the period when the contact force in not zero.

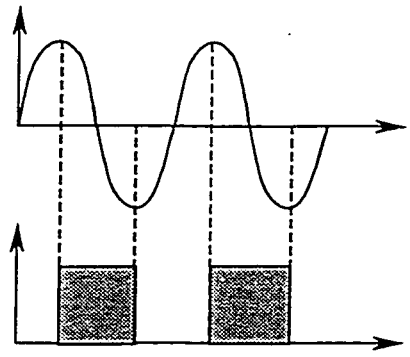

Figure 1.13 Resultant contact force under free vibration

Chandrasekaran and Nagarajan (1977) proposes a comprehensive model for the distribution of contact stresses along the wear land, and the contact force on the rake face and flank face can be obtained based on the established tool-chip stress.

Elanayar and Shin (1996) proposes a model for the contact force of flank face by considering the contact force as the frictionless indentation problem and using a generalized friction law to determine the tangential forces.

$$F_t = K_f \int_0^{2\pi} \int_0^{a(\theta)} \frac{a(\theta) f(r,\theta) r}{\sqrt{a^2(\theta) - r^2}} dr d\theta$$

where $f(r,\theta)$ is the function of cutting depth, and $a(\theta)$ defines the boundary of the contact region.

And the friction on the flank face is

$$F_2 = \sigma_c A_e = C_0 \eta^{C_1} \iint_{A_e} a^2(\theta) dr d\theta$$

where C_0 and C_1 are the constants coefficients, A_e is the contact area, and

$$\eta = 0.00067 d^{0.7423} v^{0.2115} (1 + 1.85 v d^{1.59} W)$$

is the maximum penetration depth.

These two models are both based on the theory of a rigid punch on a semi-space. The principle difference between the two models is that Elanayar's model can reflect the interference on the flank face by the variation of clearance angle, while Chandrasekaran's cannot.

It is experimentally proved by Marui et al (1983 1/2, 1995) that the relationship between contact force and the cutting tool deflection demonstrates hysteresis, as shown in the following Figure 1.14.

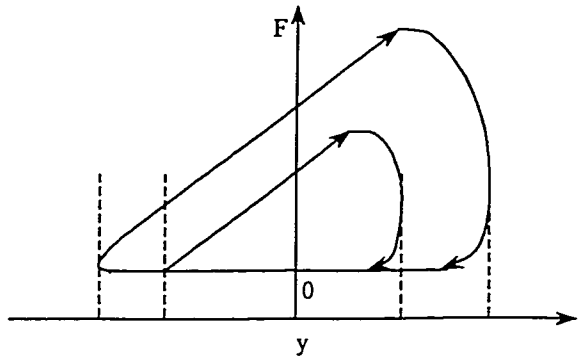

Figure 1.14 Relationship between contact force and cutting tool deflection

It is obvious in Figure 1.14 that the amplitude of the contact force increases as the amplitude of the cutting tool deflection increases. Marui et al (1983) also indicated that

the hysteretic relationship between contact force and cutting tool deflection also results in the maintenance of chatter vibration.

1.3 Cutting Dynamics in Turning

Though the actual metal cutting system has infinite degrees of freedom. However, it has been indicated in Koenigsberger and Tlusty (1970), Chiriacescu (1990), that the principle modes corresponding to the high eigen-frequencies and having high damping and stiffness values exert little influence upon the dynamic displacement between tool and workpiece and may be neglected. While the modes with very low eigen-frequencies, ranging much below the level of those arising during the machining, are not considered either for practical purposes. Consequently, the system is considered to have a finite number of degrees of freedom.

The cutting system is regarded as the machine tool together with workpiece, cutting tool, workpiece clamping device and tool clamping device. In order to describe the cutting dynamics of the metal cutting system, Koenigsberger and Tlusty (1970) presented several simplifications and assumptions.

i) The vibratory system of the machine is linear.

ii) The direction of the variable component of the cutting force is constant.

iii) The variable component of the cutting force depends only on vibration in the direction of the normal to the cut surface.

iv) The frequency of the vibration and the mutual phase shift of undulations in subsequent overlapping cuts are not influenced by the relationship of wavelength to the length of cut; this assumption corresponds to an infinite length for every cut or, practically, to planning.

And under the above assumptions, the cutting system can described as a linear second order function [Tobias (1965)],

$$m\ddot{x} + c\dot{x} + kx = F_{\Delta}$$

where m, c, k are the equivalent mass, equivalent damping coefficient, and equivalent spring stiffness respectively for the metal cutting machine.

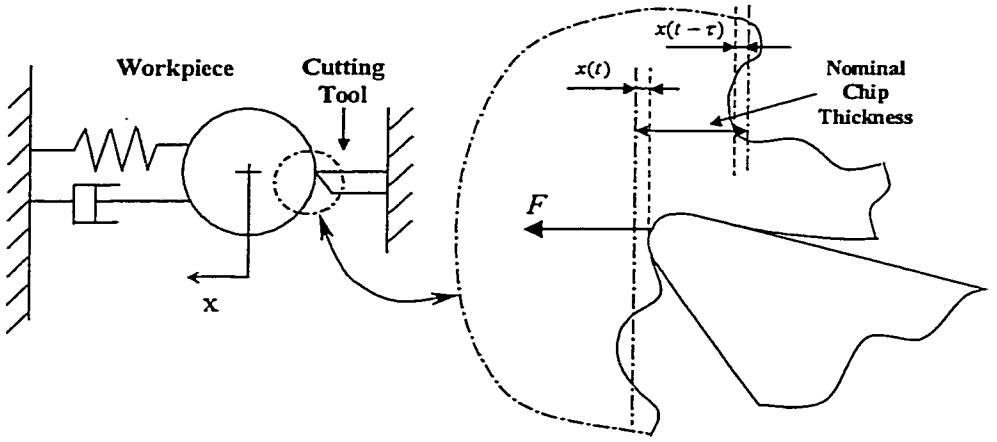

Figure 1.15 Schematic model of turning metal cutting system

Merritt (1965) and Chiriacescu (1990) developed the structure equation for the structure with n degrees of freedom,

$$\frac{y(s)}{F(s)} = \sum_{i=1}^{n} \frac{g_i}{k_i \left[\dfrac{s^2}{\omega_i^2 + 2\delta_i s/\omega_i + 1} \right]}$$

where $k_m = \frac{g_i}{k_i}$ is the directional static stiffness, ω_i is the undamped natural frequency of the modes of vibration, respectively.

Altintas (1997) presented a general machine tool structure equation as in Figure 1.16,

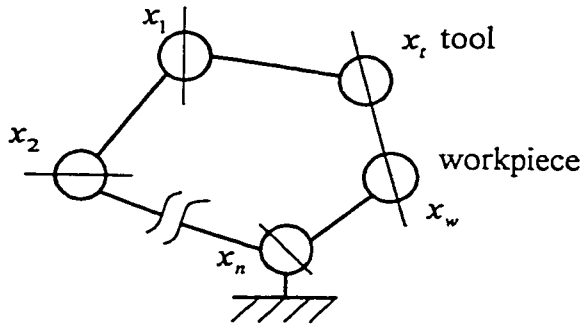

Figure 1.16 Transfer function between a tool and workpiece on the machine tools

$$x = [x_1 \quad x_2 \quad \cdots \quad x_t \quad x_w \quad \cdots \quad x_n]^T$$

$$F = [0 \quad 0 \quad \cdots \quad 1 \quad -1 \quad \cdots \quad 0]F_0$$

And the equation of motion for the system is,

$$M_x\ddot{x} + C_x\dot{x} + K_x x = F$$

where M_x, C_x and K_x are the local mass, local damping and local stiffness matrices, respectively.

Wu and Liu (1985), Minis and Tembo (1993), Elbestawi et al (1994) showed that the dynamics of the cutting system may be described by the following equations,

$$\begin{bmatrix} m_x & 0 \\ 0 & m_y \end{bmatrix}\ddot{z} + \begin{bmatrix} c_x & 0 \\ 0 & c_y \end{bmatrix}\dot{z} + \begin{bmatrix} k_x & 0 \\ 0 & k_y \end{bmatrix}z = \begin{bmatrix} F_x \\ F_y \end{bmatrix}$$

where $z = [x \quad y]^T$ represents the varying displacement along X and Y axes, m_x, m_y, c_x, c_y, k_x and k_y are the modal mass, damping, and stiffness, respectively.

Hanna and Tobias (1969) proposed the following system description with nonlinearity,

$$m\ddot{x} + f(\dot{x}) + g(x) = F_\Delta$$

The investigation of the dynamic cutting system shows that the damping function $f(\dot{x})$ can give a good approximation when it is treated as a linear function, though it maybe exhibits hysteresis. However, it is shown in Hanna and Tobias (1969), Koenigsberger and Tlusty (1970) (pp 32-34) and Chiriacescu (1990) (pp 78-79), that in some cases the static stiffness of the cutting system demonstrates the non-linear characteristic with respect to the displacement x.

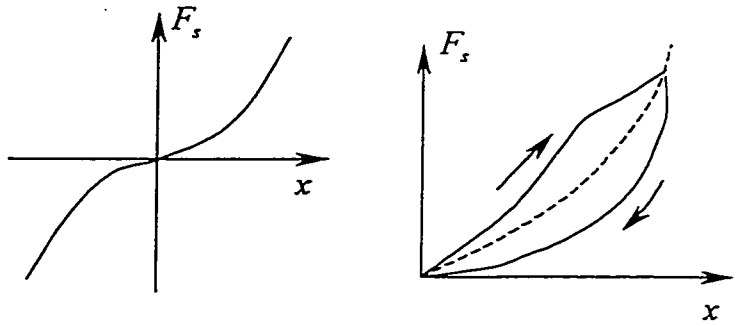

Figure 1.17 Non-linear characteristic of stiffness

Investigation in Chiriacescu(1990) show that, to a good approximation, when the static force-displacement demonstrates nonlinearity as the left figure of Figure 1.17, or the resonance tests yield results like those shown in right figure in Figure 1.17, the cutting system must be described as

$$m\ddot{v}_q + c\dot{v}_q + k(v_q) = F_q$$

where the elastic force that resist the displacement of the mass m subjected to the force F_q is replaced by nonlinearity. For the nonlinear stiffness function, Hanna and Tobias (1969) proposed the following equation,

$$k(x) = k_1 x + k_2 x^2 + k_3 x^3$$

where k_1, k_2 and k_3 are constants.

1.4 Chatter Suppression in Turning

In order to suppress the chatter occurring during the cutting process, proper control schemes are proposed. Koren, Y. (1997) reviews the progress in machine tool control during the last three decades, three types of controls are discussed: (i) servocontrol loops that control the individual axes of the machine, (ii) interpolators that coordinate the motion of several axes and (iii) adaptive control that adjusts the cutting variables in real time to maximize system performance. Rasmussen, et al (1994) improved the workpiece surface by employing a digital repetitive servo control with the design of a piezoelectric actuated cutting tool. Tarng and Wang (1993) developed an adaptive fuzzy control system for the turning processes with highly non-linear and time-varying cutting characteristics. Shiraishi et al (1991) obtained satisfactory chatter vibration control by implemented optimal control of chatter. Hwang et al (1989) implemented a fixed gain PI control and an adaptive pole assignment control technique with the feed force feedback. Chen and Chang (1991) considered the system to be linear with nonlinear time-varying perturbation and employed PI controller to treat this stabilization problem. Hwang

(1993) presented an adaptive turning force controller that has optimal robustness under the constraint of feed rate. Recently, with the advent of piezoelectric devices, more and more attention is attracted to the application of piezoactuator for metal cutting systems [Cuttino et al (1999)], [Fawcett 1990], [Liu et al (1998)], [Ge and Jouaneh (1996)]. Piezoactuator has a prominent characteristic of fast expansions with small response time. The fast response property of piezoactuator has made it a perfect controllable positioning element for the ultra-precision control.

1.5 Contributions of the Thesis

The work presented here was motivated by an industrial problem of turning metal cutting. In turning metal cutting, the occurrence of self-excited vibration, so called chatter, is undesirable as it gives rise to production problems, causing detrimental effects on the machined surface finish and decreasing the machining efficiency, and has adverse effect on the work surface finish, tool wear and tool life. Because of the small amplitude (as small as several microns), high frequency properties of chatter, it requires active vibration control providing a force to the cutting system to overcome the chatter effect. Recently, with the advent of piezoelectric devices, more and more attention is attracted to the application of piezoactuator for metal cutting systems [Cuttino et al (1999)], [Fawcett (1990)], [Liu et al (1998)]. Piezoactuator has a prominent characteristic of fast expansions with small response time. With electrical voltage applied, the piezoactuator can expand and reach its nominal displacement on the order of microseconds and a

pushing or pulling force can be excited with accelerations of more than 10,000 g's, so that the position of the cutting tool can be maneuvered to suppress the chatter effect. The fast response property of piezoactuator has made it a perfect controllable positioning element for the ultra-precision control.

With the application of piezoactuator, we are able to implement chatter suppression with ultra-precision. As a matter of fact, ultra-precision control requires a much more precise model describing the actual metal cutting system, more specifically, the cutting dynamics. There are strong indications that the relationship between the cutting force and chip thickness displays nonlinear dynamics in the cutting process [Albrecht (1965)], [Hanna and Tobias (1974)], [Pandit et al (1975)]. The mechanism of energy excitation for chatter has been successfully explained in [Fabris and D'Souza (1974)], [Kato and Marui (1974)], [Marui et al (1983)], [Marui et al (1995)], and it is concluded that chatter is the self-excited vibration caused by the hysteresis relationship between force and workpiece deflection, which ensures the system to gain energy necessary to maintain the vibration. In contrast to the linear Merchant model [Merchant (1945)], hysteresis model can better explain the experimental phenomena and as well give better correlations with the theoretical analysis of dynamic cutting process. In this thesis, we explore the relationship of cutting force fluctuation and chip thickness fluctuation as a hysteresis model where the nonlinearity dominates.

Hysteresis is recognized as one of the factors that cause undesirable chatter, resulting in instability of oscillations, inaccuracy, etc [Tao and Kokotovic (1995)][Gorbet et al

(2001)]. However, most of the hysteresis models proposed are very complicated and the non-smooth nonlinearity can severely complicate the task of controller design and analysis. This leads to the fact that the hysteresis model is never applied to the dynamic model of metal cutting when it comes to controller design. Piezoactuator with the fast response property has been introduced into the cutting system as an important controllable positioning element for the ultra-precision control; however, piezoactuator also displays hysteretic behavior and the hysteresis actuation relationship imposes a still open problem of developing control scheme with unknown hysteresis actuation [Su et al (2000)], [Tao and Kokotovic (1995)]. In addition, the adverse effect of time delay, unavoidably resulting from the regenerative effect of turning metal cutting, is another major factor that causes instability in the cutting process. Without any doubt, the combination of hysteresis and time delay in the closed-loop system has proposed an even challenging topic for the controller design in metal cutting. In this thesis, a robust controller is developed to deal with unknown hysteresis combined with time delay. The proposed robust adaptive controller ensures the suppression of chatter and global stability of the metal cutting system.

1.6 Organization of the Thesis

The present chapter provides a brief introduction and a literature survey regarding chatter vibration in metal cutting.

In Chapter 2, hysteresis models for dynamic cutting process, including cutting force model and contact force model, are presented. Active hysteresis is proved to be one of the causes of chatter occurrence as it provides the energy for chatter excitation and maintenance. Simplified mathematical hysteresis models are given and the simulations based on these models demonstrate the behaviors of passive hysteresis model, active hysteresis model, regenerative chatter effect and multi-regenerative chatter effect, which give a good correlation with the actual experimental results.

In Chapter 3, linear cutting dynamics descriptions are presented for turning system with piezoactuator, including one degree of freedom and two degrees of freedom.

In Chapter 4 – Chapter 7, in order for chatter suppression, a piezoactuator is introduced for the regulation of the machine tool displacement. Based on different developed turning models, different adaptive controllers are proposed for ultra-precision machining. In Chapter 4, piezoactuation is treated as linear actuation, while the cutting models are taken as backlash hysteresis and backlash-like hysteresis. In Chapter 5, the hysteretic property of piezoactuator introduces a still open problem of controller design. In Chapter 6, the cutting system model involves the cutting tool dynamics and piezoactuator dynamics. And in Chapter 7, type A and type B chatters are considered in the cutting system with two degrees of freedom. In order to overcome the chatter due to the hysteresis and time delay in the cutting process, several adaptive controllers based on different hysteresis descriptions for the metal cutting system of ultra-precision machining

are presented. The simulation results show that the proposed adaptive controllers significantly eliminate the chatter phenomena.

Chapter 8 provides the conclusions of the thesis and some recommendations for future work.

Chapter 2

Modeling of Dynamic Cutting Process

Introduction – In this chapter, hysteresis models for dynamic cutting process, including cutting force model and contact force model, are presented. Active hysteresis is proved to be one of the causes of chatter occurrence as it provides the energy for chatter excitation and maintenance. Simplified mathematical hysteresis models are given and the simulations based on these models demonstrate the behaviors of passive hysteresis model, active hysteresis model, regenerative chatter effect and multi-regenerative chatter effect, which give a good correlation with the actual experimental results.

2.1 Hysteresis – A Cause for Chatter Occurrence

As chatter is found to have detrimental effects to the work piece finish, tool life, etc, a large number of investigations [Shi and Tobias(1984), Wu and Liu(1985), Tarng et al(1994), Lee et al(1995)] have been performed to study the mechanism of chatter vibration in order for chatter suppression. One of the proposed mechanisms is the active hysteretic behavior appearing in the dynamic cutting process.

In view of the nonlinearity of the relationship of force and chip thickness, Albrecht(1965) gives a theoretical explanation for the closed-loop relationship of force and uncut chip thickness. Doi and Kato(1956), Kato and Marui(1974), Fabris and D'Souza(1974), Kaneko et al(1984), Marui et al(1983 1/2, 1995) have successfully explained the energy excitation of the chatter, and concluded that chatter is the self-excited vibration caused by the hysteresis relationship between force and workpiece deflection, which ensures the system to gain energy necessary to maintain the vibration.

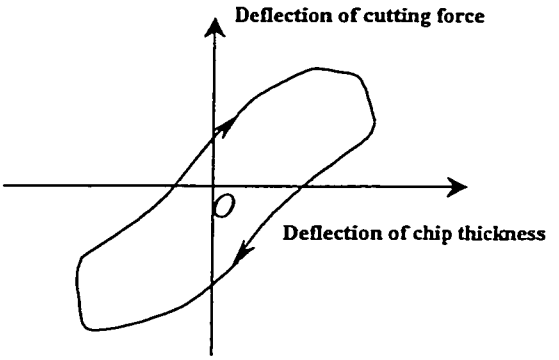

Figure 2.1 Hysteresis relationship between cutting force and chip thickness

For primary chatter, the energy excited is proportional to the area enclosed by the hysteresis [Fabris and D'Souza(1974), Doi and Kato(1956)], while for regenerative chatter, Kato and Marui(1974) provided the hysteresis relationship of force and workpiece displacement (Figure 2.2), and the energy for the chatter excitation is also proportional to the area enclosed by the hysteresis.

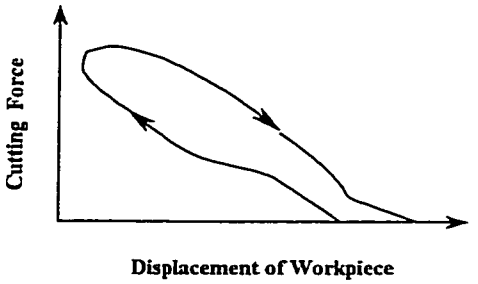

Figure 2.2 Hysteresis relationship between cutting force and workpiece displacement

In Tobias and Fishwick (1958), Tobias (1965), chatter is classified into type A and type B chatters: (a) Chatter with self-excited vibration perpendicular to the cutting direction; (b) chatter with self-excited vibration co-directional with the cutting speed, due to the deflecting cutting tool subjected to the bending effect of the force exerted on the tool tip. And the two chatter types are illustrated in the following Figure

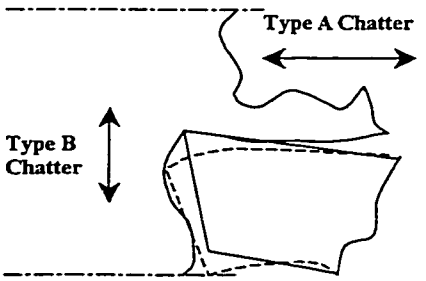

Figure 2.3 Type A and type B Chatter

Most of the current research focus on the type A chatter, however, as we can see from figure 2.3, type B chatter can also affect on the workpiece surface. Sisson and Kegg

(1969), Marui et al (1983 1/2), Marui et al (1995), Elanayar and Shin (1996) consider the contact force between the flank face and the workpiece, and different contact force models are introduced based on the elastic dynamics. Furthermore, it is experimentally proved by Marui et al (1983 1/2, 1995) that the relationship between contact force and the cutting tool deflection demonstrates hysteresis, as shown in the following Figure 2.4.

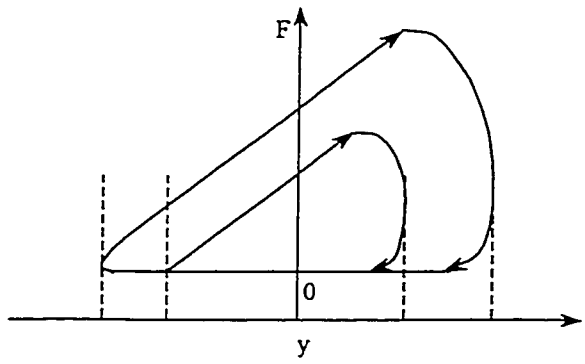

Figure 2.4 Relationship between contact force and cutting tool deflection

It is obvious in Figure 2.4 that the amplitude of the contact force increases as the amplitude of the cutting tool deflection increases. Marui et al (1983) also pointed out that the hysteretic relationship between contact force and cutting tool deflection also results in the maintenance of chatter vibration.

As indicated in the reference, the hysteresis is proved to be one the chatter mechanisms on the basis of energy excitation and maintenance. Thereafter, in the next section, we will introduce the hysteresis models into the cutting system.

2.2 Hysteresis Models in Dynamic Metal Cutting

2.2.1 Cutting/Thrust Force Models

The study on chatter requires a thorough investigation over the dynamic cutting process. When it comes to the relationship of cutting force and chip thickness, most of the existing theories on the dynamics of metal cutting employ the linear model proposed by Merchant (1946)[see, for example, Merrit (1965), Mauri et al (1988), Olgac and Hosek (1998)]

$$F_{\Delta} = k_{M} \cdot v(t) \tag{2.1}$$

where k_{M} is a constant, and $v(t)$ represents the chip thickness variation at time t. The linear Merchant model has become dominant in the modeling of metal cutting ever since it was first proposed in 1945. However, there are strong indications that any linear relationship between the cutting force and chip thickness cannot satisfactorily express the nonlinear dynamics of the cutting process [See, for example, Albrecht (1965), Hanna and Tobias (1974), Pandit, *et al* (1975)].

In order to account for the non-linearity, Hanna and Tobias (1974) proposed a nonlinear relationship between cutting force and chip thickness variation.

$$F_{\Delta} = c_1 \Delta s + c_1 (\Delta s)^2 + c_2 (\Delta s)^3 \tag{2.2}$$

where Δs represents the chip thickness variation. Shi and Tobias (1984) considered the dynamic force variation with additional penetration factor other than the chip thickness variation,

$$F_{\Delta} = c_1 \Delta s + c_1 (\Delta s)^2 + c_2 (\Delta s)^3 + c_4 \dot{x} \tag{2.3}$$

where $\dot{x}$ corresponds to the penetration rate. But, it is indicated in Szakovits and D'Souza (1976) that equation (2.2) and (2.3) does not accurately represent the dynamic cutting process which actually exhibits the relationship of hysteresis.

Albrecht (1965) gives a theoretical explanation for the closed-loop relationship of force and uncut chip thickness by introducing a time lead in the ploughing cutting force model. However, it cannot describe the phenomenon of dynamic force lagging dynamic displacement of the workpiece surface, which occurs at low frequency [Szakovits and D'Souza(1976)].

In Marui et al (1988), a phase deviation is introduced into the linear Merchant Model to describe the hysteresis relationship of the force and chip thickness, however, due to the limitation of the linear Merchant model, the metal cutting system model cannot successfully explain the nonlinearity in the dynamic cutting process, such as the low frequency experiment observation in Szakovits and D'Souza(1976) that the resultant cutting force achieves varying phase difference to chip thickness fluctuation.

Experimental results from Doi and Kato(1956), Kato and Marui(1974), Fabris and D'Souza(1974), Szakovits and D'Souza(1976), Kaneko et al(1984), Marui et al(1983 1/2, 1995) demonstrated the hysteresis relationship between cutting/thrust force and undeformed chip thickness. And the following is one of the experimental examples.

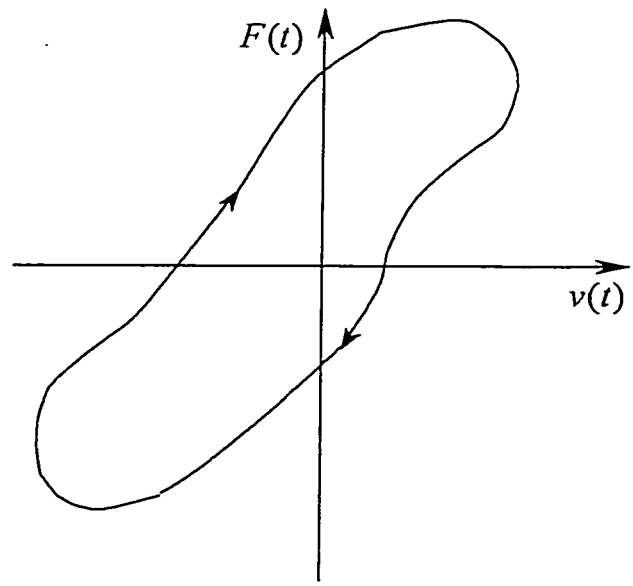

Figure 2.5 Hysteresis relationship between cutting/thrust force fluctuations and chip thickness fluctuation

The hysteresis relationship between the cutting/thrust force fluctuations and chip thickness fluctuation can be described as,

$$\begin{cases} F_{c\Delta}(t) = H_c(v(t)) \\ F_{t\Delta}(t) = H_t(v(t)) \end{cases} \tag{2.4}$$

where $F_{c\Delta}(t)$ and $F_{t\Delta}(t)$ represent the cutting force and thrust force fluctuations respectively, and $H_c(\cdot)$ and $H_t(\cdot)$ represent the functions describing hysteresis relationship between cutting/thrust force fluctuations and chip thickness fluctuation, respectively. It is noted that the hysteresis descriptions of cutting force and thrust force are different in the amplitude and hysteresis slope, etc., except that they are in the same positive direction while in chatter condition.

2.2.2 Contact/Frictional Force Models

Marui, et al (1983) investigated the contact force between flank surface and the workpiece surface by the primary chatter due to the deflection of cutting tool. The chatter mark is given experimentally as follows,

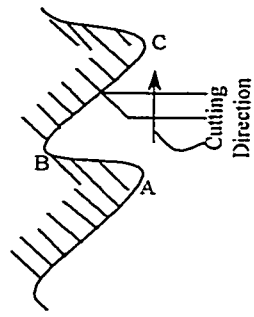

Figure 2.6 Chatter mark configuration

It is seen from Figure 2.7 that inclination of the chatter marks from A to B is large and the effective relief angle γ reaches zero or a minus value, so that the flank surface of the cutting tool will contact the workpiece surface during the this period. At the same time, a large frictional force may act on the flank surface in the vibration direction of the turning tool.

For type B chatter, the cutting tool can be taken as a beam with free end vibration. Arnold (1945), Marui et al (1983 1) give the description for the deflecting relationship of the cutting tool tip, which illustrates the cross deflection effect on workpiece surface owing to the tool tip deflection in the cutting direction.

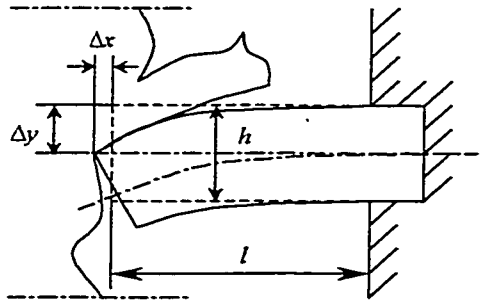

Figure 2.7 Deflection of cutting tool tip

A contact model of flank is presented in Sisson and Kegg (1969), Marui *et al* (1983 II), Elanayar and Shin (1996), which is based on the rounded tool nose model with the following assumptions.

1 The workpiece material subject to intensive compression is not "squeezed" out of the side of the cut.

2 The workpiece material is elastic and cannot be compressed permanently.

According to Sisson and Kegg (1969), Marui *et al* (1983 II), Elanayar and Shin (1996), the tool nose cannot be "perfectly" sharp, and should be represented by the rounded tool nose model, as shown in the figure below

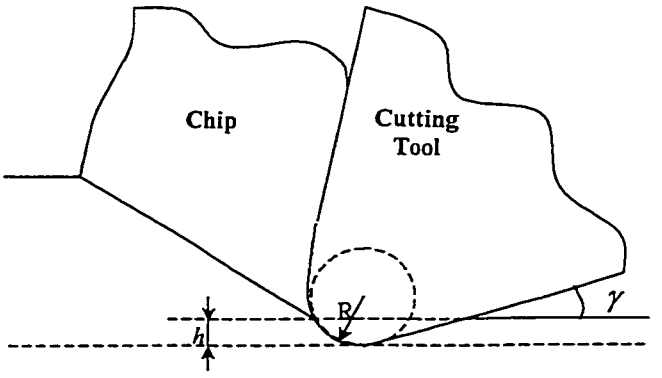

Figure 2.8 Rounded tool nose model

where R represents the tool sharpness radius. As shown in Figure 2.8, a very large negative rake angle exists at the lower part of the tool so that the workpiece material is essentially "trapped" under the tool nose and an intensive contact force is generated.

And, Marui et al (1983 1/2, 1995) experimentally presented the hysteresis relationship between the contact force and the cutting tool deflection, as shown in the following Figure.

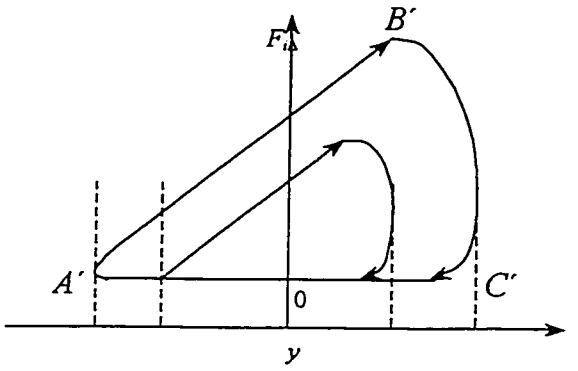

Figure 2.9 Hysteresis relationship between contact force and cutting tool deflection

The hysteresis relationship between the contact force fluctuations and y-direction fluctuation can be described as,

$$F_{i\Delta} = T(y) \tag{2.5}$$

Figure 2.6 shows that the dynamic contact force increases approximately linearly with the cutting tool amplitude enlargement and the contact force in the increasing period A' to B', when the flank face contacts the workpiece. It is shown in Figure 2.10 that after the chatter vibration reaches its positive maximum position, the separation of flank face and workpiece results in the contact force reducing to zero in a very short period (B' to C') and the contact force remains a small magnitude while the tool is deflecting upwards to

the negative maximum (C' to A'). This property of zero contact force is explained in Chiou and Liang (1999) as due to the fact that the contact force is always compressive and assumed only non-negative value. And Marui et al (1983) gives a quantitative explanation by investigating the relief angle variation.

In Marui et al (1983 1/2), the frictional force due to contact force can described as proportional to the contact force,

$$F_{nt} = k_i F_{i\Delta} \tag{2.6}$$

And the frictional force F_{nt} is in the reverse direction as the cutting force.

The hysteresis models for cutting/thrust force and contact/frictional force are set up in this section. In conclusion for this section, it is necessary to emphasize that we are searching a model that is accurate enough to describe the actual system. In order for the ultra-precision control for the turning metal cutting, linear model is not enough while the closed loop nonlinearity – hysteresis dominates the phenomenon.

2.3 Mathematical Hysteresis Models of Dynamic Cutting Process

In order for the controller design, some simplifications are required for the hysteresis models of the cutting/thrust force, contact force, and tool motions.

In order for the controller design, in this paper, we will treat the hysteresis demonstrated in the metal cutting as a backlash hysteresis due to their resemblance in profile, which is demonstrated in the following figures. For the hysteresis model of cutting/thrust force, the backlash hysteresis model is introduced in place of the actual hysteresis model.

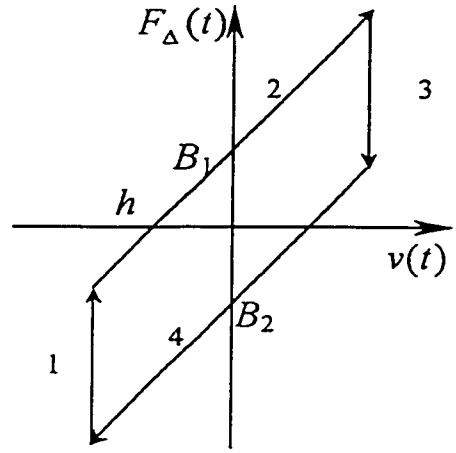

Figure 2.10 Backlash hysteresis model

In Figure 2.10, the line segments 1 and 3, 2 and 4 are parallel, and the hysteresis model of cutting force – chip thickness can be described in terms of h and B.

$$\begin{aligned} F_\Delta(t) &= H(v(t)) = H(h,B) \\ &= \begin{cases} h\cdot v(t)+B_1, & \dot{v}(t)>0 \\ h\cdot v(t)+B_2, & \dot{v}(t)<0 \\ F_\Delta(t_-) & \dot{v}(t)=0 \end{cases} \end{aligned} \tag{2.7}$$

where $v(t) = x(t) - x(t-\tau)$ is the chip thickness variation, h is the slope of the hysteresis lines and B_1, B_2 are the backlash distance. Due to the different descriptions of hysteresis model for cutting force and thrust force, we have the following description functions,

$$F_{c\Delta}(t) = H_c(v(t)) = H_c(h_c, B_c)$$
$$= \begin{cases} h_c \cdot v(t) + B_{c1}, & \dot{v}(t) > 0 \\ h_c \cdot v(t) + B_{c2}, & \dot{v}(t) < 0 \\ F_{c\Delta}(t_-) & \dot{v}(t) = 0 \end{cases} \tag{2.8}$$

and

$$F_{t\Delta}(t) = H_t(v(t)) = H_t(h_t, B_t)$$
$$= \begin{cases} h_t \cdot v(t) + B_{t1}, & \dot{v}(t) > 0 \\ h_t \cdot v(t) + B_{t2}, & \dot{v}(t) < 0 \\ F_{t\Delta}(t_-) & \dot{v}(t) = 0 \end{cases} \tag{2.9}$$

where h_c, h_t, B_{c1}, B_{c2}, B_{t1}, B_{t2} are the slopes of hysteresis and distance of hysteresis for cutting and thrust force, respectively.

For the dynamic contact force model, a triangular hysteresis model is introduced to describe the actual hysteresis model,

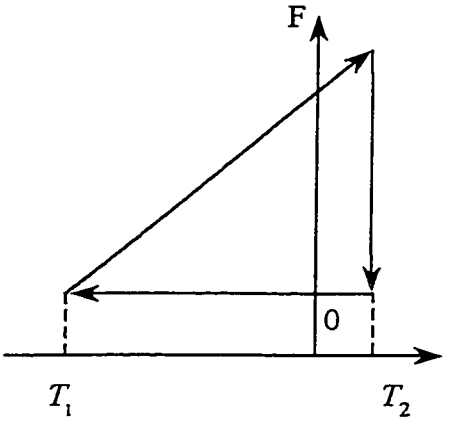

Figure 2.11 Triangular hysteresis model

The triangular hysteresis model describes the relationship of dynamic contact force and tool deflection in a simpler method and we have the following description functions:

$$F_{i\Delta} = T(x_2) = \begin{cases} h_i(x_2 - T_1) & \dot{x}_2 > 0 \\ 0 & \dot{x}_2 \le 0 \end{cases} \tag{2.10}$$

and

$$F_{nt} = k_f F_{i\Delta} \tag{2.11}$$

where h_i is the slope of the increasing line and T_1 represents the chatter amplitude.

By combining models of the cutting/thrust forces and contact/frictional forces, we have the following general description functions for dynamic cutting process.

$$\begin{cases} \Delta F_c = F_{c\Delta} + F_{ft} \\ \Delta F_t = F_{t\Delta} + F_{i\Delta} \end{cases} \tag{2.12}$$

In the following chapters, the above simplified hysteresis models will be used for controller design.

2.4 Simulation Results

In order to illustrate the effect of active hysteresis, passive hysteresis, primary chatter simulations are conducted in the following. We are taking the metal cutting system as

$$m\ddot{x} + c\dot{x} + kx = F_\Delta \tag{2.13}$$

The equivalent mass, damping coefficient and spring coefficient for the metal cutting system are,

$$m = 10 \text{ kg}, c = 5 \times 10^2 \text{ kg/s}, k = 5 \times 10^7 \text{ kg/s}^2,$$

With initial tool deflection $x_0 = 10\mu m$ and $F_\Delta = 0$, we have the force free response of the cutting system as illustrated in the following figure,

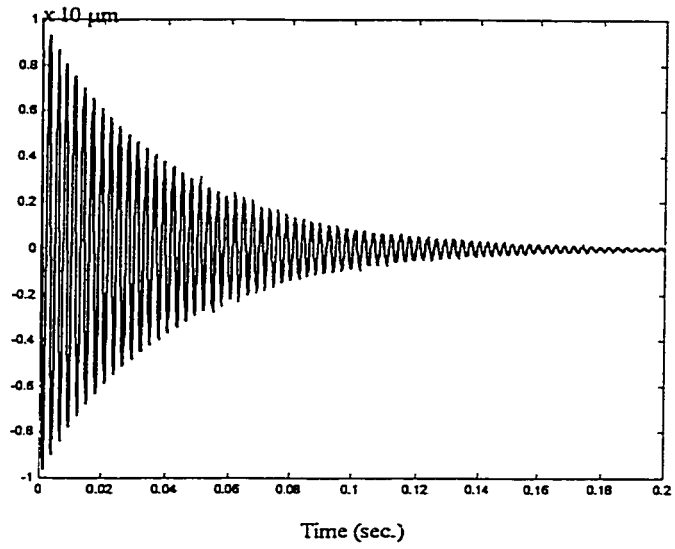

Figure 2.12 Force free response of turning system

It is clearly seen that the cutting system response is decreasing exponentially due to the damping coefficient c.

Active hysteresis is so called that the direction of the hysteresis is clockwise, while passive hysteresis is so that that the direction of the hysteresis is anti-clockwise. In order to demonstrate the effect of active hysteresis and passive hysteresis, we are going to simulate the primary chatter with coefficients for hysteresis model listed as follows,

$$h = 4 \times 10^6 \text{ N/m and } B_0 = 20 \text{ N}.$$

For active hysteresis model,

$$F_{\Delta}(t) = H(v(t)) = H(h, B)$$
$$= \begin{cases} h \cdot v(t) + B_0, & \dot{v}(t) > 0 \\ h \cdot v(t) - B_0, & \dot{v}(t) < 0 \\ F_{\Delta}(t_-) & \dot{v}(t) = 0 \end{cases}$$

where $v(t)=x$.

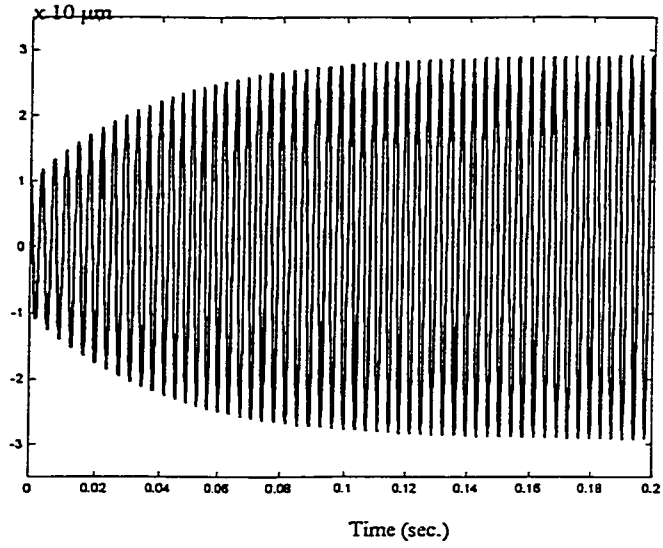

Figure 2.13 Response of turning system with active hysteresis

For passive hysteresis model,

$$F_{\Delta}(t) = H(v(t)) = H(h, B)$$
$$= \begin{cases} h \cdot v(t) - B_0, & \dot{v}(t) > 0 \\ h \cdot v(t) + B_0, & \dot{v}(t) < 0 \\ F_{\Delta}(t_-) & \dot{v}(t) = 0 \end{cases}$$

where $v(t)=x$, as primary chatter is considered in this case.

And the cutting system response is as following,

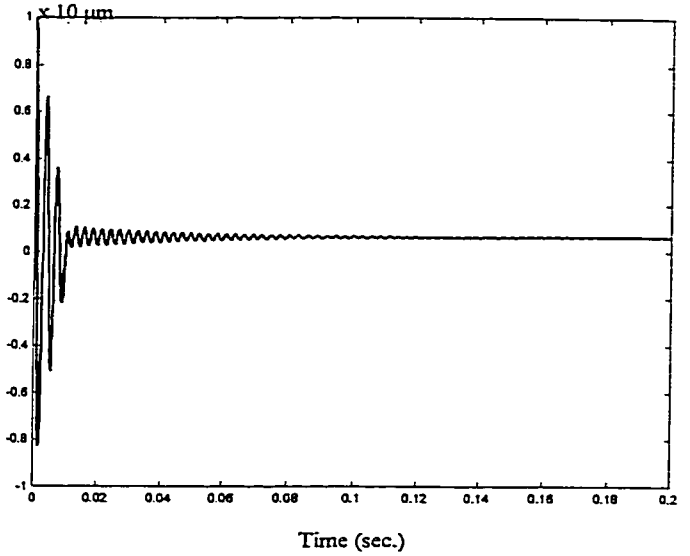

Figure 2.14 Response of turning system with passive hysteresis

It is obvious that the cutting system is much more "stable" when the cutting process is displaying passive hysteresis. As a result, based on the proposed hysteresis models, simulations (figures 2.12-2.14) give a good correlation to the theory of chatter excitation and maintenance.

In the following, we are going to present the most frequent types of chatter – regenerative chatter and multi-regenerative chatter. Taking into account (2.13), the equivalent mass, damping coefficient and spring coefficient for the metal cutting system are taken as,

$$m = 15 \text{ kg}, c = 3 \times 10^3 \text{ kg/s}, k = 6 \times 10^7 \text{ kg/s}^2,$$

And regenerative effect is considered with external force free, the cutting system response is as following,

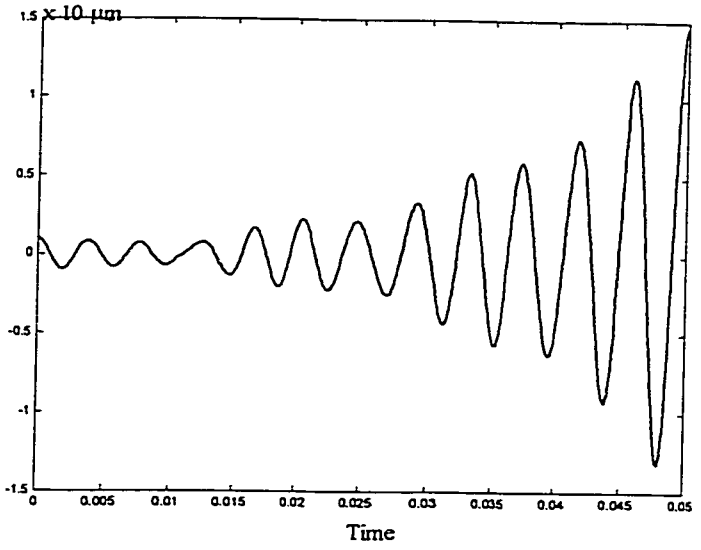

Figure 2.15 Regenerative chatter in turning

It can be seen that chatter is growing as time is going on. Theoretically, chatter can grow as the metal cutting system stays in the oscillating state, however, it is indicated that chatter cannot grow infinitely due to the multi-regenerative effect [Tlusty and Ismail(1981)], which is illustrated in the following.

In order to display the effect of multi-regenerative chatter, consider the normal depth of cut is 0.5 mm. When the chip thickness variation $v(t) < -0.5$ mm, which leads to an impossible result of (chip thickness < 0), the cutting force is reduced to 0 owing to the fact that the cutting tool moves out of contact with workpiece. And we have the following illustration for multi-regenerative chatter,

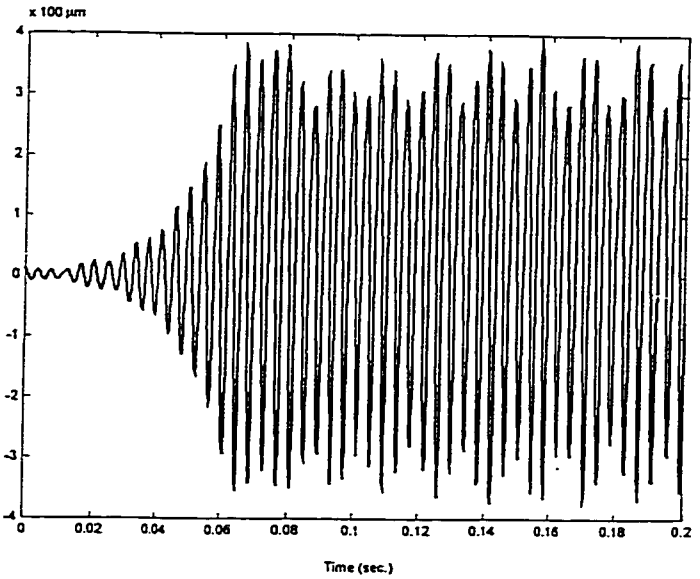

Figure 2.16 Multi-regenerative chatter in turning

Taking into account the multi-regenerative effect, it is found out that the chatter can be divided into developing and "stabilizing" periods, which also give good correlation to the experimental results [Tlusty and Ismail(1981)].

2.5 Summary

In this chapter, hysteresis models for dynamic cutting process, including cutting force model and contact force model, are presented. Active hysteresis is proved to be one of the causes of chatter occurrence as it provides the energy for chatter excitation and maintenance. Simplified mathematical hysteresis models are given and the simulations based on these models demonstrate the behaviors of passive hysteresis model, active hysteresis model, regenerative chatter effect and multi-regenerative chatter effect, which give a good correlation with the actual experimental results.

Chapter 3

Modeling of Linear Cutting Dynamics with Piezoactuator

Introduction – In this Chapter, cutting dynamics descriptions are presented for turning system with piezoactuator, including one degree of freedom and two degrees of freedom.

3.1 Cutting Tool Dynamics

The cutting system is regarded as the machine tool together with workpiece, cutting tool, workpiece clamping device and tool clamping device. In order to describe the cutting dynamics of the metal cutting system, Koenigsberger and Tlusty (1970) presented several simplifications and assumptions. i) The vibratory system of the machine is linear. ii) The direction of the variable component of the cutting force is constant. iii) The variable component of the cutting force depends only on vibration in the direction of the normal to the cut surface. iv) The frequency of the vibration and the mutual phase shift of undulations in subsequent overlapping cuts are not influenced by the relationship of wavelength to the length of cut; this assumption corresponds to an infinite length for every cut or, practically, to planning.

And under the above assumptions, the cutting system can be described as a linear second order function [Tobias (1965)],

$$m\ddot{x} + c\dot{x} + kx = F_{\Delta} \tag{3.1}$$

where m, c, k are the equivalent mass, equivalent damping coefficient, and equivalent spring stiffness respectively for the metal cutting machine.

Equation (3-1) is the description for a one DOF cutting system. And a two DOF cutting system is illustrated in Figure 3.1.

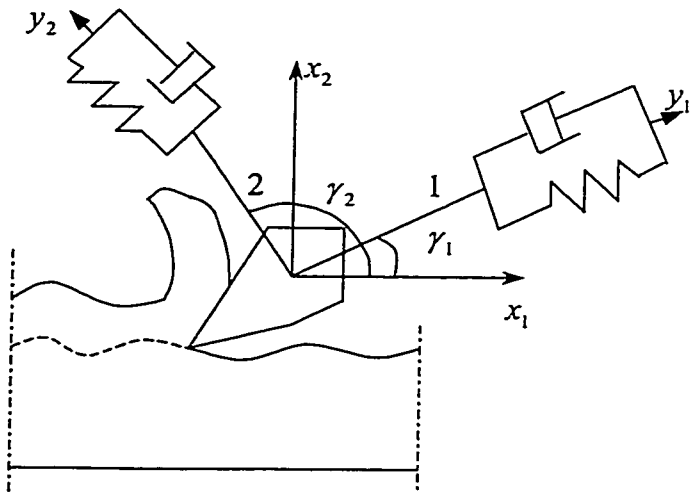

Figure 3.1 Cutting system with two degrees of freedom

In Figure 3.1, x_1 and x_2 are the displacement of the tool in the directions of freedom, and the equations of the system in these two directions can be described as,

$$\begin{bmatrix} m_1 & 0 \\ 0 & m_2 \end{bmatrix} \ddot{\bar{y}} + \begin{bmatrix} c_1 & 0 \\ 0 & c_2 \end{bmatrix} \dot{\bar{y}} + \begin{bmatrix} k_1 & 0 \\ 0 & k_2 \end{bmatrix} \bar{y} = \begin{bmatrix} F_1 \\ F_2 \end{bmatrix} = \bar{F} \tag{3.2}$$

where $\bar{y} = [y_1 \quad y_2]'$, and $m_1, m_2, c_1, c_2, k_1, k_2$ are the equivalent mass, equivalent damping coefficient, and equivalent spring stiffness respectively for the two degrees of freedom. F_1, F_2 are the forces for the two different directions.

The displacement and force components of the two degrees of freedom 1 and 2, can be described in the terms of the reference frame $X_1 - X_2$,

$$\bar{x} = \begin{bmatrix} \cos\gamma_1 & \cos\gamma_2 \\ \sin\gamma_1 & \sin\gamma_2 \end{bmatrix}^{-1} \begin{bmatrix} y_1 \\ y_2 \end{bmatrix} \tag{3.3}$$

$$\bar{F} = \begin{bmatrix} \cos\gamma_1 & \cos\gamma_2 \\ \sin\gamma_1 & \sin\gamma_2 \end{bmatrix}^{-1} \begin{bmatrix} F_x \\ F_y \end{bmatrix} \tag{3.4}$$

Substitute (3) and (4) into (2), we have,

$$\begin{bmatrix} \cos\gamma_1 & \cos\gamma_2 \\ \sin\gamma_1 & \sin\gamma_2 \end{bmatrix} \begin{bmatrix} m_1 & 0 \\ 0 & m_2 \end{bmatrix} \begin{bmatrix} \cos\gamma_1 & \cos\gamma_2 \\ \sin\gamma_1 & \sin\gamma_2 \end{bmatrix}^{-1} \begin{bmatrix} \ddot{x} \\ \ddot{y} \end{bmatrix}$$

$$+ \begin{bmatrix} \cos\gamma_1 & \cos\gamma_2 \\ \sin\gamma_1 & \sin\gamma_2 \end{bmatrix} \begin{bmatrix} k_1 & 0 \\ 0 & k_2 \end{bmatrix} \begin{bmatrix} \cos\gamma_1 & \cos\gamma_2 \\ \sin\gamma_1 & \sin\gamma_2 \end{bmatrix}^{-1} \begin{bmatrix} \dot{x} \\ \dot{y} \end{bmatrix}$$

$$+ \begin{bmatrix} \cos\gamma_1 & \cos\gamma_2 \\ \sin\gamma_1 & \sin\gamma_2 \end{bmatrix} \begin{bmatrix} k_1 & 0 \\ 0 & k_2 \end{bmatrix} \begin{bmatrix} \cos\gamma_1 & \cos\gamma_2 \\ \sin\gamma_1 & \sin\gamma_2 \end{bmatrix}^{-1} \begin{bmatrix} x \\ y \end{bmatrix} = \begin{bmatrix} F_x \\ F_y \end{bmatrix} \tag{3.5}$$

Altintas (1997) presented a general machine tool structure equation,

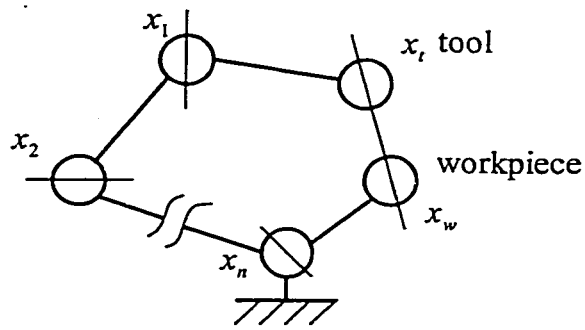

Figure 3.2 Transfer function between a tool and workpiece on the machine tools

$$x = [x_1 \quad x_2 \quad \cdots \quad x_t \quad x_w \quad \cdots \quad x_n]^T$$

$$F = [0 \quad 0 \quad \cdots \quad 1 \quad -1 \quad \cdots \quad 0]F_0$$

And the equation of motion for the system is,

$$M_x\ddot{x} + C_x\dot{x} + K_x x = F$$

where M_x, C_x and K_x are the local mass, local damping and local stiffness matrices, respectively.

Wu and Liu (1985), Minis and Tembo (1993), Elbestawi et al (1994) showed that the dynamics of the cutting system may be described by the following equations,

$$\begin{bmatrix} m_x & 0 \\ 0 & m_y \end{bmatrix}\ddot{z} + \begin{bmatrix} c_x & 0 \\ 0 & c_y \end{bmatrix}\dot{z} + \begin{bmatrix} k_x & 0 \\ 0 & k_y \end{bmatrix}z = \begin{bmatrix} F_x \\ F_y \end{bmatrix}$$

where $z = [x \quad y]^T$ represents the varying displacement along X and Y axes, m_x, m_y, c_x, c_y, k_x and k_y are the modal mass, damping, and stiffness, respectively.

In summary with all the results presented above, a general linear machine tool dynamics can be described as follows,

$$M\ddot{x} + C\dot{x} + Kx = F \tag{3.6}$$

where the local mass M, damping C, and stiffness K matrices are $R^{k\times k}$, the force vector $F \in R^{k\times 1}$. $x \in R^{k\times 1}$, and k is determined by the system model.

3.2 Piezoactuator Dynamics

The turning metal cutting system is illustrated in Figure 3.3, where the cutting tool is mounted on the tool holder with a piezoactuator as the actuator.

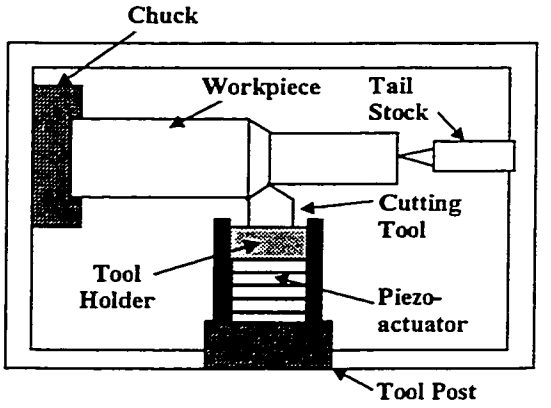

Figure 3.3 Turning metal cutting

With the advent of improved machines and processes, interest has been growing for a fast tool servo mechanism to increase the capability and capacity of existing machines. The purpose of the piezoactuator is to move the tool small distances into and out of the workpiece several times per revolution of the part, thus generating desired workpiece surfaces or correcting for errors. With electrical voltage applied, the piezoactuator can expand and reach its nominal displacement on the order of microseconds and

than 10,000 g's are possible, so that the position of the cutting tool can be maneuvered. Therefore, the chatter occurred in metal cutting can be reduced with appropriate control scheme with the help of piezoactuator [Fawcett (1990), Cuttino, et al (1999)]. Figure 3.4 demonstrates the simple section view of a piezoactuator.

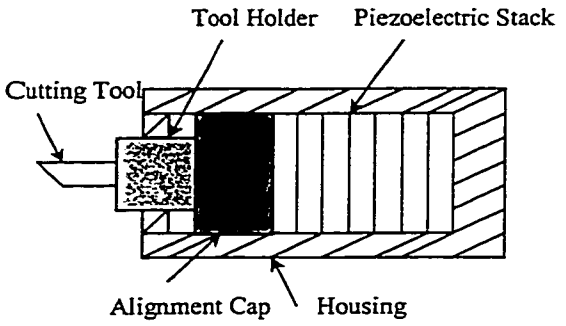

Figure 3.4 Section view of piezoactuator

Many piezoactuator models are offered with a mechanical preload so that it is possible to apply larger pulling forces to the positioning element. In order to present the description of piezoactuator model, the mechanical preload is not indicated in Figure 3.4.

Whether the piezo translator can generated force depends on its stiffness and its expansion capacity. If it is attached between two rigid walls so that it cannot expand, then it generates its maximum force, also called blocking force. However, it is only true for ideal restraints, whose spring constant k_s is infinitely large. In practice, due to fast expanding of piezo translator and the inertia of the mass load connected to the piezo translator, a pushing or pulling force can be excited and it is described as,

3.3 System Dynamics without Independent Tool Holder Dynamics

Without considering the independent tool holder dynamics, Liu et al (1998) presented a dynamic model for the turning cutting system demonstrated in the following,

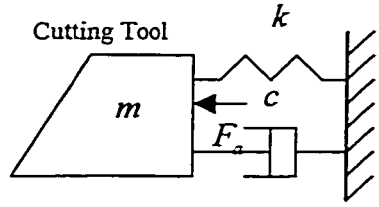

Figure 3.5 Dynamic model 1 for cutting tool with piezoactuator

And the cutting system can be described as,

$$m\ddot{x} + c\dot{x} + kx = F_{\Delta} - F_a \tag{3.8}$$

the equivalent mass of the cutting system is m, the stiffness is k, and the damping coefficient of the system is c. F_a represents the force generated by the piezoactuator due to the high speed expansion.

3.4 System Dynamics with Independent Tool Holder Dynamics

Considering the tool holder dynamics,

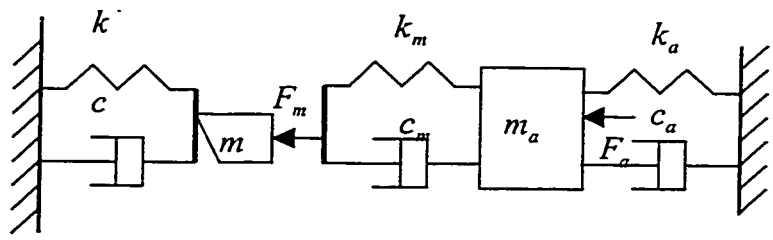

Figure 3.6 Dynamic model 2 for cutting tool with piezoactuator

From figure 3.6, the piezoactuator dynamics can be described as,

$$m_a\ddot{x}_a + c_a\dot{x}_a + k_a x_a = F_m - F_a \tag{3.9}$$

$$F_m = c_m(\dot{x} - \dot{x}_a) + k_m(x - x_a) \tag{3.10}$$

$$m\ddot{x} + c\dot{x} + kx = F_\Delta - F_m \tag{3.11}$$

Where the equivalent mass of the cutting system is m, the stiffness is k, and the damping coefficient of the cutting system is c. And m_a, c_a, k_a are respectively the equivalent mass, stiffness, and damping coefficient of the piezoactuator. F_Δ represents the cutting force fluctuation of the machine tool and is, as will be clear later, a nonlinear function with respect to the chip thickness fluctuation. F_a represents the force generated by the piezoactuator, which will also be given detailed analysis in the following section. And F_m is the reaction force between the piezoactuator and cutting tool. In Figure 3.2, F_m is represented by the force generated by the spring-damper structure.

In the following chapters, we will develop robust adaptive controllers according to these two proposed system dynamic models.

3.5 Summary

Two different dynamic system models are presented in this chapter, considering the linear cutting dynamics of turning system with piezoactuator.

Chapter 4

Chatter Suppression via Linear Piezo-actuation

Adaptive Controller Design — 1

Introduction — In this chapter, in order for chatter suppression, a piezoactuator actuation is introduced for the regulation of the machine tool displacement. Metal cutting system is modeled as a class of uncertain linear system with hysteresis and time delay and the piezoactuator is considered exhibiting linear actuation. In order to overcome the chatter due to the hysteresis and time delay in the cutting process, two adaptive controllers based on different hysteresis descriptions for the metal cutting system of ultra-precision machining are presented. The simulation results show that the proposed adaptive controllers significantly eliminate the chatter phenomena.

4.1 Dynamic Turing System Model

The schematic model of turning metal cutting system is illustrated in Figure 4.1, and the dynamic cutting process is demonstrated in the magnified contact parts of workpiece and cutting tool. In this paper, we focus on the cutting force that is perpendicular to the surface of workpiece. In Liu et al (1998), considering the piezo-actuated tool holder

assemble as a lumped mass system, the structural system may be represented by a dynamic model of turning process as illustrated in the following.

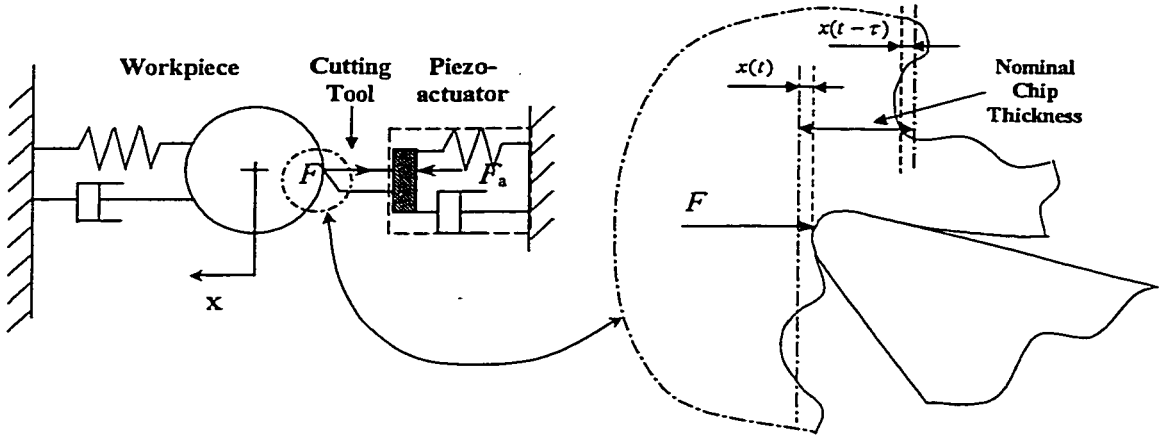

Figure 4.1 Schematic model of turning system

From Figure 4.1, the dynamical process of the above metal cutting system can be described with a linear second order function as the following [see, for example, Chiou and Liang (1998)],

$$m\ddot{x} + c\dot{x} + kx = F_{\Delta} - F_a \tag{4.1}$$

where $x(t)$ represents the fluctuating part of the depth of cut, or so called offset chip thickness(refer to Figure 4.1), m, c, k are the equivalent mass, equivalent damping coefficient, and equivalent spring stiffness respectively for the metal cutting machine, k_a is the equivalent spring stiffness for the piezoactuator and u is the control input applied to the piezoactuator. F_{Δ} represents the cutting force variation of the machine tool and is proved to be a nonlinear function with respect to the chip thickness variation.

In this chapter, we are considering linear Voltage–Displacement characteristic for piezoactuator, i.e.,

$$\Delta L = k_1 u$$

where u is the applied voltage and the k_1 is the proportionality. Due to the fact of fast expansion response of the piezoactuator, a pushing or pulling force can be excited and it is described as,

$$F_a = k_2 \Delta L$$

Where k_2 is the equivalent stiffness of the piezoactuator. Denote $k_a = k_1 k_2$, we have that the force F_a exerted on the cutting tool by the piezo actuator is proportional to the displacement $u(t)$,

$$F_a = k_a u \tag{4.2}$$

Thus, the turning cutting system can be described as,

$$m\ddot{x} + c\dot{x} + kx = F_\Delta - k_a u \tag{4.3}$$

And the block diagram illustrating the control system is as follows, with $G(s) = 1/(ms^2 + cs + k)$.

Remark: The cutting system model illustrated in Figure 4.2 is a complicated nonlinear system involving hysteresis, which can lead to instability in closed-looped operation and complicates the task of controller design and analysis [Gorbet (2001)].

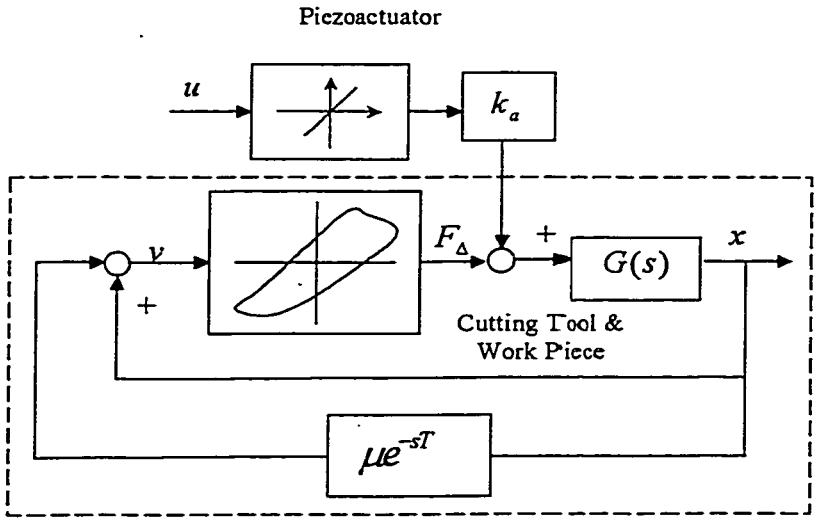

Figure 4.2 Block diagram of turning system with piezoactuator

Focusing on the above model, in the following, a robust adaptive control scheme for control input $u(t)$ will be designed to suppress the chatter effect.

4.2 Adaptive Controller Design

The control of metal cutting system is a challenging task in the presence of hysteresis nonlinearity. Hysteresis is known to be non-differentiable and severely limits the performance of the system by causing undesirable chatter. Most of the hysteresis models proposed [see, for example, Macki, et al (1993)] are very complicated and it is still unavailable for designing the control scheme with a general type of hysteresis. In this paper, we will treat the hysteresis demonstrated in the metal cutting as a backlash hysteresis in two different descriptions,

I. A dynamic backlash-like hysteresis

$$\frac{dH(v)}{dt} = \alpha\left|\frac{dv}{dt}\right|(hv - H(v)) + B_1\frac{dv}{dt} \tag{4.4}$$

where α and B_1 are constants, satisfying $h > B_1$.

II. A discontinuous time backlash hysteresis model

$$\begin{aligned} F_\Delta(t) &= H(v(t)) = H(h,B) \\ &= \begin{cases} h\cdot v(t) + B, & \dot{v}(t) > 0 \\ h\cdot v(t) - B, & \dot{v}(t) < 0 \\ 0 & \dot{v}(t) = 0 \end{cases} \end{aligned} \tag{4.5}$$

where $h > 0$ is the slope of the hysteresis lines and $B > 0$ is the backlash distance.

In Chapter 2, it is known (4.5) is used as the approximation for the actual backlash hysteresis in the cutting process. We shall now examine the solution properties of the dynamic model (4.4) and explain the corresponding switching mechanism, which is crucial for design of the controller. The equation (4.4) can be solved explicitly for v piecewise monotone,

$$H(v) = hv + f(v) \text{ with} \tag{4.6}$$

$$f(v) = [H_0 - hv_0]e^{-\alpha(v-v_0)\operatorname{sgn}\dot{v}} + e^{-\alpha v\operatorname{sgn}\dot{v}}\int_{v_0}^{v}[B_1 - h]e^{\alpha\zeta(\operatorname{sgn}\dot{v})}d\zeta$$

for $\dot{v}$ constant and $H(v_0) = H_0$. Analyzing the solution (4.6), we see that it is composed of a line with the slope h, together with a term $f(v)$. For $f(v)$, it can be easily shown that if $H(v; v_0, w_0)$ is the solution of (4.6) with initial values (v_0, w_0), then, if $\dot{v} > 0\,(\dot{v} < 0)$ and $v \to +\infty\,(-\infty)$, one has

$$\lim_{v\to\infty} H(v) = \lim_{v\to\infty}[w(v;v_0,w_0) - f(v)] = -\frac{h-B_1}{\alpha}, \tag{4.7}$$

$$\left(\lim_{v\to-\infty} H(v) = \lim_{v\to-\infty}[w(v;v_0,w_0) - f(v)] = \frac{h-B_1}{\alpha}\right).$$

It should be noted that the above convergence is exponential at the rate of α. Solution (4.6) and properties (4.7) and (4.8) show that $H(v)$ eventually satisfies the first and second conditions of (4.5). Furthermore, setting $\dot{v} = 0$ results in $\dot{w} = 0$ which satisfies the last condition of (4.5). This implies that the dynamic equation (4.4) can be used to model a class of backlash-like hysteresis and is an approximation of backlash hysteresis (4.5).

Let us use an example for specified initial data to show the switching mechanism for the dynamic model (4.4) when $\dot{v}$ changes direction. We note that when $\dot{v} > 0$ on $w(0) = 0$ and $v(0) = 0$, the solution (4.6) gives

$$H(v) = hv - \frac{h-B_1}{\alpha}(1-e^{-\alpha v}) \text{ for } v(t) \geq 0 \text{ and } \dot{v} > 0 \tag{4.8}$$

Let v_s be a positive value of v and consider now a specimen such that v is increasing along the initial curve (4.8) until a time t_s, the signal v is decreased. In this case, $H(v)$ is given by

$$H(v) = hv + \frac{h-B_1}{\alpha}[1-(2e^{-\alpha v_s} - e^{-2\alpha v})e^{\alpha v}] \text{ for } \dot{v} < 0 \tag{4.9}$$

where $v < v_s$. Equations (4.8) and (4.9) indeed show that $H(v)$ switches exponentially from the line $hv - \frac{h - B_1}{\alpha}$ to $hv + \frac{h - B_1}{\alpha}$ to generate backlash-like hysteresis curves.

To confirm the above analysis, the solutions of (4.4) can be obtained by numerical integration with v as the independent variable. Figure 4.4 shows that model (4.4) indeed generates backlash-like hysteresis curves, which confirms the above analysis. It should be mentioned that the parameter α determines the rate at which $H(v)$ switches between $-\frac{h - B_1}{\alpha}$ and $\frac{h - B_1}{\alpha}$. The larger the parameter α is, the faster the transition in $H(v)$ is going to be. However, the backlash distance is determined by $\frac{h - B_1}{\alpha}$ and the parameter must satisfy $h > B_1$. Therefore, the parameter α cannot be chosen freely. A compromise should be made in choosing a suitable parameter set $\{\alpha, h, B_1\}$ to model the required shape of backlash-like hysteresis.

It is very important to note that equation (4.7) implies that there exists a uniform bound ρ such that

$$\|f(v)\| \leq \rho \tag{4.10}$$

So, the solution of the backlash-like hysteresis (4.4) consists of a linear function and a bounded nonlinearity,

$$H(v(t)) = hv(t) + f(v(t)) \tag{4.11}$$

In the following, two adaptive controllers are presented based on continuous backlash-like hysteresis model and discontinuous backlash hysteresis model.

4.2.1 Adaptive Controller for Backlash-like Hysteresis Model

Utilizing the solution property (4.11), and substituting $v(t)$ with $x-\mu x(t-\tau)$, the backlash-like hysteresis model (4.4) for metal cutting is given as follows,

$$H\left(x-\mu x(t-\tau)\right)=h\cdot\left(x-\mu x(t-\tau)\right)+f\left(x-\mu x(t-\tau)\right) \tag{4.12}$$

where $\left\|f\left(x-\mu x(t-\tau)\right)\right\|\le\rho$.

In this case, the turning cutting system can be described as,

$$m\ddot{x}+c\dot{x}+kx=h\cdot\left(x-\mu x(t-\tau)\right)+f\left(x-\mu x(t-\tau)\right)-k_a u \tag{4.13}$$

It should be noted that by using the definition of the hysteresis model (4.4), the complicated description of the cutting model (4.3) is transformed into a simplified form, which makes the design of robust control scheme possible.

Before the controller design, the following assumptions are required,

(A1) Time delay τ remains constant during the cutting process;

(A2) m, c, k, k_a, h are bounded variables with

$$m\in[m_{\min}, m_{\max}],\ c\in[c_{\min}, c_{\max}],\ k\in[k_{\min}, k_{\max}],\ k_a\in[k_{a\min}, k_{a\max}],\ h\in[h_{\min}, h_{\max}],$$

where $m_{\min}$, $m_{\max}$, $c_{\min}$, $c_{\max}$, $k_{\min}$, $k_{\max}$, $k_{a\min}$, $k_{a\max}$, $h_{\min}$, $h_{\max}$ are known constants.

Remark: In the researches of chatter occurrence, it is commonly assumed that the revolution speed is constant [see, for example, Merrit (1965), Olgac and Hosek (1998)]. Due to the fact that m, c, k, k_a, h are physical coefficients for the metal cutting system, subjecting to internal changes or external disturbance, it is reasonable to assume that they are bounded variables.

Divided by m on both sides of (4.13) and with some manipulations, we have the following second order function with nonlinearity,

$$\ddot{x} = -\frac{c}{m}\dot{x} + \frac{-k+h}{m}x + \frac{-h\mu}{m}x(t-\tau) + \frac{1}{m}f\left(x-\mu x(t-\tau)\right) - \frac{k_a}{m}u \qquad (4.14)$$

Remark: In metal cutting, what we concern about most is the offset chip thickness $x(t)$, for it directly reflects the surface quality of the workpiece being machined, and the vibration of $x(t)$ reflects the chatter occurrence during the dynamic cutting process. In order for the chatter suppression, a robust adaptive controller is proposed in the following for the regulation of $x(t)$.

Denote,

$$a_1 = -\frac{c}{m}, \qquad a_2 = \frac{-k+h}{m}, \qquad a_3 = -\frac{h\mu}{m}, \qquad a_4 = \frac{1}{m}, \qquad b = -\frac{k_a}{m} \qquad \text{and}$$

$$g(x, x_\tau) = \frac{1}{m}f\left(x-\mu x(t-\tau)\right)$$

Equation (4.14) can be rewritten as

$$\ddot{x} = a_1\dot{x} + a_2 x + a_3 x(t-\tau) + g(x, x_\tau) + bu \tag{4.15}$$

where $g(x, x_\tau) \le \sigma = \dfrac{\rho}{m_{\min}}$.

A filtered tracking error is defined as

$$s(t) = \dot{x} + \lambda x \text{ with } \lambda > 0, \tag{4.16}$$

Remark: It has been shown [Slotine and Li (1991)] that the definition (4.16) has the following properties: (i) the equation s(t)=0 defines a time a hyper-plane on which the state x(t) decays exponentially to zero, (ii) if x(0)=0 and $|s(t)| \le \varepsilon$ with constant ε, then x(t) $\in \Omega_\varepsilon = \{x(t) \,||\, x| \le \lambda^{-1}\varepsilon\}$ for $\forall t \ge t_0$, and (iii) if $x(0) \ne 0$ and $|s(t)| \le \varepsilon$, then x(t) will converge to Ω_ε with a time-constant $1/\lambda$.

Differentiating $s(t)$ with respect to time and substituting $\ddot{x}$ with (4.14), one has,

$$\begin{aligned} \dot{s}(t) &= \ddot{x} + \lambda\dot{x} \\ &= (\lambda + a_1)\dot{x} + a_2 x + a_3 x(t-\tau) + g(x, x_\tau) + bu \end{aligned} \tag{4.17}$$

Define

$$\theta = \frac{\lambda + a_1}{b},\ \xi = \frac{a_2}{b} \text{ and } \varsigma = \frac{a_3}{b}$$

Due to the boundedness of m, c, k, k_a, h, we have $\theta \in [\theta_{\min}, \theta_{\max}]$, $\xi \in [\xi_{\min}, \xi_{\max}]$ and $\varsigma = [\varsigma_{\min}, \varsigma_{\max}]$, where $\theta_{\min}, \theta_{\max}, \xi_{\min}, \xi_{\max}, \varsigma_{\min}, \varsigma_{\max} \in R$ are constants, and they can be easily obtained with the bounds provided in assumption (A4.2).

In stead of deriving the adaptive law with the filtered error $s(t)$, we introduce a tuning error, s_ε, as follows,

$$s_\varepsilon = s - \varepsilon sat\left(\frac{s}{\varepsilon}\right) \tag{4.18}$$

where ε is a positive constant subject to the choice of designer and $sat(\cdot)$ is the saturation function.

Remark: The tuning error s_ε, becomes 0 when the absolute value of filtered error, $|s(t)| \le \varepsilon$, which is equal to creating an adaptation dead band with the range of $[-\varepsilon, \varepsilon]$.

Given the uncertain system with bounded nonlinearity (4.14), the following control and adaptation laws are presented:

$$u(t) = -\left[k_d s + \hat{\theta}\dot{x} + \hat{\xi}x + \hat{\varsigma}x(t-\tau) + k^* sat\left(\frac{s}{\varepsilon}\right)\right] \tag{4.19}$$

with

$$\dot{\hat{\theta}} = proj\left(\hat{\theta}, s_\varepsilon \dot{x}\right),\ \dot{\hat{\xi}} = proj\left(\hat{\xi}, s_\varepsilon x\right) \text{ and } \dot{\hat{\varsigma}} = proj\left(\hat{\varsigma}, s_\varepsilon x(t-\tau)\right) \tag{4.20}$$

where $k^* \ge \frac{\sigma}{b_{\min}}$. And $proj(\cdot,\cdot)$ is a projection operator, which are constructed as follows:

$$proj\left(\hat{\theta}, s_\varepsilon \dot{x}\right) = \begin{cases} 0 & \text{if } \hat{\theta} = \theta_{\max} \text{ and } s_\varepsilon \dot{x} > 0 \\ & \text{or } \hat{\theta} = \theta_{\min} \text{ and } s_\varepsilon \dot{x} < 0 \\ s_\varepsilon \dot{x} & \text{if } \theta_{\min} < \hat{\theta} < \theta_{\max} \\ & \text{or } \hat{\theta} = \theta_{\max} \text{ and } s_\varepsilon \dot{x} \le 0 \\ & \text{or } \hat{\theta} = \theta_{\min} \text{ and } s_\varepsilon \dot{x} \ge 0 \end{cases} \tag{4.21}$$

$$proj(\hat{\xi}, s_\varepsilon x) = \begin{cases} 0 & \text{if } \hat{\xi} = \xi_{\max} \text{ and } s_\varepsilon x > 0 \\ & \text{or } \hat{\xi} = \xi_{\min} \text{ and } s_\varepsilon x < 0 \\ s_\varepsilon x & \text{if } \xi_{\min} < \hat{\xi} < \xi_{\max} \\ & \text{or } \hat{\xi} = \xi_{\max} \text{ and } s_\varepsilon x \le 0 \\ & \text{or } \hat{\xi} = \xi_{\min} \text{ and } s_\varepsilon x \ge 0 \end{cases} \tag{4.22}$$

$$proj(\hat{\varsigma}, s_\varepsilon x(t-\tau)) = \begin{cases} 0 & \text{if } \hat{\varsigma} = \varsigma_{\max} \text{ and } s_\varepsilon x(t-\tau) > 0 \\ & \text{or } \hat{\varsigma} = \varsigma_{\min} \text{ and } s_\varepsilon x(t-\tau) < 0 \\ s_\varepsilon x(t-\tau) & \text{if } \varsigma_{\min} < \hat{\varsigma} < \varsigma_{\max} \\ & \text{or } \hat{\varsigma} = \varsigma_{\max} \text{ and } s_\varepsilon x(t-\tau) \le 0 \\ & \text{or } \hat{\varsigma} = \varsigma_{\min} \text{ and } s_\varepsilon x(t-\tau) \ge 0 \end{cases} \tag{4.23}$$

Remark: As shown in Figure 4.3, the term $k^* sat\left(\frac{s}{\varepsilon}\right)$ is continuous for $s \in [-\infty, +\infty]$. The smaller ε is chosen, the higher control accuracy may result in. However, if ε is chosen too small, the slope of the linear function in the region $s \in [-\varepsilon, +\varepsilon]$ would be so large that the adaptive controller has a "jumping" effect, and it would cause undesirable high frequency chatter phenomena while stabilizing the system. So, ε should be properly chosen to ensure the control performance requirements and to avoid the undesirable chatter phenomena.

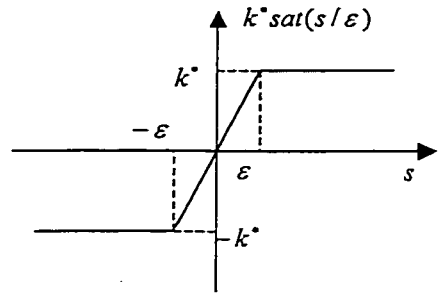

Figure 4.3 Relationship between $k^* sat\left(\frac{s}{\varepsilon}\right)$ and s

The stability of the closed-loop system described by (4.14) and (4.19)–(4.23) is established in the following theorem.

Theorem: For the system model (4.14), the robust adaptive controller specified by equations (4.19) – (4.23) ensures that all the closed loop signals are bounded; moreover, the state x will converge to $\Omega_\varepsilon = \{x(t) \,||\, x| \leq \lambda^{-1}\varepsilon\}$ for $\forall t \geq t_0$.

Proof: To establish the global boundedness, a Lyapunov function candidate is defined as follows,

$$V(t) = \frac{1}{2}\left[\frac{1}{b}s_\varepsilon^2(t) + (\hat{\theta} - \theta)^2 + (\hat{\xi} - \xi)^2 + (\hat{\varsigma} - \varsigma)^2\right] \tag{4.24}$$

Since the discontinuity at $|s| = \varepsilon$ is of the first kind and since $s_\varepsilon = 0$ when $|s| \leq \varepsilon$, it follows that the derivative $\dot{V}$ exists for all s, and given by

$$\dot{V}(t) = 0 \text{ when } |s| \leq \varepsilon$$

When $|s| > \varepsilon$, notice the fact that $s_\varepsilon \dot{s}_\varepsilon = s_\varepsilon \dot{s}$, and differentiating $V(t)$ with respect to time yields

$$\dot{V}(t) = \frac{1}{b}s_\varepsilon \dot{s} + (\hat{\theta} - \theta)\dot{\hat{\theta}} + (\hat{\xi} - \xi)\dot{\hat{\xi}} + (\hat{\varsigma} - \varsigma)\dot{\hat{\varsigma}}$$

$$= s_\varepsilon u + \frac{1}{b}s_\varepsilon\left[(\lambda + a_1)\dot{x} + a_2 x + a_3 x(t-\tau) + g(x, x_\tau)\right]$$
$$+ (\hat{\theta} - \theta)\dot{\hat{\theta}} + (\hat{\xi} - \xi)\dot{\hat{\xi}} + (\hat{\varsigma} - \varsigma)\dot{\hat{\varsigma}}$$

$$= -k_d s_\varepsilon s + s_\varepsilon\left[-\hat{\theta}\dot{x} - \hat{\xi}x - \hat{\varsigma}x(t-\tau) - k^* sat(\frac{s}{\varepsilon})\right]$$
$$+ s_\varepsilon\left[\theta\dot{x} + \xi x + \varsigma x(t-\tau) + \frac{1}{b}g(x, x_\tau)\right]$$
$$+ (\hat{\theta} - \theta)\dot{\hat{\theta}} + (\hat{\xi} - \xi)\dot{\hat{\xi}} + (\hat{\varsigma} - \varsigma)\dot{\hat{\varsigma}}$$

From the fact that $|s| > \varepsilon$, it is easy to see $|s| > |s_\varepsilon|$, so one has,

$$\dot{V}(t) \le -k_d s_\varepsilon^2 + s_\varepsilon\left[-\hat{\theta}\dot{x} - \hat{\xi}x - \hat{\varsigma}x(t-\tau) - k^* sat(\frac{s}{\varepsilon})\right]$$
$$+ s_\varepsilon\left[\theta\dot{x} + \xi x + \varsigma x(t-\tau) + \frac{1}{b}g(x, x_\tau)\right] + (\hat{\theta} - \theta)\dot{\hat{\theta}} + (\hat{\xi} - \xi)\dot{\hat{\xi}} + (\hat{\varsigma} - \varsigma)\dot{\hat{\varsigma}}$$

By using adaptive laws (4.19) – (4.23) and noticing that $(\hat{\theta} - \theta) \cdot proj(\hat{\theta}, s_\varepsilon \dot{x}) \le (\hat{\theta} - \theta) \cdot s_\varepsilon \dot{x}$ and $(\hat{\xi} - \xi) \cdot proj(\hat{\xi}, s_\varepsilon x) \le (\hat{\xi} - \xi) \cdot s_\varepsilon x$, $(\hat{\varsigma} - \varsigma) proj(\hat{\varsigma}, s_\varepsilon x(t-\tau)) \le (\hat{\varsigma} - \varsigma) s_\varepsilon x(t-\tau)$, the above inequality becomes,

$$\dot{V}(t) \le -k_d s_\varepsilon^2 + s_\varepsilon\left[-\hat{\theta}\dot{x} - \hat{\xi}x - \hat{\varsigma}x(t-\tau) - k^* sat(\frac{s}{\varepsilon})\right]$$
$$+ s_\varepsilon\left[\theta\dot{x} + \xi x + \varsigma x(t-\tau) + \frac{1}{b}g(x, x_\tau)\right]$$
$$+ (\hat{\theta} - \theta)s_\varepsilon\dot{x} + (\hat{\xi} - \xi)s_\varepsilon x + (\hat{\varsigma} - \varsigma)s_\varepsilon x(t-\tau)$$

$$\le -k_d s_\varepsilon^2 - k^*|s_\varepsilon| + s_\varepsilon \frac{g(x, x_\tau)}{b}$$

$$\le -k_d s_\varepsilon^2 - k^*|s_\varepsilon| + \frac{\sigma}{b_{\min}}|s_\varepsilon|$$

$$\le -k_d s_\varepsilon^2$$

Therefore, all signals in the system are bounded. Since $s(t)$ is uniformly bounded, by the standard filter theory and the definition of $s(t)$ in (4.16), it can be shown that both $x(t)$ and $\dot{x}(t)$ are also uniformly ultimately bounded. To complete the proof and establish

asymptotic convergence of $x(t)$, it is necessary to show that $s_\varepsilon(t) \to 0$ as $t \to \infty$. This can be accomplished by applying Barbalat's Lemma to the continuous, nonnegative function:

$$V_1(t) = V(t) - \int_0^t \left(\dot{V}(\tau) + k_d s_\varepsilon^2(\tau)\right) d\tau \text{ with } \dot{V}_1(t) = -k_d s_\varepsilon^2(t) \tag{4.25}$$

It can easily be shown that every term on the right side of (4.17) is bounded, hence $\dot{s}(t)$ is bounded. This implies $\dot{V}_1(t)$ is a uniformly continuous function of time. Since $V_1(t)$ is bounded below by 0, and $\dot{V}_1(t) \le 0$ for all t, use of Barbalat's lemma proves that $\dot{V}_1(t) \to 0$ as $t \to \infty$ and hence from (4.25) that $s_\varepsilon(t) \to 0$ as $t \to \infty$. Remark for equation (4.16) indicates that $x(t) \to \Omega_\varepsilon$ as $t \to \infty$. This completes the proof. ■

Remark: The above theorem proves the convergence of $x(t)$, that is, the chatter effect will be significantly suppressed in metal cutting with the proposed adaptive controller.

4.2.2 Adaptive Controller for Backlash Hysteresis Model

As known in the cutting force modeling part, the backlash hysteresis model with uncertainties is introduced in place of the actual hysteresis model for the sake of controller design. In this case, the turning cutting system can be described as,

$$m\ddot{x} + c\dot{x} + kx = F_\Delta - k_a u \tag{4.26}$$

with F_Δ in the description of (4.5).

Before the controller design, the following assumptions are required,

(A4.3) Time delay τ remains constant during the cutting process;

(A4.4) m, c, k, k_a, h, h_a and B are bounded variables with

$$m \in [m_{\min}, m_{\max}],\ c \in [c_{\min}, c_{\max}],\ k \in [k_{\min}, k_{\max}],\ k_a \in [k_{a\min}, k_{a\max}],\ h \in [h_{\min}, h_{\max}],$$

$$B=B_0+\Delta B \text{ with } \Delta B<\rho_B$$

where $m_{\min}$, $m_{\max}$, $c_{\min}$, $c_{\max}$, $k_{\min}$, $k_{\max}$, $k_{a\min}$, $k_{a\max}$, $h_{\min}$, $h_{\max}$, B_0 and ρ_B are known constants.

In order for the chatter suppression, a robust adaptive controller is proposed for the regulation of $x(t)$. Divided by m on both sides of (4.26) and with some manipulations, we have the following second order function with nonlinearity,

$$\ddot{x} = -\frac{c}{m}\dot{x} - \frac{k}{m}x + \frac{F_\Delta}{m} - \frac{k_a \cdot u}{m} \tag{4.27}$$

A filtered tracking error is defined as

$$s(t) = \dot{x} + \lambda x \text{ with } \lambda > 0, \tag{4.28}$$

Differentiating $s(t)$ with respect to time and substituting $\ddot{x}$ with (4.27), one has,

$$\begin{aligned} \dot{s}(t) &= \ddot{x} + \lambda \dot{x} \\ &= (\lambda - \frac{c}{m})\dot{x} - \frac{k}{m}x + \frac{F_\Delta}{m} - \frac{k_a u}{m} - \frac{k_a f_a(u)}{m} \end{aligned} \tag{4.29}$$

Define

$$\theta_1 = \frac{m}{k_a}(\lambda - \frac{c}{m}),\ \theta_2 = \frac{h-k}{k_a},\ \theta_3 = -\frac{\mu h}{k_a},\ \theta_4 = \begin{cases} \frac{B}{k_a} & \dot{v} > 0 \\ -\frac{B}{k_a} & \dot{v} < 0 \end{cases} \tag{4.30}$$

Due to the boundedness of m, c, k, k_a, h, we have $\theta_i \in [\theta_{i\min}, \theta_{i\max}]$, i=1,2,3,4, where $\theta_{i\min}, \theta_{i\max} \in R$ are constants, and they can be easily obtained with the bounds provided in assumption (A4.4).

In order to avoid undesirable high frequency chatter phenomena caused by the designed adaptive controller, in stead of deriving the adaptive law with the filtered error $s(t)$, we introduce a tuning error, s_ε, as follows,

$$s_\varepsilon = s - \varepsilon sat\left(\frac{s}{\varepsilon}\right)$$

where ε is a positive constant subject to the choice of designer and $sat(\cdot)$ is the saturation function.

Given the turning metal cutting system (4.27), the following control and adaptation laws are presented:

$$u(t) = k_d s_\varepsilon + \hat{\theta}_1 \dot{x} + \hat{\theta}_2 x + \hat{\theta}_3 x + \hat{\theta}_4 x_\tau + k^* sat(\frac{s}{\varepsilon}) \tag{4.31}$$

with

$$\dot{\hat{\theta}}_i = proj\left(\hat{\theta}_i, g_i\right) \tag{4.32}$$

where

$$k^* = \frac{\rho_B}{k_{a\min}} \tag{4.33}$$

and g_i are defined in the following. $proj(\cdot,\cdot)$ is a projection operator, which are constructed as follows:

$$proj\left(\hat{\theta}_i, g_i\right) = \begin{cases} 0 & \text{if } \hat{\theta}_i = \theta_{i\max} \text{ and } g_i > 0 \\ & \text{or } \hat{\theta}_i = \theta_{i\min} \text{ and } g_i < 0 \\ g_i & \text{if } \theta_{i\min} < \hat{\theta}_i < \theta_{i\max} \\ & \text{or } \hat{\theta}_i = \theta_{i\max} \text{ and } g_i \le 0 \\ & \text{or } \hat{\theta}_i = \theta_{i\min} \text{ and } g_i \ge 0 \end{cases} \tag{4.34}$$

The different θ_i and g_i $(i = 1,2,3,4)$ are defined respectively as follows,

$$proj\left(\hat{\theta}_1, s_\varepsilon \dot{x}\right) = \begin{cases} 0 & \text{if } \hat{\theta}_1 = \theta_{1\max} \text{ and } s_\varepsilon \dot{x} > 0 \\ & \text{or } \hat{\theta}_1 = \theta_{1\min} \text{ and } s_\varepsilon \dot{x} < 0 \\ s_\varepsilon \dot{x} & \text{if } \theta_{1\min} < \hat{\theta}_1 < \theta_{1\max} \\ & \text{or } \hat{\theta}_1 = \theta_{1\max} \text{ and } s_\varepsilon \dot{x} \le 0 \\ & \text{or } \hat{\theta}_1 = \theta_{1\min} \text{ and } s_\varepsilon \dot{x} \ge 0 \end{cases} \tag{4.35}$$

$$proj\left(\hat{\theta}_2, s_\varepsilon x\right) = \begin{cases} 0 & \text{if } \hat{\theta}_2 = \theta_{2\max} \text{ and } s_\varepsilon x > 0 \\ & \text{or } \hat{\theta}_2 = \theta_{2\min} \text{ and } s_\varepsilon x < 0 \\ s_\varepsilon x & \text{if } \theta_{2\min} < \hat{\theta}_2 < \theta_{2\max} \\ & \text{or } \hat{\theta}_2 = \theta_{2\max} \text{ and } s_\varepsilon x \le 0 \\ & \text{or } \hat{\theta}_2 = \theta_{2\min} \text{ and } s_\varepsilon x \ge 0 \end{cases} \tag{4.36}$$

$$proj\left(\hat{\theta}_3, s_\varepsilon x_r\right) = \begin{cases} 0 & \text{if } \hat{\theta}_3 = \theta_{3\max} \text{ and } s_\varepsilon x_r > 0 \\ & \text{or } \hat{\theta}_3 = \theta_{3\min} \text{ and } s_\varepsilon x_r < 0 \\ s_\varepsilon x_r & \text{if } \theta_{3\min} < \hat{\theta}_3 < \theta_{3\max} \\ & \text{or } \hat{\theta}_3 = \theta_{3\max} \text{ and } s_\varepsilon x_r \le 0 \\ & \text{or } \hat{\theta}_3 = \theta_{3\min} \text{ and } s_\varepsilon x_r \ge 0 \end{cases} \tag{4.37}$$

$$proj\left(\hat{\theta}_4, s_\varepsilon\right) = \begin{cases} 0 & \text{if } \hat{\theta}_4 = \theta_{4\max} \text{ and } s_\varepsilon > 0 \\ & \text{or } \hat{\theta}_4 = \theta_{4\min} \text{ and } s_\varepsilon < 0 \\ s_\varepsilon & \text{if } \theta_{4\min} < \hat{\theta}_4 < \theta_{4\max} \\ & \text{or } \hat{\theta}_4 = \theta_{4\max} \text{ and } s_\varepsilon \le 0 \\ & \text{or } \hat{\theta}_4 = \theta_{4\min} \text{ and } s_\varepsilon \ge 0 \end{cases} \tag{4.38}$$

The stability of the closed-loop system described by (4.26) and (4.31)-(4.38) is established in the following theorem.

Theorem: For the system model (4.26), the robust adaptive controller specified by equations (4.31) – (4.38) ensures that all the closed loop signals are bounded; moreover, the state x will converge to $\Omega_\varepsilon = \{x(t) \,||\, x| \le \lambda^{-1}\varepsilon\}$ within a time constant $1/\lambda$.

Proof: To establish the global boundedness, a Lyapunov function candidate is defined as follows,

$$V(t)=\frac{1}{2}\left[\frac{m}{k_a h_a}s_\varepsilon^2(t)+(\hat{\theta}_1-\theta_1)^2+(\hat{\theta}_2-\theta_2)^2+(\hat{\theta}_3-\theta_3)^2+(\hat{\theta}_4-\theta_4)^2\right] \quad (4.39)$$

Since the discontinuity at $|s|=\varepsilon$ is of the first kind and since $s_\varepsilon=0$ when $|s|\le\varepsilon$, it follows that the derivative $\dot{V}$ exists for all s, and given by

$$\dot{V}(t)=0 \text{ when } |s|\le\varepsilon$$

When $|s|>\varepsilon$, notice the fact that $s_\varepsilon\dot{s}_\varepsilon=s_\varepsilon\dot{s}$, and differentiating $V(t)$ with respect to time yields

$$\begin{aligned}\dot{V}(t)&=\frac{m}{k_a h_a}s_\varepsilon\dot{s}+(\hat{\theta}_1-\theta_1)\dot{\hat{\theta}}_1+(\hat{\theta}_2-\theta_2)\dot{\hat{\theta}}_2+(\hat{\theta}_3-\theta_3)\dot{\hat{\theta}}_3+(\hat{\theta}_4-\theta_4)\dot{\hat{\theta}}_4\\&=\frac{m}{k_a h_a}s_\varepsilon\left((\lambda-\frac{c}{m})\dot{x}-\frac{k}{m}x+\frac{F_\Delta}{m}-\frac{k_a\cdot u}{m}\right)\\&\quad+(\hat{\theta}_1-\theta_1)\dot{\hat{\theta}}_1+(\hat{\theta}_2-\theta_2)\dot{\hat{\theta}}_2+(\hat{\theta}_3-\theta_3)\dot{\hat{\theta}}_3+(\hat{\theta}_4-\theta_4)\dot{\hat{\theta}}_4 \quad (4.40)\end{aligned}$$

In the following, the proof is constructed with the two conditions (i) $\dot{v}(t)>0$ and (ii) $\dot{v}(t)<0$;

(i) When $\dot{v}(t)>0$, by substituting $F_\Delta=hv+B$, one has,

$$\begin{aligned}\dot{V}(t)&=\frac{m}{k_a h_a}s_\varepsilon\left((\lambda-\frac{c}{m})\dot{x}-\frac{k}{m}x+\frac{h(x-\mu x_\tau)+B}{m}-\frac{k_a\cdot u}{m}\right)\\&\quad+(\hat{\theta}_1-\theta_1)\dot{\hat{\theta}}_1+(\hat{\theta}_2-\theta_2)\dot{\hat{\theta}}_2+(\hat{\theta}_3-\theta_3)\dot{\hat{\theta}}_3+(\hat{\theta}_4-\theta_4)\dot{\hat{\theta}}_4\end{aligned}$$

Noting that $B=B_0+\Delta B$,

$$\dot{V}(t)=\frac{m}{k_a}s_\varepsilon\left((\lambda-\frac{c}{m})\dot{x}+\frac{h-k}{m}x+\frac{-\mu h}{m}x_\tau+\frac{B_0}{m}+\frac{\Delta B}{m}\right)-s_\varepsilon u$$

$$+(\hat{\theta}_1-\theta_1)\dot{\hat{\theta}}_1+(\hat{\theta}_2-\theta_2)\dot{\hat{\theta}}_2+(\hat{\theta}_3-\theta_3)\dot{\hat{\theta}}_3+(\hat{\theta}_4-\theta_4)\dot{\hat{\theta}}_4$$

$$=\theta_1 s_\varepsilon \dot{x}+\theta_2 s_\varepsilon x+\theta_3 s_\varepsilon x_r+\theta_4 s_\varepsilon+\frac{\Delta B}{k_a}s_\varepsilon-s_\varepsilon u$$

$$+(\hat{\theta}_1-\theta_1)\dot{\hat{\theta}}_1+(\hat{\theta}_2-\theta_2)\dot{\hat{\theta}}_2+(\hat{\theta}_3-\theta_3)\dot{\hat{\theta}}_3+(\hat{\theta}_4-\theta_4)\dot{\hat{\theta}}_4$$

And using the property $(\hat{\theta}_i-\theta_i)proj(\hat{\theta}_i,g_i)\le(\hat{\theta}_i-\theta_i)\cdot g_i$, we have,

$$\dot{V}(t)\le\theta_1 s_\varepsilon \dot{x}+\theta_2 s_\varepsilon x+\theta_3 s_\varepsilon x_r+\theta_4 s_\varepsilon+\frac{\Delta B}{k_a}s_\varepsilon-s_\varepsilon u$$

$$+(\hat{\theta}_1-\theta_1)s_\varepsilon\dot{x}+(\hat{\theta}_2-\theta_2)s_\varepsilon x+(\hat{\theta}_3-\theta_3)s_\varepsilon x_r+(\hat{\theta}_4-\theta_4)s_\varepsilon$$

$$=\hat{\theta}_1 s_\varepsilon \dot{x}+\hat{\theta}_2 s_\varepsilon x+\hat{\theta}_3 s_\varepsilon x_r+\hat{\theta}_4 s_\varepsilon+\frac{\Delta B}{k_a}s_\varepsilon-s_\varepsilon u$$

Using the adaptive law, one obtains,

$$\dot{V}(t)\le-k_d s_\varepsilon s-k^* s_\varepsilon sat(\frac{s}{\varepsilon})+\frac{\rho_B}{k_{a\min}}|s_\varepsilon|$$

$$=-k_d s_\varepsilon^2-k^*|s_\varepsilon|+\frac{\rho_B}{k_{a\min}}|s_\varepsilon|$$

$$\le-k_d s^2 \qquad (4.41)$$

(ii) When $\dot{v}<0$, by substituting $F_\Delta=hv-B$, and following the same procedure, it is clear that by using the control law (4.31),

$$\dot{V}(t)\le-k_d s^2 \qquad (4.42)$$

Therefore, for all the conditions, $\dot{V}(t)\le-k_d s_\varepsilon^2$, and all signals in the system are bounded. Since $s(t)$ is uniformly bounded, by the standard filter theory and the definition of $s(t)$ in (4.28), it can be shown that both $x(t)$ and $\dot{x}(t)$ are also uniformly ultimately bounded. To complete the proof and establish asymptotic convergence of $x(t)$, it is necessary to

show that $s(t) \to 0$ as $t \to \infty$. This can be accomplished by applying Barbalat's Lemma to the continuous, nonnegative function:

$$V_1(t) = V(t) - \int_0^t \left(\dot{V}(\tau) + k_d s_\varepsilon^2(\tau)\right) d\tau \text{ with } \dot{V}_1(t) = -k_d s_\varepsilon^2(t) \tag{4.43}$$

It can easily be shown that every term on the right side of (4.43) is bounded, hence $\dot{s}(t)$ is bounded. This implies $\dot{V}_1(t)$ is a uniformly continuous function of time. Since $V_1(t)$ is bounded below by 0, and $\dot{V}_1(t) \le 0$ for all t, use of Barbalat's lemma proves that $\dot{V}_1(t) \to 0$ as $t \to \infty$ and hence from (4.43) that $s(t) \to 0$ as $t \to \infty$. Remark for equation (4.28) indicates that $x(t) \to \Omega_\varepsilon$ as $t \to \infty$. This completes the proof. ■

Remark: The above theorem proves the convergence of $x(t)$, that is, the chatter effect will be significantly suppressed in metal cutting with the proposed adaptive controller.

4.3 Simulation Results

For controller 1 with backlash-like hysteresis description, parameters of the backlash-like hysteresis model are taken as, $\alpha = 1$, $h = 4500$, and $B_1 = 200$. Using the input signal $v(t) = 0.02\sin(t)$, the backlash-like hysteresis for the cutting system can be illustrated as in the Figure 4.4.

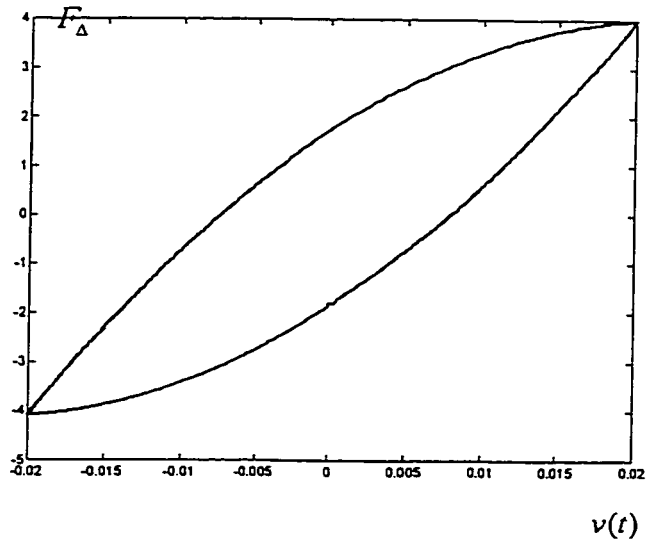

Figure 4.4 Backlash-like hysteresis of metal cutting system

To illustrate the preceding results, we consider the turning system (4.4) with the following parameters. For the turning cutting system, take $m = 50kg$ with $m_{\min} = 25kg$ and $m_{\max} = 100kg$, $c = 1$ with $c_{\min} = 0.5$ and $c_{\max} = 5$, $k = 7\times10^6$ N/m with $k_{\min} = 6\times10^6$ N/m and $k_{\max} = 8\times10^6$ N/m, and $\mu = 1$. For the piezo actuator, $k_a = 5\times10^7$ N/m with $k_{a\min} = 4.5\times10^7$ N/m and $k_{a\max} = 5.5\times10^7$ N/m. And from Figure 4.4, we take $\rho = 5$.

The simulation in Figure 4.5 shows that the turning cutting system without control is in chattering condition due to the small damping coefficient and the presence of hysteresis.

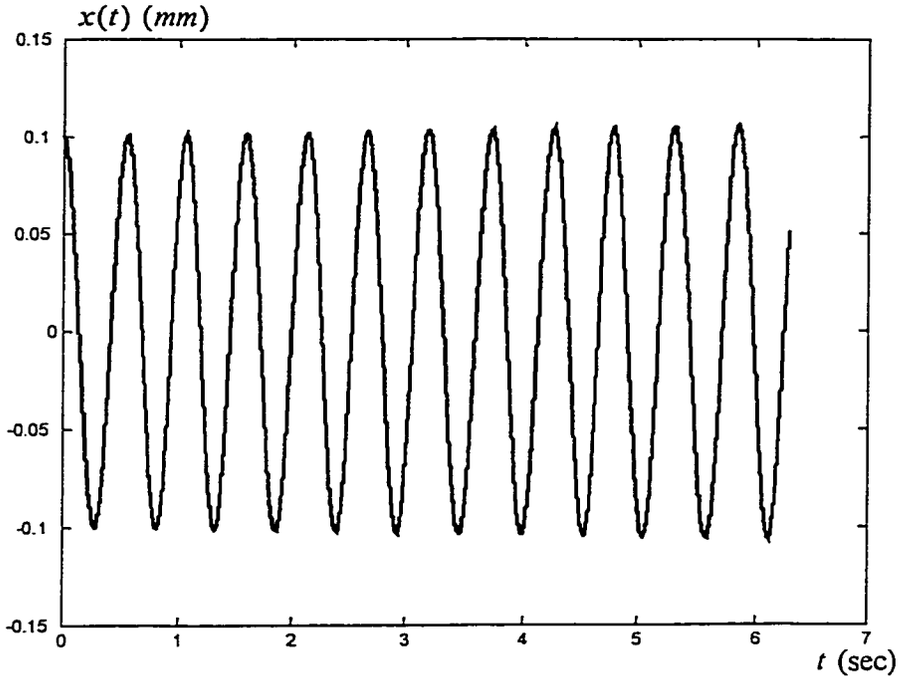

Figure 4.5 Turning system without control (chattering)

In order to eliminate the chatter in the turning cutting, the adaptive controller (4.19)–(4.23) is introduced into the system.

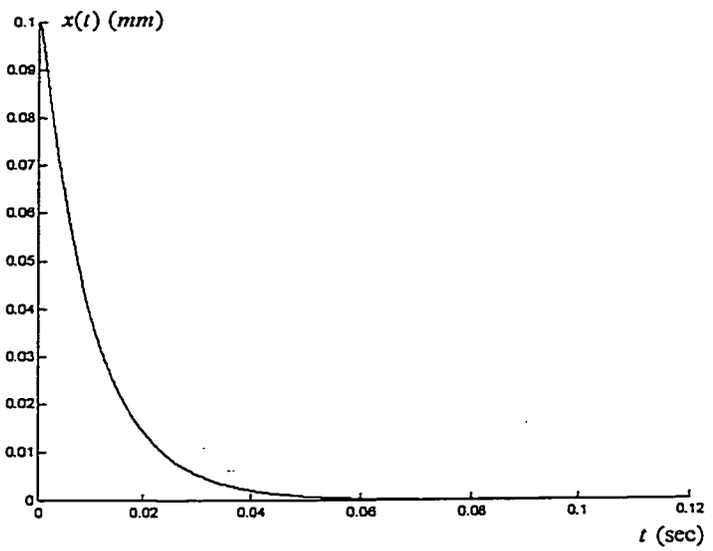

Figure 4.6 Turning system with proposed adaptive controller

In metal cutting, as what we concern about most is the offset chip thickness $x(t)$, we should choose proper λ of the tracking error $s(t)$ so that $x(t)$ is much more "sensitive" to the adaptive control than $\dot{x}(t)$. $\lambda = 100$ is considered in the tracking error equation. And the simulation of the turning system with the adaptive controller is shown in Fig.8, which shows clearly that the proposed adaptive controller results in suppression of chatter.

For controller 2 with backlash hysteresis description, we have the following typical experimental data for turning metal cutting system [Liu et al (1998)]. The equivalent mass, damping coefficient and spring coefficient are respectively, m = 15 kg, $c = 3 \times 10^3$ kg/s, $k = 6 \times 10^7$ kg/s^2. And we can have a reasonable range for these system coefficients as, $m \in [10, 20]$ kg, $c \in [2, 4] \times 10^3$ kg/s, $k \in [5, 7] \times 10^7$ kg/s^2.

For the hysteresis model for cutting force, we take the following from the experimental data of Szakovits and D'Souza (1976),

$$h = 4 \times 10^6 \text{ N/m and } B = 20 \text{ N}$$

with $h \in [3, 5] \times 10^6$ N/m and $B \in [10, 30]$ N.

For the piezoactuator, the spring coefficient is considered to be k_a=7 $\times$ 10^7 N/m [Cuttino et al (1999)]. In this chapter, the piezoactuator is considered to display linear property. Thus the piezoactuator displacement is taken as the control input for convenience.

The simulation in Figure 4.7 illustrates the turning cutting system with initial tool deflection 10 μm, and it is in chattering condition in the presence of active hysteresis.

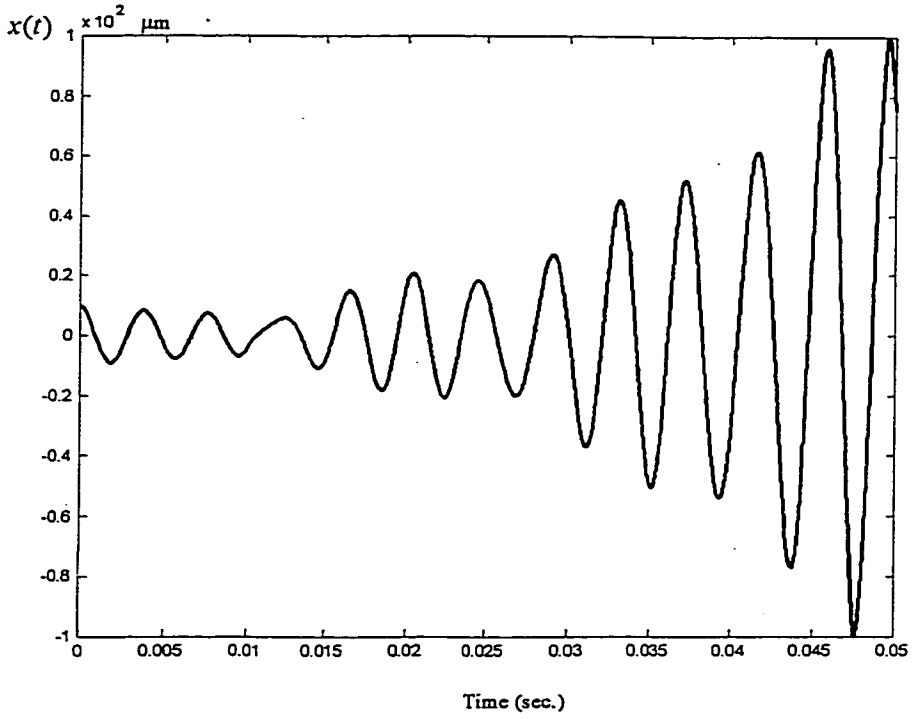

Figure 4.7 Turning cutting system without control (chattering)

It can be seen that chatter is growing as time is going on. Theoretically, chatter can grow as the metal cutting system stays in the oscillating state, however, it is indicated that chatter can not grow infinitely due to the multi-regenerative effect [Tlusty and Ismail (1981)], which is not discussed in the controller design.

It is easy to obtain $\theta_{1\min} = -8\times10^{-5}$, $\theta_{1\max} = -3\times10^{-5}$, $\theta_{2\min} = -1$, $\theta_{2\max} = 1$, $\theta_{3\min} = -1$, $\theta_{3\max} = 0$, $\theta_{4\min} - 5\times10^{-6}$, $\theta_{4\max} = 5\times10^{-6}$. And we are taking the initial data as, $\theta_1 = -5\times10^{-5}$, $\theta_2 = 0.2$, $\theta_3 = -0.3$, $\theta_4 = 1\times10^{-6}$, $k_d = 1\times10^{-6}$, and $k^* = 5\times10^{-6}$.

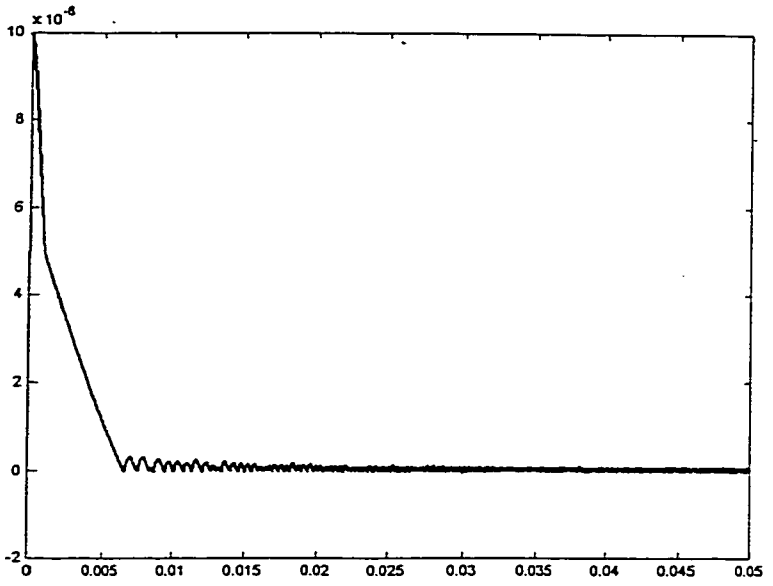

Figure 4.8 Turning cutting system with proposed adaptive controller

And the piezoactuator displacement is illustrated in the following figure 4.9.

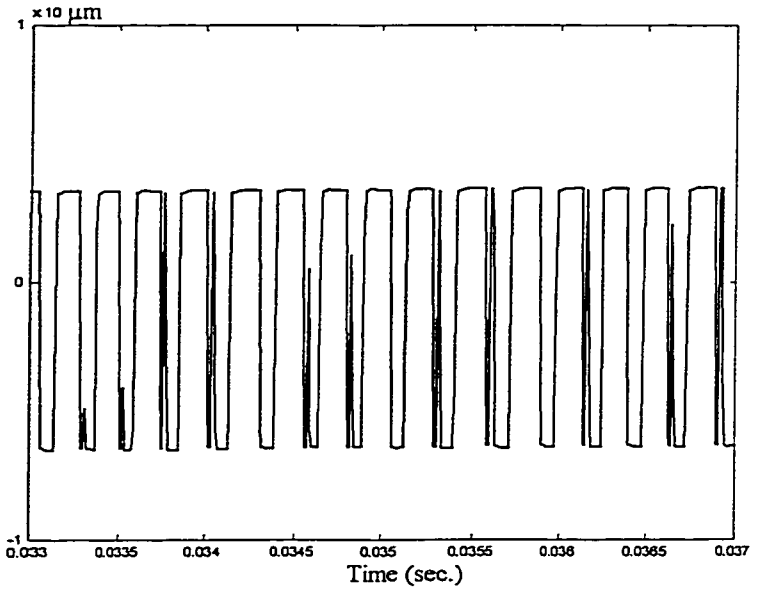

Figure 4.9 Controlled displacement of piezoactuator

In this case, $\lambda = 100$ is chosen in the tracking error equation. And the simulation of the turning system with the adaptive controller is shown in Figure 4.8, which shows clearly that the proposed adaptive controller results in suppression of chatter.

4.4 Summary

In this chapter, in order for chatter suppression, a piezoactuator is introduced for the regulation of the machine tool displacement and metal cutting system is modeled as a class of uncertain linear system with hysteresis and time delay. In order to overcome the chatter due to the hysteresis and time delay during the cutting process, an adaptive controller for the metal cutting system of ultra-precision is presented. The simulation results show that the proposed adaptive controller significantly eliminates the chatter phenomena.

Chapter 5

Chatter Suppression via Nonlinear Piezo-actuation

Adaptive Controller Design – 2

Introduction – In this chapter, in order for chatter suppression, a piezoactuator with hysteretic relationship is introduced for the regulation of the machine tool displacement. The metal cutting system is modeled as a class of uncertain linear system with hysteresis and time delay and the piezoactuator exhibits nonlinear hysteretic actuation. In order to overcome the chatter due to the hysteresis and time delay during the cutting process, an adaptive controller for the metal cutting system of ultra-precision is presented. The simulation results show that the proposed adaptive controller significantly eliminates the chatter phenomena.

5.1 Turning System Model with Hysteresis

In Liu et al (1998), considering the piezo-actuated tool holder assemble as a lumped mass system, the structural system may be represented by a dynamic model of turning process as illustrated in the following,

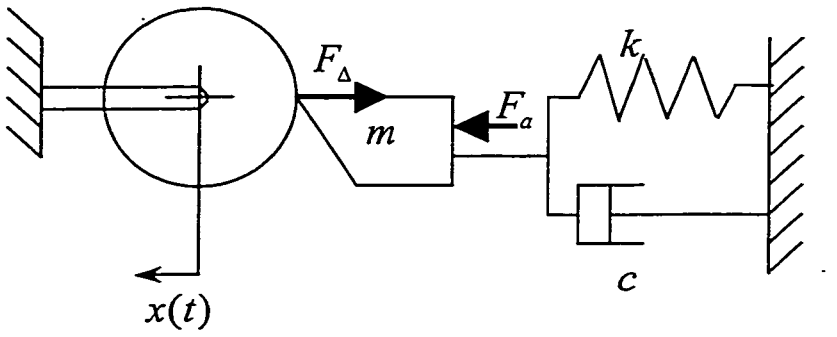

Figure 5.1 Dynamic model of turning process

In Figure 5.1, the equivalent mass of the cutting system is m, the stiffness is k, and the damping coefficient of the system is c. F_a represents the force generated by the piezoactuator due to the high speed expansion. And the cutting system can be described as,

$$m\ddot{x} + c\dot{x} + kx = F_\Delta - F_a \tag{5.1}$$

with $F_a = F_a(u)$ as the description of the generated force on the cutting tool and the voltage applied on the piezoactuator.

As known in the cutting force modeling part, the backlash hysteresis model with uncertainty for the relationship of cutting force and uncut chip thickness is introduced in place of the actual hysteresis model for the sake of controller design.

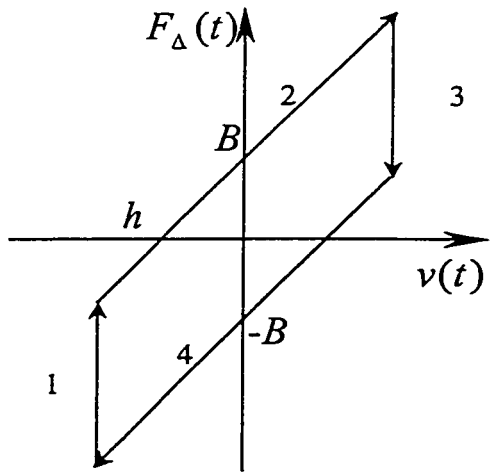

Figure 5.2 Backlash hysteresis model

In Figure 5.2, the line segments 1 and 3, 2 and 4 are parallel, and the hysteresis model of cutting force – chip thickness can be described in terms of h and B.

$$F_\Delta(t) = H(v(t)) = H(h,B) = \begin{cases} h \cdot v(t) + B, & \dot{v}(t) > 0 \\ h \cdot v(t) - B, & \dot{v}(t) < 0 \\ F_\Delta(t_-) & \dot{v}(t) = 0 \end{cases} \tag{5.2}$$

where h is the slope of the hysteresis lines and $B > 0$ is the backlash distance. The hysteresis in cutting force can approximately described as Figure 5.2 because of its resemblance in profile with the various experimental data and figures in [Fabris and D'souza (1974)][Szakovits and D'souza (1976)].

Force F_a generated by piezoactuator serves as the force provided by the active vibration control. To find out the description of F_a, we should first find out the relationship between the stimulated piezo expansion and the voltage applied to the piezoactuator,

which demonstrates the nonlinear close-loop characteristic of hysteresis [Cuttino et al (1999)][Fripp and Hagood (1995)] as shown in Figure 5.3.

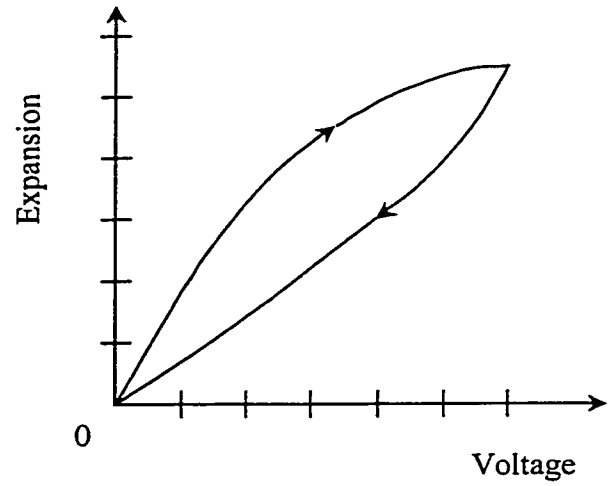

Figure 5.3 Hysteresis curves of a piezoactuator

Figure 5.3 is a typical relationship graph of expansion – voltage for piezoactuator. As can be seen, the expansion of a piezoactuator is not exactly proportional to the electric field strength. How much a piezoactuator expands at a given voltage depends on whether the voltage is increasing or decreasing, demonstrating closed loop hysteresis. And the hysteresis relationship can be described as,

$$\Delta L = H_a(u) \tag{5.3}$$

where u denotes the applied voltage, and ΔL denotes the expansion of the piezoactuator. $H_a(\cdot)$ denotes the hysteresis function for the relationship of piezoactuator expansion via applied voltage. It should be noted that the piezoactuator can generate force depending on its stiffness and its expansion capacity.

$$F_a = k_a \Delta L = k_a H_a(u) \tag{5.4}$$

Hysteresis is known to be non-differentiable and severely limits the performance of the system by causing undesirable chatter. Moreover, the hysteresis behaviour demonstrated in the actuator signals makes it impossible to achieve a high accuracy positioning. Most of the hysteresis models proposed [see, for example, Macki, et al (1993)] are very complicated and it is still unavailable for designing the control scheme with a general type of hysteresis.

For the sake of controller design, a continuous time dynamic backlash-like hysteresis [Su, et al(2000)] as described in Chapter 4 is employed to describe the hysteresis demonstrated in the relationship of force-expansion of piezoactuator,

$$\frac{dH_a(z)}{dt} = \alpha\left|\frac{dz}{dt}\right|\left(h_a z - H_a(z)\right) + B_a\frac{dz}{dt} \tag{5.5}$$

where α, h_a and B_a are constants, satisfying $h_a > B_a$.

As shown in [Su, et al(2000)], the solution of the backlash-like hysteresis (5.5) consists of a linear function and a bounded nonlinearity,

$$H_a(u) = h_a u + f(u) \tag{5.6}$$

with a uniform bound ρ such that

$$\|f(u)\| \le \rho_a \tag{5.7}$$

Thus, the expansion of the piezoactuator due to the applied voltage is $h_a \cdot u + f_a(u)$, with h_a denoting the slope of the backlash-like hysteresis, and $\|f_a(u)\| \le \rho_a$, ρ_a is a constant bound.

In this case, the force-expansion relationship $F_a(u)$ can be described as,

$$F_a(u) = k_a\left(h_a \cdot u + f_a(u)\right) \tag{5.8}$$

where k_a is the stiffness of the piezoactuator. Therefore, in order for controller design, the metal cutting system (5.1) can be simplified as,

$$m\ddot{x} + c\dot{x} + kx = F_\Delta - k_a\left(h_a \cdot u + f_a(u)\right) \tag{5.9}$$

with F_Δ in the description of (5.2).

And the block diagram illustrating the control system is as follows, where $G(s) = 1/(ms^2 + cs + k)$.

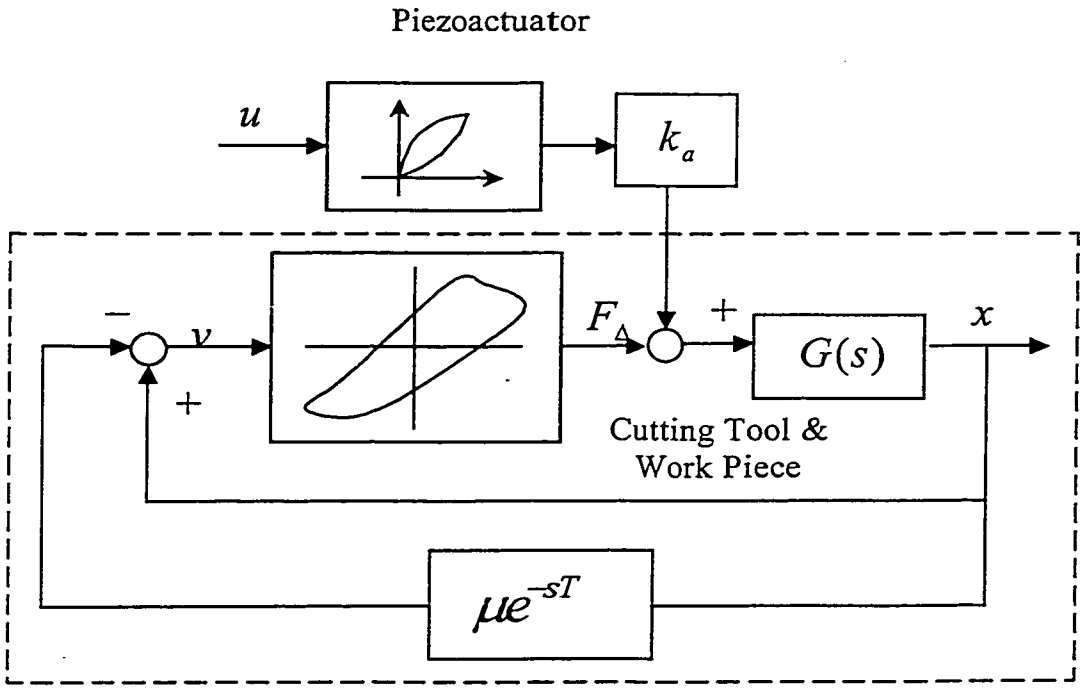

Figure 5.4 Block diagram of turning metal cutting system with piezoactuator

Remark: The cutting system model illustrated in Figure6 is a complicated nonlinear system involving hysteresis, which can lead to instability in closed-looped operation and complicates the task of controller design and analysis [Gorbet et al (2001)].

Focusing on the above model, in the following, a robust adaptive control scheme for control input $u(t)$ will be designed to suppress the chatter effect.

5.2 Adaptive Controller Design

As indicated in Figure 5.4, the metal cutting system displays hysteretic nonlinearities. However, hysteresis is known to be non-differentiable and severely limits the performance of the system by causing undesirable chatter. Moreover, the hysteresis behaviour demonstrated in the actuator signals makes it impossible to achieve a high accuracy positioning.

Before the controller design, the following assumptions are required,

(A5.1) Time delay τ remains constant during the cutting process;

(A5.2) $m, c, k, k_a, h,\ h_a$ are bounded variables with

$$m \in [m_{\min}, m_{\max}],\ c \in [c_{\min}, c_{\max}],\ k \in [k_{\min}, k_{\max}],$$

$$k_a \in [k_{a\min}, k_{a\max}],\ h \in [h_{\min}, h_{\max}],\ h_a \in [h_{a\min}, h_{a\max}]$$

$$B=B_0+\Delta B \text{ with } \Delta B<\rho_B$$

where $m_{\min}$, $m_{\max}$, $c_{\min}$, $c_{\max}$, $k_{\min}$, $k_{\max}$, $k_{a\min}$, $k_{a\max}$, $h_{\min}$, $h_{\max}$, $h_{a\min}$, $h_{a\max}$, B_0 and ρ_B are known constants.

Remark: In the researches of chatter occurrence, it is commonly assumed that the rotation speed is constant [Kaneko et al (1984)][Kondo et al (1997)]. Due to the fact that m, c, k, k_a, h, h_a are physical coefficients for the metal cutting system, subjecting to internal changes or external disturbance, it is reasonable to assume that they are bounded variables.

In order for the chatter suppression, a robust adaptive controller is proposed for the regulation of $x(t)$. Divided by m on both sides of (5.9) and with some manipulations, we have the following second order function with nonlinearity,

$$\ddot{x} = -\frac{c}{m}\dot{x} - \frac{k}{m}x + \frac{F_\Delta}{m} - \frac{k_a h_a \cdot u}{m} - \frac{k_a f_a(u)}{m} \tag{5.10}$$

A filtered tracking error is defined as

$$s(t) = \dot{x} + \lambda x \text{ with } \lambda > 0, \tag{5.11}$$

Remark: It has been shown [Slotine and Li] that the definition (5.11) has the following properties: (i) the equation $s(t)$=0 defines a time a hyper-plane on which the state $x(t)$ decays exponentially to zero, (ii) if $x(0)$=0 and $|s(t)| \le \varepsilon$ with constant ε, then

$x(t) \in \Omega_\varepsilon = \{x(t) \,||\, x| \leq \lambda^{-1}\varepsilon\}$ for $\forall t \geq t_0$, and (iii) if $x(0) \neq 0$ and $|s(t)| \leq \varepsilon$, then x(t) will converge to Ω_ε with a time-constant $1/\lambda$.

Differentiating $s(t)$ with respect to time and substituting $\ddot{x}$ with (5.10), one has,

$$\dot{s}(t) = \ddot{x} + \lambda\dot{x}$$

$$= (\lambda - \frac{c}{m})\dot{x} - \frac{k}{m}x + \frac{F_\Delta}{m} - \frac{k_a h_a \cdot u}{m} - \frac{k_a f_a(u)}{m} \tag{5.12}$$

Define

$$\theta_1 = \frac{m}{k_a h_a}(\lambda - \frac{c}{m}),\ \theta_2 = \frac{h-k}{k_a h_a},\ \theta_3 = -\frac{\mu h}{k_a h_a},\ \theta_4 = \begin{cases} \dfrac{B}{k_a h_a} & \dot{v} > 0 \\ -\dfrac{B}{k_a h_a} & \dot{v} < 0 \end{cases} \tag{5.13}$$

Due to the boundedness of m, c, k, k_a, h, we have $\theta_i \in [\theta_{i\min}, \theta_{i\max}]$, i=1,2,3,4, where $\theta_{i\min}, \theta_{i\max} \in R$ are constants, and they can be easily obtained with the bounds provided in assumption (A5.2).

Given the turning metal cutting system (5.10), the following control and adaptation laws are presented:

$$u(t) = k_d s + \hat{\theta}_1\dot{x} + \hat{\theta}_2 x + \hat{\theta}_3 x + \hat{\theta}_4 x_\tau + k^* sign(s) \tag{5.14}$$

with

$$\dot{\hat{\theta}}_i = proj(\hat{\theta}_i, g_i) \tag{5.15}$$

where

$$k^* = \frac{\rho_B + k_{a\max}\rho_a}{k_{a\min}h_{a\min}} \tag{5.16}$$

and g_i are defined in the following. $proj(\cdot,\cdot)$ is a projection operator, which are constructed as follows:

$$proj\left(\hat{\theta}_i, g_i\right) = \begin{cases} 0 & \text{if } \hat{\theta}_i = \theta_{i\max} \text{ and } g_i > 0 \\ & \text{or } \hat{\theta}_i = \theta_{i\min} \text{ and } g_i < 0 \\ g_i & \text{if } \theta_{i\min} < \hat{\theta}_i < \theta_{i\max} \\ & \text{or } \hat{\theta}_i = \theta_{i\max} \text{ and } g_i \le 0 \\ & \text{or } \hat{\theta}_i = \theta_{i\min} \text{ and } g_i \ge 0 \end{cases} \tag{5.17}$$

The different θ_i and g_i $(i = 1,2,3,4)$ are defined respectively as follows,

$$proj\left(\hat{\theta}_1, s\dot{x}\right) = \begin{cases} 0 & \text{if } \hat{\theta}_1 = \theta_{1\max} \text{ and } s\ \dot{x} > 0 \\ & \text{or } \hat{\theta}_1 = \theta_{1\min} \text{ and } s\ \dot{x} < 0 \\ s\dot{x} & \text{if } \theta_{1\min} < \hat{\theta}_1 < \theta_{1\max} \\ & \text{or } \hat{\theta}_1 = \theta_{1\max} \text{ and } s\ \dot{x} \le 0 \\ & \text{or } \hat{\theta}_1 = \theta_{1\min} \text{ and } s\ \dot{x} \ge 0 \end{cases} \tag{5.18}$$

$$proj\left(\hat{\theta}_2, s\ x\right) = \begin{cases} 0 & \text{if } \hat{\theta}_2 = \theta_{2\max} \text{ and } s\ x > 0 \\ & \text{or } \hat{\theta}_2 = \theta_{2\min} \text{ and } s\ x < 0 \\ s\ x & \text{if } \theta_{2\min} < \hat{\theta}_2 < \theta_{2\max} \\ & \text{or } \hat{\theta}_2 = \theta_{2\max} \text{ and } s\ x \le 0 \\ & \text{or } \hat{\theta}_2 = \theta_{2\min} \text{ and } s\ x \ge 0 \end{cases} \tag{5.19}$$

$$proj\left(\hat{\theta}_3, s\ x_r\right) = \begin{cases} 0 & \text{if } \hat{\theta}_3 = \theta_{3\max} \text{ and } s\ x_r > 0 \\ & \text{or } \hat{\theta}_3 = \theta_{3\min} \text{ and } s\ x_r < 0 \\ s\ x_r & \text{if } \theta_{3\min} < \hat{\theta}_3 < \theta_{3\max} \\ & \text{or } \hat{\theta}_3 = \theta_{3\max} \text{ and } s\ x_r \le 0 \\ & \text{or } \hat{\theta}_3 = \theta_{3\min} \text{ and } s\ x_r \ge 0 \end{cases} \tag{5.20}$$

$$proj\left(\hat{\theta}_4, s\ \right) = \begin{cases} 0 & \text{if } \hat{\theta}_4 = \theta_{4\max} \text{ and } s\ > 0 \\ & \text{or } \hat{\theta}_4 = \theta_{4\min} \text{ and } s\ < 0 \\ s & \text{if } \theta_{4\min} < \hat{\theta}_4 < \theta_{4\max} \\ & \text{or } \hat{\theta}_4 = \theta_{4\max} \text{ and } s\ \le 0 \\ & \text{or } \hat{\theta}_4 = \theta_{4\min} \text{ and } s\ \ge 0 \end{cases} \tag{5.21}$$

The stability of the closed-loop system described by (5.9) and (5.14)-(5.21) is established in the following theorem.

Theorem: For the system model (5.9), the robust adaptive controller specified by equations (5.14) – (5.21) ensures that all the closed loop signals are bounded; moreover, the state x will converge to $\Omega_\varepsilon = \{x(t) \,||\, x \,| \le \lambda^{-1}\varepsilon\}$ for $\forall t \ge t_0$.

Proof: To establish the global boundedness, a Lyapunov function candidate is defined as follows,

$$V(t) = \frac{1}{2}\left[\frac{m}{k_a h_a} s^2(t) + (\hat{\theta}_1 - \theta_1)^2 + (\hat{\theta}_2 - \theta_2)^2 + (\hat{\theta}_3 - \theta_3)^2 + (\hat{\theta}_4 - \theta_4)^2\right] \tag{5.22}$$

Differentiating $V(t)$ with respect to time yields

$$\dot{V}(t) = \frac{m}{k_a h_a} s\,\dot{s} + (\hat{\theta}_1 - \theta_1)\dot{\hat{\theta}}_1 + (\hat{\theta}_2 - \theta_2)\dot{\hat{\theta}}_2 + (\hat{\theta}_3 - \theta_3)\dot{\hat{\theta}}_3 + (\hat{\theta}_4 - \theta_4)\dot{\hat{\theta}}_4$$

$$= \frac{m}{k_a h_a} s \left((\lambda - \frac{c}{m})\dot{x} - \frac{k}{m} x + \frac{F_\Delta}{m} - \frac{k_a h_a \cdot u}{m} - \frac{k_a f_a(u)}{m} \right)$$

$$+ (\hat{\theta}_1 - \theta_1)\dot{\hat{\theta}}_1 + (\hat{\theta}_2 - \theta_2)\dot{\hat{\theta}}_2 + (\hat{\theta}_3 - \theta_3)\dot{\hat{\theta}}_3 + (\hat{\theta}_4 - \theta_4)\dot{\hat{\theta}}_4 \qquad (5.23)$$

In the following, the proof is constructed with the two conditions (i) $\dot{v}(t) > 0$ and (ii) $\dot{v} < 0$;

(i) When $\dot{v}(t) > 0$, by substituting $F_\Delta = hv + B$, one has,

$$\dot{V}(t) = \frac{m}{k_a h_a} s \left((\lambda - \frac{c}{m})\dot{x} - \frac{k}{m} x + \frac{h(x - \mu x_\tau) + B}{m} - \frac{k_a h_a \cdot u}{m} - \frac{k_a f_a(u)}{m} \right)$$

$$+ (\hat{\theta}_1 - \theta_1)\dot{\hat{\theta}}_1 + (\hat{\theta}_2 - \theta_2)\dot{\hat{\theta}}_2 + (\hat{\theta}_3 - \theta_3)\dot{\hat{\theta}}_3 + (\hat{\theta}_4 - \theta_4)\dot{\hat{\theta}}_4$$

Noting that $B = B_0 + \Delta B$,

$$\dot{V}(t) = \frac{m}{k_a h_a} s \left((\lambda - \frac{c}{m})\dot{x} + \frac{h - k}{m} x + \frac{-\mu h}{m} x_\tau + \frac{B_0}{m} + \frac{\Delta B}{m} - \frac{k_a f_a(u)}{m} \right) - s\,u$$

$$+ (\hat{\theta}_1 - \theta_1)\dot{\hat{\theta}}_1 + (\hat{\theta}_2 - \theta_2)\dot{\hat{\theta}}_2 + (\hat{\theta}_3 - \theta_3)\dot{\hat{\theta}}_3 + (\hat{\theta}_4 - \theta_4)\dot{\hat{\theta}}_4$$

$$= \theta_1 s\,\dot{x} + \theta_2 s\,x + \theta_3 s\,x_\tau + \theta_4 s + \frac{\Delta B - k_a f_a(u)}{k_a h_a} s - s\,u$$

$$+ (\hat{\theta}_1 - \theta_1)\dot{\hat{\theta}}_1 + (\hat{\theta}_2 - \theta_2)\dot{\hat{\theta}}_2 + (\hat{\theta}_3 - \theta_3)\dot{\hat{\theta}}_3 + (\hat{\theta}_4 - \theta_4)\dot{\hat{\theta}}_4$$

And using the property $(\hat{\theta}_i - \theta_i)proj(\hat{\theta}_i, g_i) \le (\hat{\theta}_i - \theta_i) \cdot g_i$, we have,

$$\dot{V}(t) \le \theta_1 s\ \dot{x} + \theta_2 s\ x + \theta_3 s\ x_r + \theta_4 s\ + \frac{\Delta B - k_a f_a(u)}{k_a h_a} s\ - s\ u$$

$$+ (\hat{\theta}_1 - \theta_1) s\ \dot{x} + (\hat{\theta}_2 - \theta_2) s\ x + (\hat{\theta}_3 - \theta_3) s\ x_r + (\hat{\theta}_4 - \theta_4) s$$

$$= \hat{\theta}_1 s\ \dot{x} + \hat{\theta}_2 s\ x + \hat{\theta}_3 s\ x_r + \hat{\theta}_4 s\ + \frac{\Delta B - k_a f_a(u)}{k_a h_a} s\ - s\ u$$

Using the adaptive law, one obtains,

$$\dot{V}(t) \le -k_d s\ s - k^* s\ sign(s) + \frac{\rho_B + k_{a\max}\rho_a}{k_{a\min} h_{a\min}} |s\ |$$

$$= -k_d s^2 - k^* |s\ | + \frac{\rho_B + k_{a\max}\rho_a}{k_{a\min} h_{a\min}} |s_\varepsilon|$$

$$\le -k_d s^2 \qquad (5.24)$$

(ii) When $\dot{v} < 0$, by substituting $F_\Delta = hv - B$, and using the same proof process, it is clear that by using the control law (5.14),

$$\dot{V}(t) \le -k_d s^2 \qquad (5.25)$$

Therefore, for all the conditions, $\dot{V}(t) \le -k_d s^2$, and all signals in the system are bounded. Since $s(t)$ is uniformly bounded, by the standard filter theory and the definition of $s(t)$ in (5.11), it can be shown that both $x(t)$ and $\dot{x}(t)$ are also uniformly ultimately bounded. To complete the proof and establish asymptotic convergence of $x(t)$, it is necessary to show that $s(t) \to 0$ as $t \to \infty$. This can be accomplished by applying Barbalat's Lemma to the continuous, nonnegative function:

$$V_1(t) = V(t) - \int_0^t \left(\dot{V}(\tau) + k_d s^2(\tau)\right) d\tau \text{ with } \dot{V}_1(t) = -k_d s^2(t) \qquad (5.26)$$

It can easily be shown that every term on the right side of (5.26) is bounded, hence $\dot{s}(t)$ is bounded. This implies $\dot{V}_1(t)$ is a uniformly continuous function of time. Since $V_1(t)$ is bounded below by 0, and $\dot{V}_1(t) \leq 0$ for all t, use of Barbalat's lemma proves that $\dot{V}_1(t) \to 0$ as $t \to \infty$ and hence from (5.26) that $s(t) \to 0$ as $t \to \infty$. Remark for equation (5.11) indicates that $x(t) \to \Omega_\varepsilon$ as $t \to \infty$. This completes the proof. ■

Remark: The above theorem proves the convergence of $x(t)$, that is, the chatter effect will be significantly suppressed in metal cutting with the proposed adaptive controller.

5.3 Simulation Results

We have the following typical experimental data for turning metal cutting system [Liu et al (1998)].

The equivalent mass, damping coefficient and spring coefficient are respectively, m = 15 kg, $c = 3 \times 10^3$ kg/s, $k = 6 \times 10^7$ kg/s^2. And we can have a reasonable range for these system coefficients as, $m \in [10, 20]$ kg, $c \in [2, 4] \times 10^3$ kg/s, $k \in [5, 7] \times 10^7$ kg/s^2.

For the hysteresis model for cutting force, we have the following,

$$h = 4 \times 10^6 \text{ N/m and } B = 20 \text{ N}$$

with $h \in [3, 5] \times 10^6$ N/m and $B \in [10, 30]$ N.

For the piezoactuator hysteresis, we have,

$$h_a = 2.5 \times 10^{-8} \text{ m/V}, B_a = 0.1 \times 10^{-6} \text{ m}, \alpha = 0.02$$

with $h_a \in [2.0, 3.0] \times 10^{-8}$ m/V and using the backlash-like hysteresis description (5.5), we have the following hysteresis illustration for the piezoactuator.

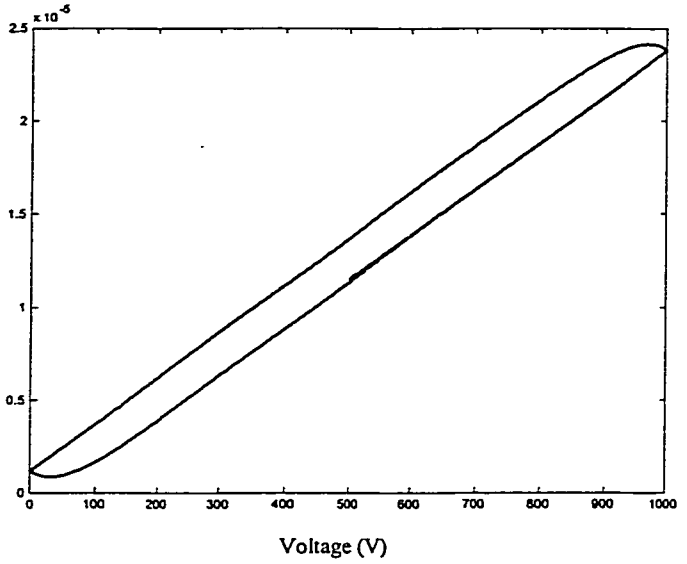

Figure 5.5 Hysteretic relationship between piezo expansion and applied voltage

The simulation in Figure 5.6 illustrates the turning cutting system with initial tool deflection 10 μm, and it is in chattering condition in the presence of active hysteresis.

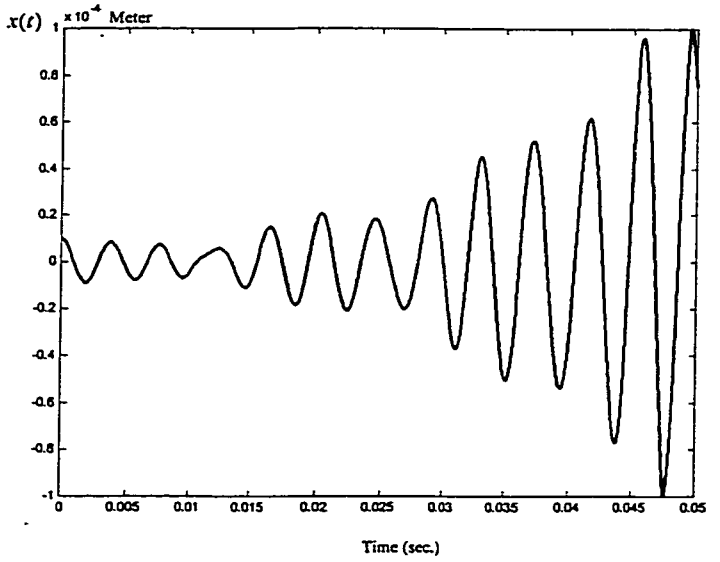

Figure 5.6 Turning cutting system without control (chattering)

It is easy to obtain $\theta_{1\min} = -3.2 \times 10^3$, $\theta_{1\max} = -1.2 \times 10^3$, $\theta_{2\min} = -4 \times 10^7$, $\theta_{2\max} = 4 \times 10^7$, $\theta_{3\min} = -4 \times 10^7$, $\theta_{3\max} = 0$, $\theta_{4\min} = -200$, $\theta_{4\max} = 200$ and $\rho_a = 1.2 \times 10^{-6}$. And we are taking the initial data as, $\theta_1 = -2000$, $\theta_2 = 0.8 \times 10^7$, $\theta_3 = -1.2 \times 10^7$, $\theta_4 = 100$, $k_d = 40$, and $k^* = 60$.

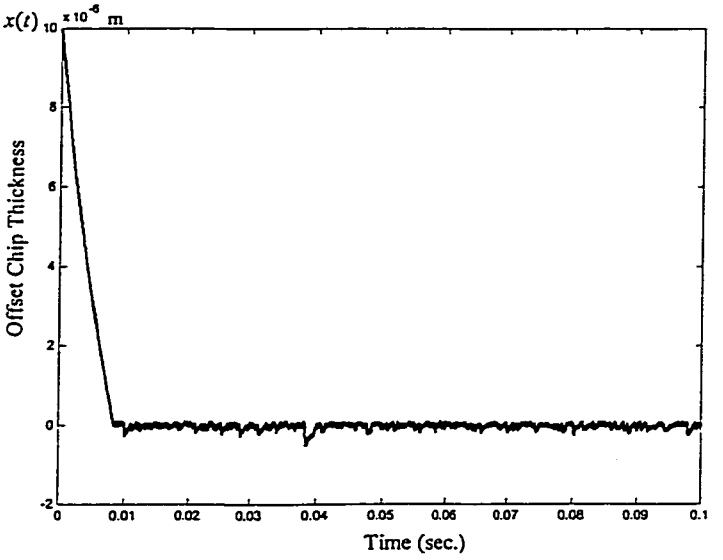

Figure 5.7 Turning cutting system with proposed adaptive controller

In metal cutting, because what we concern about most is the offset chip thickness $x(t)$, we should choose proper λ of the tracking error $s(t)$ so that $x(t)$ is much more "sensitive" to the adaptive control than $\dot{x}(t)$. $\lambda = 100$ is considered in the tracking error equation. And the simulation of the turning system with the adaptive controller is shown in Figure 5.7, which shows clearly that the proposed adaptive controller results in suppression of chatter.

5.4 Summary

In this paper, in order for chatter suppression, a piezoactuator characteristic of hysteresis is introduced for the regulation of the machine tool displacement and metal cutting system is modeled as a class of uncertain linear system with hysteresis and time delay. In order to overcome the chatter due to the hysteresis and time delay during the cutting process, an adaptive controller for the metal cutting system of ultra-precision is presented. The simulation results show that the proposed adaptive controller significantly eliminates the chatter phenomena.

Chapter 6

Chatter Suppression of Turning System with Tool Holder Dynamics

Adaptive Controller Design – 3

Introduction – In this chapter, in order for chatter suppression, a piezoactuator with hysteretic relationship is introduced for the regulation of the machine tool displacement. The cutting system model involves the cutting tool dynamics and piezoactuator dynamics, while the piezoactuator exhibits nonlinear hysteretic actuation. An adaptive controller for the metal cutting system of ultra-precision is presented. The simulation results show that the proposed adaptive controller significantly eliminates the chatter phenomena.

6.1 Turning System with Tool Holder Dynamics

Considering the piezoactuator as an independent free mechanical body with the cutting tool, we have the following illustration for the cutting dynamics.

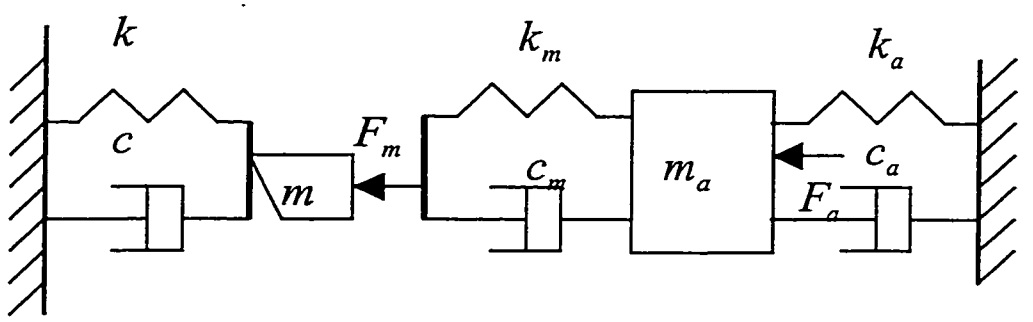

Figure 6.1 Dynamic model of turning cutting system with piezoactuator

In Figure 6.1, the equivalent mass of the cutting system is m, the stiffness is k, and the damping coefficient of the cutting system is c. And m_a, c_a, k_a are respectively the equivalent mass, stiffness, and damping coefficient of the piezoactuator. F_Δ represents the cutting force fluctuation of the machine tool and is, as will be clear later, a nonlinear function with respect to the chip thickness fluctuation. F_a represents the force generated by the piezoactuator, which will also be given detailed analysis in the following section. And F_m is the reaction force between the piezoactuator and cutting tool. In Figure 6.1, F_m is represented by the force generated by the spring-damper structure. From Figure 6.1, the piezoactuator dynamics is,

$$m_a\ddot{x}_a + c_a\dot{x}_a + k_b x_a = F_m - F_a(u) \tag{6.1}$$

where x_a represents the displacement of the piezoactuator with u denoting the voltage applied on the piezoactuator. And the dynamics of the cutting system can be described as,

$$m\ddot{x} + c\dot{x} + kx = F_\Delta - F_m \tag{6.2}$$

While the reaction force F_m can be described as,

$$F_m = c_m(\dot{x} - \dot{x}_a) + k_m(x - x_a) \tag{6.3}$$

In the above dynamic functions, $x(t)$ represents the fluctuating part of the depth of cut, or so called offset chip thickness. In metal cutting system, what we concern about most is the offset chip thickness $x(t)$, for it directly reflects the surface quality of the workpiece being machined, and the vibration of $x(t)$ reflects the chatter occurrence during the dynamic cutting process. The objective of the controller design is to regulate the offset chip thickness $x(t)$ so that $x \to 0$ as $t \to \infty$. To achieve this control objective, we need to investigate the detailed descriptions for both F_Δ and F_a.

With the hysteresis relationships of F_Δ via v and F_a via u, we can illustrate the turning metal cutting system (6.1)-(6.3) with a block diagram as Figure 5, where $G(s) = 1/(ms^2 + cs + k)$, $G_a(s) = 1/(m_a s^2 + c_a s + b)$ and $G_m(s) = 1/(c_m s + k_m)$.

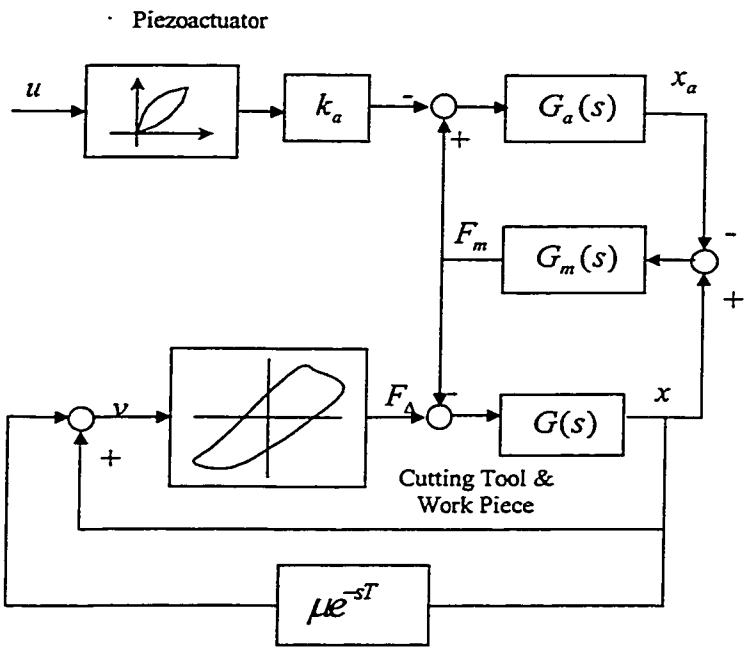

Figure 6.2 Block diagram of turning metal cutting system with piezoactuator

Remark: The cutting system model illustrated in Figure 6.2 is a complicated nonlinear system involving hysteresis, which can lead to instability in closed-looped operation and complicates the task of controller design and analysis [Gorbet et al (2001)].

Focusing on the above model, in the following, a robust adaptive control scheme for control input $u(t)$ will be designed to suppress the chatter effect.

6.2 Adaptive Controller Design

As indicated in Figure 6.2, the metal cutting system displays hysteretic nonlinearity. However, hysteresis is known to be non-differentiable and severely limits the

performance of the system by causing undesirable chatter. Moreover, the hysteresis behaviour demonstrated in the actuator signals makes it impossible to achieve a high accuracy positioning.

The hysteresis in cutting force can be approximately described as Figure 6.3 because of its resemblance in profile with the various experimental results.

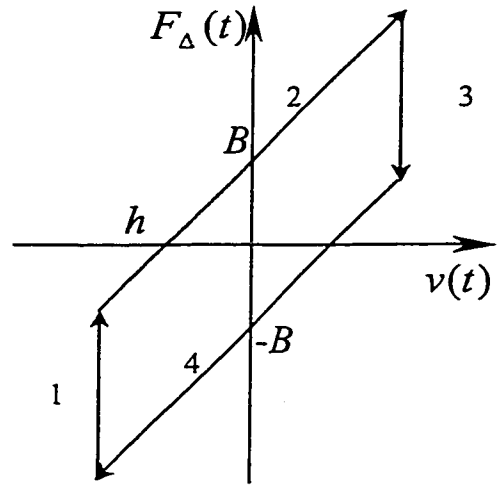

Figure 6.3 Backlash hysteresis model

In Figure 6.3, the line segments 1 and 3, 2 and 4 are parallel, and the hysteresis model of cutting force – chip thickness can be described in terms of h and B.

$$F_\Delta(t) = H(v(t)) = H(h, B) = \begin{cases} h \cdot v(t) + B, & \dot{v}(t) > 0 \\ h \cdot v(t) - B, & \dot{v}(t) < 0 \\ F_\Delta(t_-) & \dot{v}(t) = 0 \end{cases} \tag{6.4}$$

where h is the slope of the hysteresis lines and $B > 0$ is the backlash distance.

Force F_a generated by piezoactuator serves as the force provided by the active vibration control.

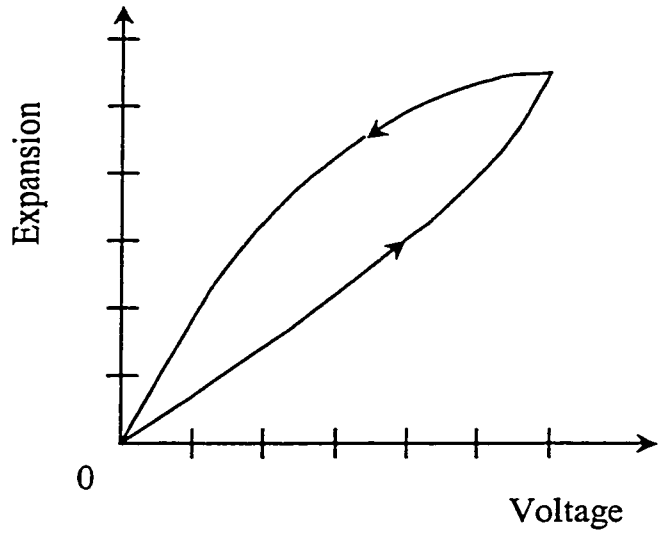

Figure 6.4 Hysteresis curves of a piezoactuator

Figure 6.4 is a typical relationship graph of expansion – voltage for piezoactuator. As can be seen, the expansion of a piezoactuator is not exactly proportional to the electric field strength, demonstrating closed loop hysteresis. And the hysteresis relationship can be described as,

$$\Delta L = H_a(u)$$

where u denotes the applied voltage, and ΔL denotes the expansion of the piezoactuator. $H_a(\cdot)$ denotes the hysteresis function for the relationship of piezoactuator expansion via applied voltage. And the pushing or pulling force can be excited and it is described as,

$$F_a = k_a \Delta L = k_a H_a(u) \tag{6.5}$$

Backlash hysteresis model is discontinuous itself and may not be amenable to controller design for the nonlinear systems. A continuous time dynamic backlash-like hysteresis is employed to describe the hysteresis demonstrated in the relationship of force-expansion of piezoactuator [Su et al (2000)],

$$\frac{dH_a(z)}{dt} = \alpha\left|\frac{dz}{dt}\right|\left(h_a z - H_a(z)\right) + B_a\frac{dz}{dt} \tag{6.6}$$

where α, h_a and B_a are constants, satisfying $h_a > B_a$.

As shown in [Su et al (2000)], the solution of the backlash-like hysteresis (6.6) consists of a linear function and a bounded nonlinearity,

$$H_a(u) = h_a u + f(u) \tag{6.7}$$

with a uniform bound ρ_a such that

$$\|f(u)\| \le \rho_a \tag{6.8}$$

In this case, sum up (6.1) and (6.3) to eliminate F_m in the dynamic functions and the turning cutting system can be described as,

$$m\ddot{x} + c\dot{x} + kx + m_a\ddot{x}_a + c_a\dot{x}_a + k_a x_a = F_\Delta - k_a\left(h_a \cdot u + f_a(u)\right) \tag{6.9}$$

with F_Δ in the description of (6.4).

Before the controller design, the following assumptions are required,

(A6.1) Time delay τ remains constant during the cutting process;

(A6.2) m, c, k, k_a, h, h_a, and B are bounded variables with

$$m \in [m_{\min}, m_{\max}],\ c \in [c_{\min}, c_{\max}],\ k \in [k_{\min}, k_{\max}],$$

$$k_a \in [k_{a\min}, k_{a\max}],\ h \in [h_{\min}, h_{\max}],\ h_a \in [h_{a\min}, h_{a\max}]$$

$$B=B_0+\Delta B \text{ with } \Delta B<\rho_B$$

where $m_{\min}$, $m_{\max}$, $c_{\min}$, $c_{\max}$, $k_{\min}$, $k_{\max}$, $k_{a\min}$, $k_{a\max}$, $h_{\min}$, $h_{\max}$, $h_{a\min}$, $h_{a\max}$, B_0 are known constants.

In order for the chatter suppression, a robust adaptive controller is proposed for the regulation of $x(t)$. Divided by m on both sides of (6.9) and with some manipulations, we have the following second order function with nonlinearity,

$$\ddot{x} = -\frac{c}{m}\dot{x} - \frac{k}{m}x - \frac{m_a}{m}\ddot{x}_a - \frac{c_a}{m}\dot{x}_a - \frac{k_a}{m}x_a + \frac{F_\Delta}{m} - \frac{k_a h_a \cdot u}{m} - \frac{k_a f_a(u)}{m} \qquad (6.10)$$

A filtered tracking error is defined as

$$s(t) = \dot{x} + \lambda x \text{ with } \lambda > 0, \qquad (6.11)$$

Differentiating $s(t)$ with respect to time and substituting $\ddot{x}$ with (6.10), one has,

$$\dot{s}(t) = \ddot{x} + \lambda\dot{x}$$

$$= (\lambda - \frac{c}{m})\dot{x} - \frac{k}{m}x - \frac{m_a}{m}\ddot{x}_a - \frac{c_a}{m}\dot{x}_a - \frac{b}{m}x_a + \frac{F_\Delta}{m} - \frac{k_a h_a \cdot u}{m} - \frac{k_a f_a(u)}{m} \qquad (6.12)$$

Define

$$\theta_1 = \frac{m}{k_a h_a}(\lambda - \frac{c}{m}) \quad \theta_2 = \frac{h-k}{k_a h_a} \quad \theta_3 = -\frac{\mu h}{k_a h_a}$$

$$\theta_4 = \frac{m_a}{k_a h_a} \quad \theta_5 = \frac{c_a}{k_a h_a} \quad \theta_6 = \frac{b}{k_a h_a} \quad \theta_4 = \begin{cases} \frac{B}{k_a h_a} & \dot{v} > 0 \\ -\frac{B}{k_a h_a} & \dot{v} < 0 \end{cases}$$

Due to the boundedness of m, c, k, k_a, h, h_a, we have $\theta_i \in [\theta_{i\min}, \theta_{i\max}]$, i=1,...,7, where $\theta_{i\min}, \theta_{i\max} \in R$ are constants, and they can be easily obtained with the bounds provided in assumption (A6.2).

In order to avoid undesirable high frequency chatter phenomena caused by the designed adaptive controller, in stead of deriving the adaptive law with the filtered error $s(t)$, we introduce a tuning error, s_ε, as follows,

$$s_\varepsilon = s - \varepsilon sat\left(\frac{s}{\varepsilon}\right) \tag{6.13}$$

where ε is a positive constant subject to the choice of designer and $sat(\cdot)$ is the saturation function.

Given the turning metal cutting system (6.9), the following control and adaptation laws are presented:

$$u(t) = k_d s + \hat{\theta}_1 \dot{x} + \hat{\theta}_2 x + \hat{\theta}_3 x_\tau + \hat{\theta}_4 \ddot{x}_a + \hat{\theta}_5 \dot{x}_a + \hat{\theta}_6 x_a + \hat{\theta}_7 x_\tau + k^* sat(\frac{s}{\varepsilon}) \tag{6.14}$$

with

$$\dot{\hat{\theta}}_i = proj\left(\hat{\theta}_i, g_i\right) \tag{6.15}$$

where

$$k^* = \frac{\rho_B + k_{a\max}\rho_a}{k_{a\min}h_{a\min}} \tag{6.16}$$

and $k_d > 0$. $proj(\cdot,\cdot)$ is a projection operator, which are constructed as follows:

$$proj(\hat{\theta}_i, \gamma_i g_i) = \begin{cases} 0 & \text{if } \hat{\theta}_i = \theta_{i\max} \text{ and } g_i > 0 \\ & \text{or } \hat{\theta}_i = \theta_{i\min} \text{ and } g_i < 0 \\ \gamma_i g_i & \text{if } \theta_{i\min} < \hat{\theta}_i < \theta_{i\max} \\ & \text{or } \hat{\theta}_i = \theta_{i\max} \text{ and } g_i \le 0 \\ & \text{or } \hat{\theta}_i = \theta_{i\min} \text{ and } g_i \ge 0 \end{cases} \tag{6.17}$$

where $\gamma_i > 0$ (i=1,...7) are constants, and the different g_i ($i = 1,...,7$) are defined respectively as follows,

$$g_1 = s_\varepsilon \dot{x},\ g_2 = s_\varepsilon x,\ g_3 = s_\varepsilon x_r,\ g_4 = s_\varepsilon \ddot{x}_a,\ g_5 = s_\varepsilon \dot{x}_a,\ g_6 = s_\varepsilon x_a,\ g_7 = s_\varepsilon$$

Remark: It can be easily proved that the projection operators for $\hat{\theta}_i$ satisfies i) $\hat{\theta}_i(t) \in [\theta_{i\min}, \theta_{i\max}]$ if $\hat{\theta}_i(0) \in [\theta_{i\min}, \theta_{i\max}]$; and ii) $(\hat{\theta}_i - \theta_i) proj(\hat{\theta}_i, g_i) \le (\hat{\theta}_i - \theta_i) \cdot g_i$.

The stability of the closed-loop system described by (6.9) and (6.14)–(6.17) is established in the following theorem.

Theorem: For the system model (6.9), the robust adaptive controller specified by equations (6.14) – (6.17) ensures that all the closed loop signals are bounded; moreover, the state x will converge to $\Omega_\varepsilon = \{x(t) \,||\, x| \le \lambda^{-1}\varepsilon\}$ for $\forall t \ge t_0$.

Proof: To establish the global boundedness, a Lyapunov function candidate is defined as follows,

$$V(t) = \frac{1}{2}\left[\frac{m}{k_a h_a} s_\varepsilon^2(t) + \sum_{i=1}^{7} \frac{1}{\gamma_i}(\hat{\theta}_i - \theta_i)^2\right] \tag{6.18}$$

Since the discontinuity at $|s| = \varepsilon$ is of the first kind and since $s_\varepsilon = 0$ when $|s| \le \varepsilon$, it follows that the derivative $\dot{V}$ exists for all s, and given by

$$\dot{V}(t) = 0 \text{ when } |s| \le \varepsilon$$

When $|s| > \varepsilon$, notice the fact that $s_\varepsilon \dot{s}_\varepsilon = s_\varepsilon \dot{s}$, and differentiating $V(t)$ with respect to time yields

$$\begin{aligned}\dot{V}(t) &= \frac{m}{k_a h_a} s_\varepsilon \dot{s} + \sum_{i=1}^{7} (\hat{\theta}_i - \theta_i)\dot{\hat{\theta}}_i \\ &= \frac{m}{k_a h_a} s_\varepsilon \left((\lambda - \frac{c}{m})\dot{x} - \frac{k}{m}x - \frac{m_a}{m}\ddot{x}_a - \frac{c_a}{m}\dot{x}_a - \frac{b}{m}x_a + \frac{F_\Delta}{m} - \frac{k_a h_a \cdot u}{m} - \frac{k_a f_a(u)}{m} \right) \\ &\quad + \sum_{i=1}^{7} (\hat{\theta}_i - \theta_i)\dot{\hat{\theta}}_i \end{aligned} \tag{6.19}$$

In the following, the proof is constructed with the two conditions (i) $\dot{v}(t) > 0$ and (ii) $\dot{v} < 0$;

(i) When $\dot{v}(t) > 0$, by substituting $F_\Delta = hv + B$, one has,

$$\begin{aligned}\dot{V}(t) = \frac{m}{k_a h_a} s_\varepsilon \Bigg(&(\lambda - \frac{c}{m})\dot{x} - \frac{k}{m}x - \frac{m_a}{m}\ddot{x}_a - \frac{c_a}{m}\dot{x}_a - \frac{b}{m}x_a \\ &+ \frac{h(x - \mu x_\tau) + B}{m} - \frac{k_a h_a \cdot u}{m} - \frac{k_a f_a(u)}{m} \Bigg) + \sum_{i=1}^{7} \frac{1}{\gamma_i}(\hat{\theta}_i - \theta_i)\dot{\hat{\theta}}_i \end{aligned}$$

Noting that $B = B_0 + \Delta B$,

$$\dot{V}(t) = \frac{m}{k_a h_a} s_\varepsilon \Bigg((\lambda - \frac{c}{m})\dot{x} + \frac{h-k}{m}x - \frac{m_a}{m}\ddot{x}_a - \frac{c_a}{m}\dot{x}_a - \frac{b}{m}x_a$$

$$+\frac{-\mu h}{m}\dot{x}_\tau+\frac{B_0}{m}+\frac{\Delta B}{m}-\frac{k_a f_a(u)}{m}\Big)-s_\varepsilon u+\sum_{i=1}^{7}\frac{1}{\gamma_i}(\hat{\theta}_i-\theta_i)\dot{\hat{\theta}}_i$$

$$=\theta_1 s_\varepsilon\dot{x}+\theta_2 s_\varepsilon x+\theta_3 s_\varepsilon x_\tau+\theta_4 s_\varepsilon\ddot{x}_a+\theta_5 s_\varepsilon\dot{x}_a+\theta_6 s_\varepsilon x_a+\theta_7 s_\varepsilon$$

$$+\frac{\Delta B-k_a f_a(u)}{k_a h_a}s_\varepsilon-s_\varepsilon u+\sum_{i=1}^{7}\frac{1}{\gamma_i}(\hat{\theta}_i-\theta_i)\dot{\hat{\theta}}_i$$

And using the property $(\hat{\theta}_i-\theta_i)proj(\hat{\theta}_i,\gamma_i g_i)\le(\hat{\theta}_i-\theta_i)\cdot\gamma_i g_i$, we have,

$$\dot{V}(t)\le\theta_1 s_\varepsilon\dot{x}+\theta_2 s_\varepsilon x+\theta_3 s_\varepsilon x_\tau+\theta_4 s_\varepsilon\ddot{x}_a+\theta_5 s_\varepsilon\dot{x}_a+\theta_6 s_\varepsilon x_a+\theta_7 s_\varepsilon$$

$$+\frac{\Delta B-k_a f_a(u)}{k_a h_a}s_\varepsilon-s_\varepsilon u+(\hat{\theta}_1-\theta_1)s_\varepsilon\dot{x}+(\hat{\theta}_2-\theta_2)s_\varepsilon x+(\hat{\theta}_3-\theta_3)s_\varepsilon x_\tau$$

$$+(\hat{\theta}_4-\theta_4)s_\varepsilon\ddot{x}_a+(\hat{\theta}_5-\theta_5)s_\varepsilon\dot{x}_a+(\hat{\theta}_6-\theta_6)s_\varepsilon x_a+(\hat{\theta}_7-\theta_7)s_\varepsilon$$

$$=\hat{\theta}_1 s_\varepsilon\dot{x}+\hat{\theta}_2 s_\varepsilon x+\hat{\theta}_3 s_\varepsilon x_\tau+\hat{\theta}_4 s_\varepsilon\ddot{x}_a+\hat{\theta}_5 s_\varepsilon\dot{x}_a+\hat{\theta}_6 s_\varepsilon x_a$$

$$+\hat{\theta}_7 s_\varepsilon+\frac{\Delta B-k_a f_a(u)}{k_a h_a}s_\varepsilon-s_\varepsilon u$$

Using the adaptive law, one obtains,

$$\dot{V}(t)\le-k_d s_\varepsilon^2-k^*s_\varepsilon sat(\frac{s}{\varepsilon})+\frac{\rho_B+k_{a\max}\rho_a}{k_{a\min}h_{a\min}}|s_\varepsilon|$$

$$=-k_d s_\varepsilon^2-k^*|s_\varepsilon|+\frac{\rho_B+k_{a\max}\rho_a}{k_{a\min}h_{a\min}}|s_\varepsilon|$$

$$\le-k_d s_\varepsilon^2 \qquad (6.20)$$

(ii) When $\dot{v}<0$, by substituting $F_\Delta=hv-B$, and using the same proof process, it is easy to achieve by using the control law (6.14),

$$\dot{V}(t)\le-k_d s_\varepsilon^2 \qquad (6.21)$$

Therefore, for all the conditions, $\dot{V}(t) \le -k_d s_\varepsilon^2$, and all signals in the system are bounded. Since $s(t)$ is uniformly bounded, by the standard filter theory and the definition of $s(t)$ in (6.11), it can be shown that both $x(t)$ and $\dot{x}(t)$ are also uniformly ultimately bounded. To complete the proof and establish asymptotic convergence of $x(t)$, it is necessary to show that $s(t) \to 0$ as $t \to \infty$. This can be accomplished by applying Barbalat's Lemma to the continuous, nonnegative function:

$$V_1(t) = V(t) - \int_0^t \left(\dot{V}(\tau) + k_d s_\varepsilon^2(\tau)\right) d\tau \text{ with } \dot{V}_1(t) = -k_d s_\varepsilon^2(t) \tag{6.22}$$

It can easily be shown that every term on the right side of (6.22) is bounded, hence $\dot{s}(t)$ is bounded. This implies $\dot{V}_1(t)$ is a uniformly continuous function of time. Since $V_1(t)$ is bounded below by 0, and $\dot{V}_1(t) \le 0$ for all t, use of Barbalat's lemma proves that $\dot{V}_1(t) \to 0$ as $t \to \infty$ and hence from (6.22) that $s_\varepsilon(t) \to 0$ as $t \to \infty$. Remark for equation (6.10) indicates that $x(t) \to \Omega_\varepsilon$ as $t \to \infty$. This completes the proof. ■

Remark: The above theorem proves the convergence of $x(t)$, that is, the chatter effect will be significantly suppressed in metal cutting with the proposed adaptive controller.

6.3 Simulation Results

The equivalent mass, damping coefficient and spring coefficient for the metal cutting system are,

$$m = 15 \text{ kg}, c = 3 \times 10^3 \text{ kg/s}, k = 6 \times 10^7 \text{ kg/s}^2.$$

And we can have a reasonable range for these system coefficients as, $m \in [10, 20]$ kg, $c \in [2, 4] \times 10^3$ kg/s, $k \in [5, 7] \times 10^7$ kg/s^2.

For the piezoactuator,

$$m_a = 2 \text{ kg}, c_a = 1 \times 10^3 \text{ kg/s}, b = 5 \times 10^7 \text{ kg/s}^2 \text{ and } k_a = 7 \times 10^7 \text{ kg/s}^2$$

with $k \in [6, 8] \times 10^7$ kg/s^2.

For the hysteresis model for cutting force, we have the following,

$$h = 4 \times 10^6 \text{ N/m and } B_0 = 20 \text{ N}$$

with $h \in [3, 5] \times 10^6$ N/m and $\rho_B = 10$ N.

For the piezoactuator hysteresis, we have,

$$h_a = 2.5 \times 10^{-8} \text{ m/V}, B_a = 0.1 \times 10^{-6} \text{ m}, \alpha = 0.02$$

with $h_a \in [0.9, 1.1] \times 10^{-6}$ m/V and using the backlash-like hysteresis description (6.6), we have the following hysteresis illustration for the piezoactuator (Figure 6.5).

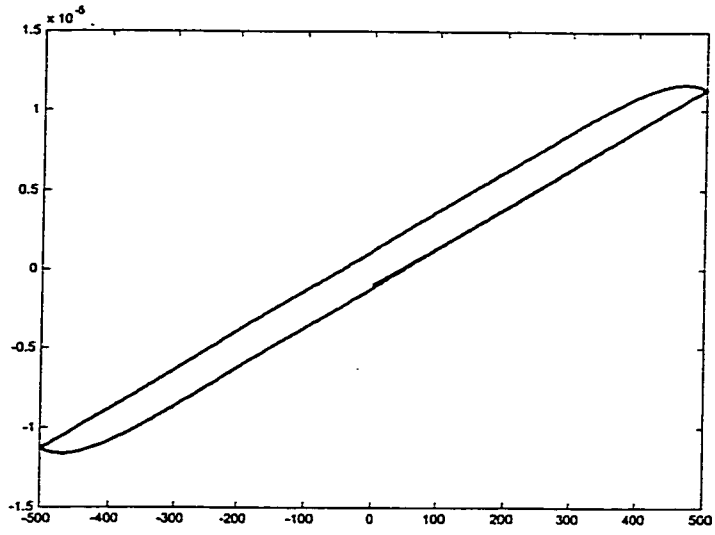

Figure 6.5 Hysteresis relationship between piezo expansion and applied voltage

The simulation in Figure 6.6 illustrates the turning cutting system with initial tool deflection 10 μm, and it is in chattering condition in the presence of active hysteresis.

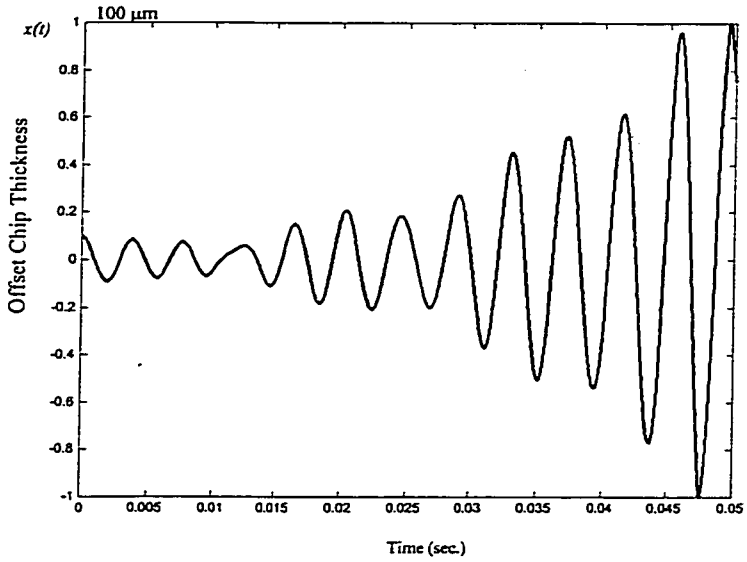

Figure 6.6 Turning cutting system without piezoactuation

It is easy to obtain $\theta_{1\min} = 0.8\times10^{4}$, $\theta_{1\max} = 3.2\times10^{4}$, $\theta_{2\min} = -6\times10^{7}$, $\theta_{2\max} = -1\times10^{7}$, $\theta_{3\min} = -5\times10^{6}$, $\theta_{3\max} = -1\times10^{6}$, $\theta_{4\min} = 0$, $\theta_{4\max} = 2$, $\theta_{5\min} = 300$, $\theta_{5\max} = 1000$, $\theta_{6\min} = 3\times10^{7}$, $\theta_{6\max} = 5\times10^{7}$, $\theta_{7\min} = -20$, $\theta_{7\max} = 20$. And we are taking the initial data as, $\theta_1 = 1\times10^{4}$, $\theta_2 = -3\times10^{7}$, $\theta_3 = 2\times10^{6}$, $\theta_4 = 1$, $\theta_5 = 600$, $\theta_6 = 4\times10^{7}$, $\theta_7 = 0$, and the controller parameters $\gamma_1 = 5\times10^{8}$, $\gamma_2 = 5\times10^{14}$, $\gamma_3 = 5\times10^{17}$, $\gamma_4 = 1\times10^{2}$, $\gamma_5 = 1\times10^{9}$, $\gamma_6 = 1\times10^{17}$, $\gamma_7 = 1$, $k_d = 1$, and $k^* = 40$ and $\varepsilon = 1\times10^{-7}$.

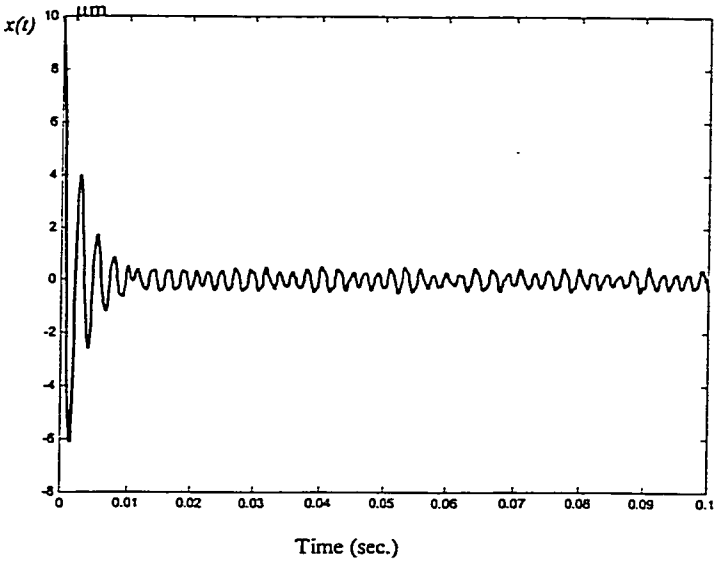

Figure 6.7 Turning cutting system with proposed adaptive controller

In metal cutting, because what we concern about most is the offset chip thickness $x(t)$, we should choose proper λ of the tracking error $s(t)$ so that $x(t)$ is much more "sensitive" to the adaptive control than $\dot{x}(t)$. $\lambda = 2000$ is considered in the tracking error equation. And the simulation of the turning system with the adaptive controller is

shown in Figure 6.7, which shows clearly that the proposed adaptive controller results in suppression of chatter.

6.4 Summary

In this paper, in order for chatter suppression, a piezoactuator is introduced for the regulation of the machine tool displacement and metal cutting system is modeled as a class of uncertain linear system with hysteresis and time delay. In order to overcome the chatter due to the hysteresis and time delay in the cutting process, an adaptive controller for the metal cutting system of ultra-precision is presented. The simulation results show that the proposed adaptive controller significantly eliminates the chatter phenomena.

Chapter 7

Chatter Suppression of Cutting System with 2-DOF via Nonlinear Piezoactuation

Adaptive Controller Design – 4

Introduction – In this chapter, type A and type B chatters are considered in the cutting system with two degrees of freedom. In order to suppress the chatter, the piezoactuator is introduced for the ultra-precision control, and a robust adaptive control scheme is proposed for regulation of machine tools. Simulation results show significant reduction of chatter.

7.1 Turning System of 2-DOF

As discussed in Chapter 3, for a metal cutting system, a general machine tool structure can be described as follows,

$$M\ddot{x} + C\dot{x} + Kx = F \tag{7.1}$$

where the local mass M, damping C, and stiffness K matrices are $R^{2\times2}$, and the force vector $F \in R^{2\times1}$. $x \in R^{2\times1}$. For a two degree-of-freedom cutting system, it can be illustrated in Figure 6.1

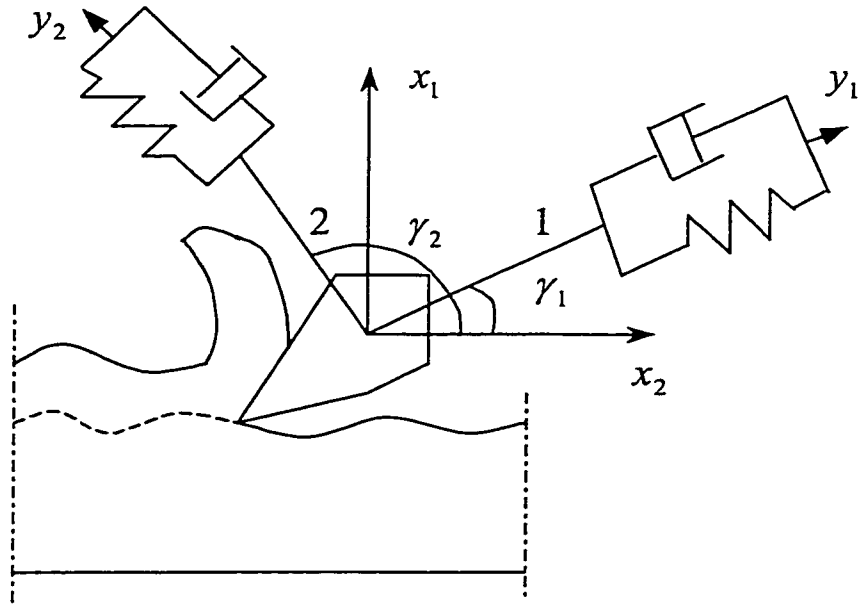

Figure 7.1 Cutting system with 2 degrees of freedom

In Figure 7.1, x_1 and x_2 represent the relative displacement between the cutting tool and the workpiece in the reference directions, which are normal to the workpiece surface and along with the cutting direction, respectively. And y_1 and y_2 are the displacement of the tool in the directions of freedom.

As discussed in the modeling of the cutting system, for the hysteresis model of cutting/thrust force, the backlash hysteresis model is introduced in place of the actual hysteresis model.

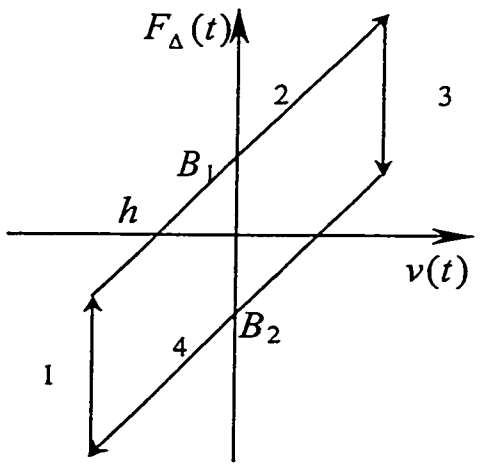

Figure 7.2 Backlash hysteresis model

And we have the description functions for the forces in the cutting force direction and thrust force direction.

$$\begin{cases} \Delta F_c = F_{c\Delta} + F_{fi} \\ \Delta F_t = F_{t\Delta} + F_{i\Delta} \end{cases} \tag{7.2}$$

where

$$\begin{aligned} F_{c\Delta}(t) &= H_c(v(t)) = H_c(h_c, B_c) \\ &= \begin{cases} h_c \cdot v(t) + B_{c1}, & \dot{v}(t) > 0 \\ h_c \cdot v(t) + B_{c2}, & \dot{v}(t) < 0 \\ F_{c\Delta}(t_-) & \dot{v}(t) = 0 \end{cases}, \end{aligned} \tag{7.3}$$

where h_c is unknown constant and $h_c \in [h_{c\min}, h_{c\max}]$, $B_{c1} = B_{c10} + \Delta B_{c1}$ and $B_{c2} = B_{c20} + \Delta B_{c2}$, while C_{c1} and C_{c2} are constants. And $v(t) = x_1(t) - x_1(t-\tau)$ denotes the chip thickness variation. And

$$
\begin{aligned}
F_{t\Delta}(t) &= H_t(v(t)) = H_t(h_t, B_t) \\
&= \begin{cases} h_t \cdot v(t) + B_{t1}, & \dot{v}(t) > 0 \\ h_t \cdot v(t) + B_{t2}, & \dot{v}(t) < 0 \\ F_{t\Delta}(t_-) & \dot{v}(t) = 0 \end{cases},
\end{aligned} \tag{7.4}
$$

where h_t is unknown constant and $h_t \in [h_{t\min}, h_{t\max}]$, $B_{t1} = B_{t10} + \Delta B_{t1}$ and $B_{t2} = B_{t20} + \Delta B_{t2}$, while C_{t1} and C_{t2} are constants.

For the dynamic contact force model, a triangular hysteresis model is introduced to describe the actual hysteresis model,

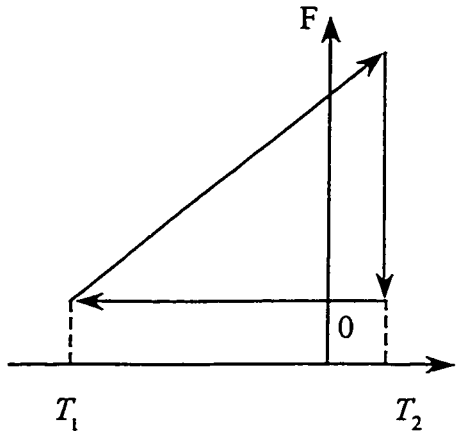

Figure 7.3 Triangular hysteresis model

And the contact force due to the flank contact is described as follows,

$$
\begin{aligned}
F_{i\Delta} &= T(x_2) \\
&= \begin{cases} h_i(x_2 - T_1) & \dot{x}_2 > 0 \\ 0 & \dot{x}_2 \le 0 \end{cases}
\end{aligned} \tag{7.5}
$$

and

$$F_{ft} = k_f T(x_2)$$
$$= \begin{cases} k_f h_i (x_2 - T_l) & \dot{x}_2 > 0, \\ 0 & \dot{x}_2 \le 0 \end{cases} \tag{7.6}$$

where T_l is the maximum displacement of x_2, and h_i, T_l, k_f are unknown constants, with $h_i \in [h_{i\min}, h_{i\max}]$, $T_l \in [T_{l\min}, T_{l\max}]$, and $k_f \in [k_{f\min}, k_{f\max}]$.

For the piezoactuator with hysteretic relationship between expansion and applied voltage as illustrated in Figure , we would like to consider using the backlash-like hysteresis model.

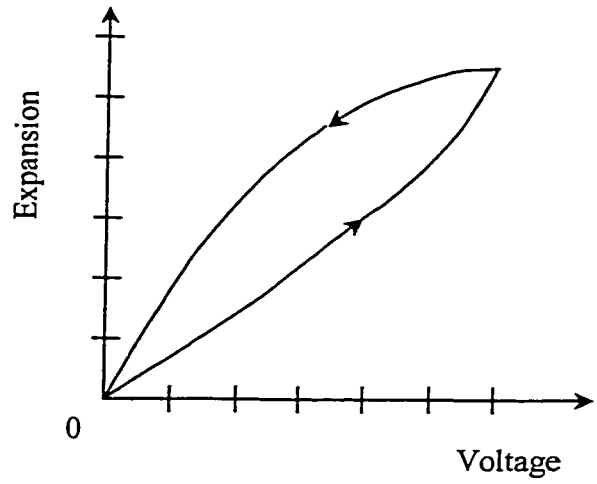

Figure 7.4 Hysteretic relationship between expansion and applied voltage

In order for amiable controller design, we are using backlash-like hysteresis as,

$$\frac{dH_a(z)}{dt} = \alpha \left| \frac{dz}{dt} \right| (h_a z - H_a(z)) + B_a \frac{dz}{dt} \tag{7.7}$$

where α, h_a and B_a are constants, satisfying $h_a > B_a$.

In summary, the block diagram of the turning metal cutting system is demonstrated as follows,

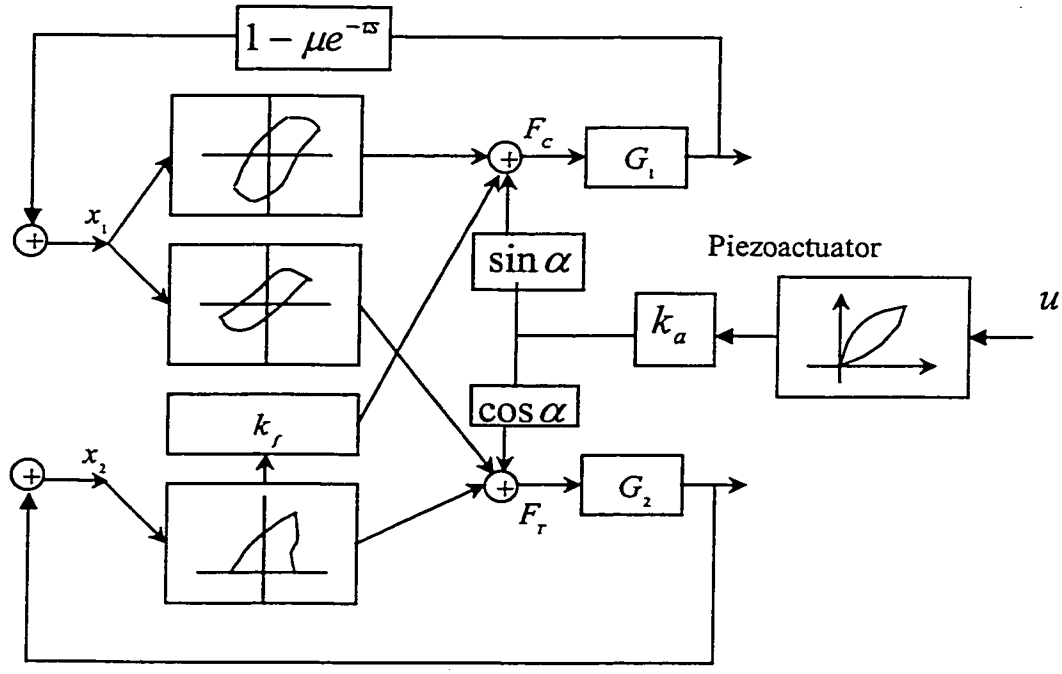

Figure 7.5 Block Diagram of turning metal cutting system of 2-DOF with piezoactuator

As the backlash hysteresis model described in (7.3) and (7.4) is so complicated that it would be tedious for the adaptive controller design. In this chapter, we will introduce the backlash-like hysteresis model in place of the backlash hysteresis demonstrated in the cutting dynamics.

7.2 Adaptive Controller Design

As in Chapter 4, using the expression of backlash-like hysteresis to replace the backlash hysteresis model, we have

$$F_{c\Delta} = H_c(v(t)) = h_c v(t) + f_c(v), \tag{7.8}$$

where h_c is an unknown constant with $h_c \in [h_{c\min}, h_{c\max}]$, and $\|f_c(v)\| \le \rho_c$, ρ_c is a constant bound. And $v(t) = x_1(t) - \mu x_1(t-\tau)$ denotes the chip thickness variation, $\mu \in [0,1]$ is the overlap factor. Also for the thrust force model, we have,

$$F_{t\Delta} = H_t(v(t)) = h_t v(t) + f_t(v), \tag{7.9}$$

where h_t is an unknown constant with $h_t \in [h_{t\min}, h_{t\max}]$ and $\|f_t(v)\| \le \rho_t$, ρ_t is a constant bound. While the contact/frictional forces are described as (7.5) and (7.6), respectively.

Thus the metal cutting system (7.1) can be described as,

$$M\ddot{x} + C\dot{x} + Kx = \begin{bmatrix} \Delta F_c - F_a(u)\sin\alpha \\ \Delta F_t - F_a(u)\cos\alpha \end{bmatrix}$$

$$= \begin{bmatrix} h_c \\ h_t \end{bmatrix}(x_1 - \mu x_{1\tau}) + \begin{bmatrix} f_c \\ f_t \end{bmatrix} + \begin{bmatrix} k_f \\ 1 \end{bmatrix} T(x_2) - \begin{bmatrix} \sin\alpha \\ \cos\alpha \end{bmatrix} F_a(u) \tag{7.10}$$

As a matter of fact, the relationship of the expansion of the piezoactuator and the applied voltage demonstrates the hysteresis. As discussed in chapter 3, noting the properties of backlash-like hysteresis, the force-expansion relationship $F_a(u)$ can be described as,

$$F_a(u) = k_a(h_a \cdot u + f_a(u)) \tag{7.7}$$

where u is the applied voltage, k_a is the stiffness of the piezoactuator, and h_a is the slope of the piezoactuator hysteresis. k_a and h_a are constants and $\|f_a(u)\| \le \rho_a$.

As a result, we have the following system description,

$$M\ddot{x} + C\dot{x} + Kx = \begin{bmatrix} h_c \\ h_t \end{bmatrix}(x_1 - \mu x_{1\tau}) + \begin{bmatrix} f_c(v) \\ f_t(v) \end{bmatrix} + \begin{bmatrix} k_f \\ 1 \end{bmatrix} T(x_2) - \begin{bmatrix} \sin\alpha \\ \cos\alpha \end{bmatrix} k_a h_a u - \begin{bmatrix} \sin\alpha \\ \cos\alpha \end{bmatrix} k_a f_a(u) \tag{7.8}$$

Noting the fact that $rank(M) = 2$, left multiplying M^{-1} on both sides of (df-2), one has,

$$\begin{aligned} \ddot{x} = & -M^{-1}C\dot{x} - M^{-1}Kx \\ & + M^{-1}\begin{bmatrix} h_c \\ h_t \end{bmatrix} x_1 - M^{-1}\begin{bmatrix} h_c \\ h_t \end{bmatrix} \mu x_{1\tau} + M^{-1}\begin{bmatrix} k_f \\ 1 \end{bmatrix} T(x_2) \\ & + M^{-1}\left(\begin{bmatrix} f_c(v) \\ f_t(v) \end{bmatrix} - \begin{bmatrix} \sin\alpha \\ \cos\alpha \end{bmatrix} k_a f_a(u) \right) - M^{-1}\begin{bmatrix} \sin\alpha \\ \cos\alpha \end{bmatrix} k_a h_a u \end{aligned} \tag{7.9}$$

Define a filtered tracking error as the follows,

$$s = p^T \dot{x} + \lambda p^T x \tag{7.10}$$

where $\lambda \in R$ and $p \in R^{n\times 1}$ are given by the designer.

Remark: In metal cutting, what we concern about most is the offset chip thickness $x_1(t)$, for it directly reflects the surface quality of the workpiece being machined, and the vibration of $x_1(t)$ reflects the chatter occurrence during the dynamic cutting process, while the vibration of $x_2(t)$ has no direct detrimental effect on the workpiece quality. As

a result, in order for the chatter suppression, we choose the p to be $[1 \quad 0]$, so that a robust adaptive controller is proposed in the following for the regulation of $p^T x(t)$, i.e., $x_1(t)$.

Differentiating $s(t)$ with respect to time and substituting $\ddot{x}$ with (7.9), one has,

$$\begin{aligned}\dot{s}(t) &= p^T \ddot{x} + \lambda p^T \dot{x} \\ &= -p^T (M^{-1}C - \lambda I)\dot{x} - p^T M^{-1} K x \\ &\quad + p^T M^{-1} \begin{bmatrix} h_c \\ h_t \end{bmatrix} x_1 - p^T M^{-1} \begin{bmatrix} h_c \\ h_t \end{bmatrix} \mu x_{1r} + p^T M^{-1} \begin{bmatrix} k_f \\ 1 \end{bmatrix} T(x_2) \\ &\quad + p^T M^{-1} \left(\begin{bmatrix} f_c(v) \\ f_t(v) \end{bmatrix} - \begin{bmatrix} \sin\alpha \\ \cos\alpha \end{bmatrix} k_a f_a(u) \right) - p^T M^{-1} \begin{bmatrix} \sin\alpha \\ \cos\alpha \end{bmatrix} k_a h_a u \end{aligned} \tag{7.11}$$

In order to eliminate the chatter phenomena aroused, we introduce a tuning error, s_ε,

$$s_\varepsilon = s - \varepsilon sat(\frac{s}{\varepsilon}) \tag{7.12}$$

where ε is an arbitrary positive constant and $sat(\cdot)$ is the saturation function.

Define $l = \left(p^T M^{-1} \begin{bmatrix} \sin\alpha \\ \cos\alpha \end{bmatrix} k_a h_a \right)$ and θ_i (i=1,...,6),

$$\theta_1 = -l^{-1} p^T (M^{-1}C - \lambda I) \;,\; \theta_2 = -l^{-1} p^T M^{-1} K \;,\; \theta_3 = l^{-1} p^T M^{-1} \begin{bmatrix} h_c \\ h_t \end{bmatrix},$$

$$\theta_4 = -l^{-1} p^T M^{-1} \begin{bmatrix} h_c \\ h_t \end{bmatrix} \mu \;,\; \theta_5 = \begin{cases} l^{-1} p^T M^{-1} \begin{bmatrix} k_f \\ 1 \end{bmatrix} h_i & \dot{x}_2 > 0 \\ 0 & \dot{x}_2 \le 0 \end{cases}, \; \theta_6 = \begin{cases} l^{-1} p^T M^{-1} \begin{bmatrix} k_f \\ 1 \end{bmatrix} h_i T_1 & \dot{x}_2 > 0 \\ 0 & \dot{x}_2 \le 0 \end{cases}$$

Due to the boundedness of M, C, K, k_a, h_a, h_t, h_i, μ and T_1, we have

$$\theta_i \in [\theta_{i\min}, \theta_{i\max}]$$

where $\theta_{i\min}, \theta_{i\max} \in R$ (i=1,...,6) are constants.

Given the metal cutting system, the following control and adaptation laws are presented:

$$u(t) = k_d s + \hat{\theta}_1 \dot{x} + \hat{\theta}_2 x + \hat{\theta}_3 x_1 + \hat{\theta}_4 x_{1\tau} + \hat{\theta}_5 x_2 + \hat{\theta}_6 + k^* sat\left(\frac{s}{\varepsilon}\right) \tag{7.13}$$

with

$$\dot{\hat{\theta}}_i = proj\left(\hat{\theta}_i, g_i\right) \tag{7.14}$$

where

$$k^* = \left\|\tilde{q}_1^T\right\|_\infty \max(\rho_c, \rho_t) + \left|\tilde{q}_2\right|_{\max} \rho_a \tag{7.15}$$

And $proj(\cdot,\cdot)$ is a projection operator, which are constructed as follows:

$$proj\left(\hat{\theta}_i, g_i\right) = \begin{cases} 0 & \text{if } \hat{\theta}_i = \theta_{i\max} \text{ and } g_i > 0 \\ & \text{or } \hat{\theta}_i = \theta_{i\min} \text{ and } g_i < 0 \\ g_i & \text{if } \theta_{i\min} < \hat{\theta}_i < \theta_{i\max} \\ & \text{or } \hat{\theta}_i = \theta_{i\max} \text{ and } g_i \le 0 \\ & \text{or } \hat{\theta}_i = \theta_{i\min} \text{ and } g_i \ge 0 \end{cases} \tag{7.16}$$

The different g_i (i=1,...,6) are defined respectively as follows,

$$g_1 = s_\varepsilon \dot{x},\ g_2 = s_\varepsilon x,\ g_3 = s_\varepsilon x_1,\ g_4 = s_\varepsilon x_{1\tau},\ g_5 = s_\varepsilon x_2,\ g_6 = s_\varepsilon \tag{7.17}$$

The stability of the closed-loop system described by (7.8) and (7.13)-(7.17) is established in the following theorem.

Theorem: For the system model (7.8), the robust adaptive controller specified by equations (7.13) – (7.17) ensures that all the closed loop signals are bounded; moreover, the state $p^T x$ will converge to $\Omega_\varepsilon = \{p^T x(t) \,||\, p^T x| \leq \lambda^{-1}\varepsilon\}$ for $\forall t \geq t_0$.

Proof: To establish the global boundedness, a Lyapunov function candidate is defined as follows,

$$V(t) = \frac{1}{2}\left[l^{-1} s_\varepsilon^2(t) + \sum_{i=1}^{6} (\hat{\theta}_i - \theta_i)^2 \right] \tag{7.18}$$

Since the discontinuity at $|s| = \varepsilon$ is of the first kind and since $s_\varepsilon = 0$ when $|s| \leq \varepsilon$, it follows that the derivative $\dot{V}$ exists for all s, and given by

$$\dot{V}(t) = 0 \text{ when } |s| \leq \varepsilon \tag{7.19}$$

When $|s| > \varepsilon$, notice the fact that $s_\varepsilon \dot{s}_\varepsilon = s_\varepsilon \dot{s}$, and differentiating $V(t)$ with respect to time yields

$$\begin{aligned}
\dot{V}(t) &= l^{-1} s_\varepsilon \dot{s} + \sum_{i=1}^{6} (\hat{\theta}_i - \theta_i)^T \dot{\hat{\theta}}_i \\
&= l^{-1} s_\varepsilon \Big\{ - p^T (M^{-1}C - \lambda I)\dot{x} - p^T M^{-1} K x \\
&\quad + p^T M^{-1} \begin{bmatrix} h_c \\ h_t \end{bmatrix} x_1 - p^T M^{-1} \begin{bmatrix} h_c \\ h_t \end{bmatrix} \mu x_{1\tau} + p^T M^{-1} \begin{bmatrix} k_f \\ 1 \end{bmatrix} T(x_2) \\
&\quad + p^T M^{-1} \left(\begin{bmatrix} f_c(v) \\ f_t(v) \end{bmatrix} - \begin{bmatrix} \sin\alpha \\ \cos\alpha \end{bmatrix} k_a f_a(u) \right) - p^T M^{-1} \begin{bmatrix} \sin\alpha \\ \cos\alpha \end{bmatrix} k_a h_a u \Big\}
\end{aligned}$$

$$+\sum_{i=1}^{6}(\hat{\theta}_i-\theta_i)^T\dot{\hat{\theta}}_i$$

$$=\theta_1^T s_\varepsilon\dot{x}+\theta_2^T s_\varepsilon x+\theta_3^T s_\varepsilon x_1+\theta_4^T s_\varepsilon x_{1\tau}+\tilde{l}_1 s_\varepsilon T(x_2)+s_\varepsilon\tilde{q}_1^T\begin{bmatrix}f_c(v)\\f_t(v)\end{bmatrix}$$

$$+s_\varepsilon\tilde{q}_2 f_a(u)-s_\varepsilon u+\sum_{i=1}^{6}(\hat{\theta}_i-\theta_i)^T\dot{\hat{\theta}}_i$$

And using the property $(\hat{\theta}_i-\theta_i)proj(\hat{\theta}_i,g_i)\le(\hat{\theta}_i-\theta_i)\cdot g_i$, we have,

$$\dot{V}(t)\le\hat{\theta}_1^T s_\varepsilon\dot{x}+\hat{\theta}_2^T s_\varepsilon x+\hat{\theta}_3^T s_\varepsilon x_1+\hat{\theta}_4^T s_\varepsilon x_{1\tau}+s_\varepsilon\tilde{q}_1^T\begin{bmatrix}f_c(v)\\f_t(v)\end{bmatrix}+s_\varepsilon\tilde{q}_2 f_a(u)-s_\varepsilon u$$

$$+s_\varepsilon\tilde{l}_1 T(x_2)+\sum_{i=5}^{6}(\hat{\theta}_i-\theta_i)^T\dot{\hat{\theta}}_i$$

$$=-k_d s_\varepsilon s-k^* s_\varepsilon sat\left(\frac{s_\varepsilon}{\varepsilon}\right)+s_\varepsilon\tilde{q}_1^T\begin{bmatrix}f_c(v)\\f_t(v)\end{bmatrix}+s_\varepsilon\tilde{q}_2 f_a(u)$$

$$+s_\varepsilon\tilde{l}_1 T(x_2)-s_\varepsilon u_T+(\hat{\theta}_5-\theta_5)^T\dot{\hat{\theta}}_5+(\hat{\theta}_6-\theta_6)^T\dot{\hat{\theta}}_6$$

where $u_T(t)=\hat{\theta}_5 x_2+\hat{\theta}_6+k^* sat\left(\frac{s}{\varepsilon}\right)$. Since $|s_\varepsilon|=s_\varepsilon sat(\frac{s}{\varepsilon})$ for $|s|>\varepsilon$, and from the fact that $|s|>\varepsilon$, it is easy to see $|s|>|s_\varepsilon|$, so one has,

$$\dot{V}(t)\le-k_d s_\varepsilon^2-k^*|s_\varepsilon|+|s_\varepsilon|\left\|\tilde{q}_1^T\right\|_\infty\max(\rho_c,\rho_t)+|s_\varepsilon|\left|\tilde{q}_2\right|_{\max}\rho_a$$

$$+s_\varepsilon\tilde{l}_1 T(x_2)-s_\varepsilon u_T+(\hat{\theta}_5-\theta_5)^T\dot{\hat{\theta}}_5+(\hat{\theta}_6-\theta_6)^T\dot{\hat{\theta}}_6$$

$$\le-k_d s_\varepsilon^2+s_\varepsilon\tilde{l}_1 T(x_2)-s_\varepsilon u_T+(\hat{\theta}_5-\theta_5)^T\dot{\hat{\theta}}_5+(\hat{\theta}_6-\theta_6)^T\dot{\hat{\theta}}_6$$

In the following, we will construct the proof under the conditions of $\dot{x}_2\ge 0$ and $\dot{x}_2<0$.

(1) Under the condition of $\dot{x}_2 \geq 0$, substituting $T(x_2) = h_i(x_2 - T_1)$, we have the following inequality,

$$\dot{V}(t) \leq -k_d s_\varepsilon^2 + s_\varepsilon \tilde{I}_1 h_i(x_2 - T_1) - s_\varepsilon u_T + (\hat{\theta}_{T1} - \theta_{T1})^T \dot{\hat{\theta}}_{T1} + (\hat{\theta}_{T2} - \theta_{T2})^T \dot{\hat{\theta}}_{T2}$$

Once again, using the property $(\hat{\theta}_i - \theta_i) proj(\hat{\theta}_i, g_i) \leq (\hat{\theta}_i - \theta_i) \cdot g_i$, we have,

$$\begin{aligned} \dot{V}(t) &\leq -k_d s_\varepsilon^2 + \theta_5 s_\varepsilon x_2 + \theta_6 s_\varepsilon - s_\varepsilon u_T + (\hat{\theta}_5 - \theta_5)^T s_\varepsilon x_2 + (\hat{\theta}_6 - \theta_6)^T s_\varepsilon \\ &= -k_d s_\varepsilon^2 \end{aligned} \tag{7.20}$$

(2) Under the condition of $\dot{x} \leq 0$, in the same process, it is easy to see that,

$$\dot{V}(t) \leq -k_d s_\varepsilon^2 \tag{7.21}$$

Therefore, for all the conditions, $\dot{V}(t) \leq -k_d s_\varepsilon^2$, and all signals in the system are bounded. Since $s(t)$ is uniformly bounded, by the standard filter theory and the definition of $s(t)$, it can be shown that both $x(t)$ and $\dot{x}(t)$ are also uniformly ultimately bounded. To complete the proof and establish asymptotic convergence of $x(t)$, it is necessary to show that $s_\varepsilon(t) \to 0$ as $t \to \infty$. This can be accomplished by applying Barbalat's Lemma to the continuous, nonnegative function:

$$V_1(t) = V(t) - \int_0^t \left(\dot{V}(\tau) + k_d s_\varepsilon^2(\tau)\right) d\tau \text{ with } \dot{V}_1(t) = -k_d s_\varepsilon^2(t) \tag{7.22}$$

It can easily be shown that every term on the right side of (7.22) is bounded, hence $\dot{s}(t)$ is bounded. This implies $\dot{V}_1(t)$ is a uniformly continuous function of time. Since $V_1(t)$ is bounded below by 0, and $\dot{V}_1(t) \leq 0$ for all t, use of Barbalat's lemma proves that

$\dot{V}_1(t) \to 0$ as $t \to \infty$ and hence from (7.27) that $s_\varepsilon(t) \to 0$ as $t \to \infty$. Remark for equation (7.10) indicates that $p^T x(t) \to \Omega_\varepsilon$ as $t \to \infty$. This completes the proof. ■

Remark: The above theorem proves the convergence of $p^T x(t)$. As we choose $p = [1 \quad 0]$, it would lead to the convergence of $x_1(t)$, that is, the chatter effect will be significantly suppressed in metal cutting with the proposed adaptive controller.

7.3 Simulation Results

We are taking the system coefficients to be, $M = \begin{bmatrix} m_c & 0 \\ 0 & m_t \end{bmatrix}$, $C = \begin{bmatrix} c_c & 0 \\ 0 & c_t \end{bmatrix}$, $K = \begin{bmatrix} k_c & 0 \\ 0 & k_t \end{bmatrix}$.

The equivalent mass, damping coefficient and spring coefficient for the metal cutting system are,

$$m_c = 15 \text{ kg}, c_c = 3 \times 10^3 \text{ kg/s}, k_c = 6 \times 10^7 \text{ kg/s}^2$$

$$m_t = 1 \text{ kg}, c_t = 3 \times 10^2 \text{ kg/s}, k_t = 6 \times 10^5 \text{ kg/s}^2$$

And we can have a reasonable range for these system coefficients as, $m_c \in [10, 20]$ kg, $c_c \in [2, 4] \times 10^3$ kg/s, $k_c \in [5, 7] \times 10^7 \text{ kg/s}^2$, $m_t \in [0.5, 1.5]$ kg, $c_t \in [2, 4] \times 10^2$ kg/s, $k_t \in [5, 7] \times 10^5 \text{ kg/s}^2$.

For the piezoactuator,

$$k_a = 7 \times 10^7 \text{ kg/s}^2 \text{ with } k_a \in [6, 8] \times 10^7 \text{ kg/s}^2.$$

For the hysteresis model for cutting force, we have the following,

$$h_c = 4 \times 10^6 \text{ N/m and } B_{c0} = 20 \text{ N}$$

with $h_c \in [3, 5] \times 10^6$ N/m and $\rho_B = 10$ N.

And the hysteresis model for contact/frictional force, we have the following,

$$h_t = 2 \times 10^6 \text{ N/m}, T_1 = 1 \times 10^{-6} \text{ and } k_f = 5 \times 10^3$$

with $h_t \in [1, 3] \times 10^6$ N/m, $T_1 \in [0.5, 1.5] \times 10^{-6}$, and $k_f \in [3, 4] \times 10^3$.

For the piezoactuator hysteresis, we have,

$$h_a = 2.5 \times 10^{-8} \text{ m/V}, B_a = 0.1 \times 10^{-6} \text{ m}, \alpha = 0.02$$

with $h_a \in [0.9, 1.1] \times 10^{-6}$ m/V.

The simulation in Figure 7.6 illustrates the turning cutting system with initial tool deflection 10 μm, and it is in chattering condition in the presence of active hysteresis.

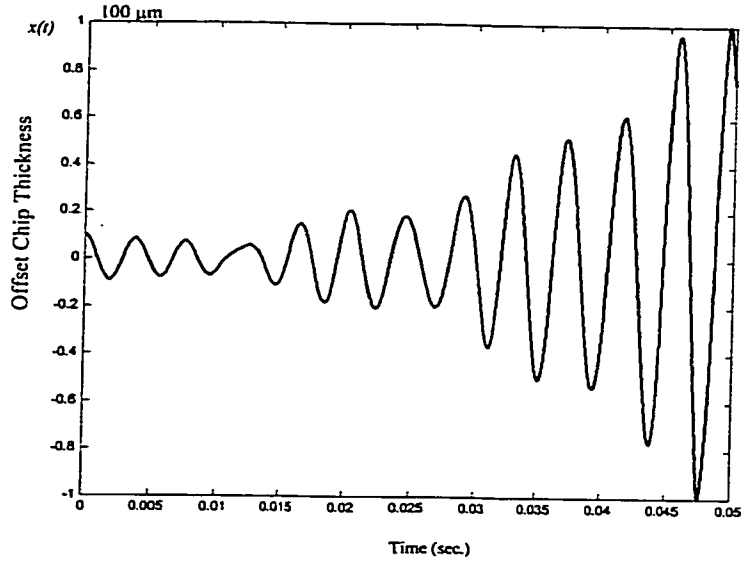

Figure 7.6 Turning cutting system without control

We take the following limits as, $\theta_{1\min} = 0$, $\theta_{1\max} = 5\times10^{4}$, $\theta_{2\min} = -5\times10^{7}$, $\theta_{2\max} = 0$, $\theta_{3\min} = -5\times10^{6}$, $\theta_{3\max} = 0$, $\theta_{4\min} = 0$, $\theta_{4\max} = 2$, $\theta_{5\min} = 100$, $\theta_{5\max} = 1000$, $\theta_{6\min} = 2\times10^{5}$, $\theta_{6\max} = 6\times10^{5}$. And we are taking the initial data as, $\theta_1 = 2\times10^{4}$, $\theta_2 = -3\times10^{7}$, $\theta_3 = 2\times10^{6}$, $\theta_4 = 1$, $\theta_5 = 300$, $\theta_6 = 4\times10^{5}$, and the controller parameters $k_d = 1$, and $k^* = 40$ and $\varepsilon = 1\times10^{-7}$, $\lambda = 500$.

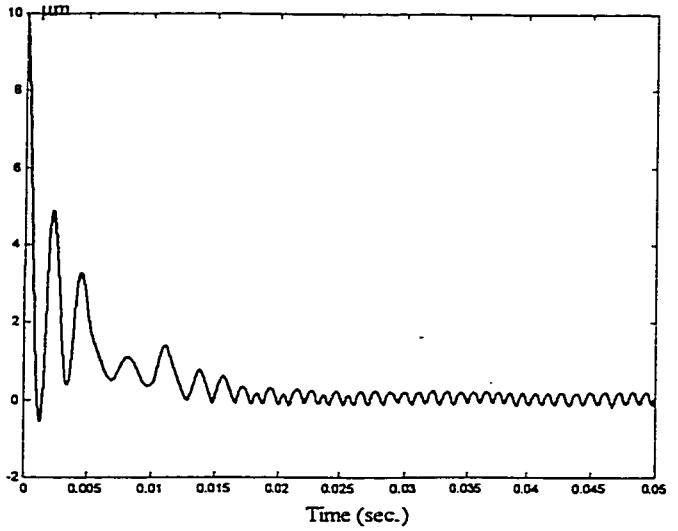

Figure 7.7 Turning system with proposed adaptive controller

And the simulation of the turning system with the adaptive controller is shown in Figure 7.7, which shows clearly that the proposed adaptive controller results in suppression of chatter.

7.4 Summary

In this chapter, type A and type B chatters are considered in the cutting system with two degrees of freedom. In order to suppress the chatter, the piezoactuator is introduced for the ultra-precision control, and a robust adaptive control scheme is proposed for regulation of machine tools. Simulation results show significant reduction of chatter.

Chapter 8

Conclusions and Future Work

8.1 Conclusions

In this thesis, hysteresis models for metal cutting process are considered and incorporated into the adaptive controller design for chatter suppression. Because of the small amplitude (as small as several microns), high frequency properties of chatter, it requires active vibration control providing a force to the cutting system to overcome the chatter effect. Recently, with the advent of piezoelectric devices, more and more attention in metal cutting system is attracted to the application of piezoactuator, which has a prominent characteristic of fast expansions with small response time. With the application of piezoactuator, in order to design a proper control scheme for the chatter suppression, it is necessary to investigate thoroughly over the dynamic cutting process, or the relationship of cutting force and chip thickness. And ultra-precision control requires much more accurate model in metal cutting where nonlinearity dominates. In this thesis, rather than using the commonly accepted linear Merchant model, the relationship of cutting force variation and chip thickness variation is treated as a nonlinear hysteresis model, which has been proved to be able to explain the nonlinearity of the turning metal cutting process in a way that is much more accurate. In this thesis, the turning cutting

systems is described as a class of uncertain systems with hysteresis and time delay. Piezoactuator with the fast response property has been introduced into the cutting system as an important controllable positioning element for the ultra-precision control; however, piezoactuator also displays hysteretic behavior and the hysteresis actuation relationship imposes a still open problem of developing control scheme with unknown hysteresis actuation. In this paper, considering type A and type B chatters, different metal cutting dynamics structures, and linear or nonlinear piezoactuation, robust adaptive control schemes for the chatter suppression in metal cutting are developed, as well as to ensure global stability of the turning metal cutting system. The novelty is that hysteresis model is for the first time incorporated into the controller design for metal cutting system. The simulation results for controller design show significant reduction of chatter by the proposed adaptive controller.

8.2 Future Work

1. It is indicated in the references [Fabris and D'Souza (1974), Szakovits and D'Souza (1976)] that the demonstrated hysteresis is frequency dependent. However, there are still problems about how the hysteresis changes as the cutting conditions change. For example, whether or not and how the slope and distance of hysteresis change as the vibration magnitude is changing. In order to obtain a much more accurate hysteresis model for ultra-precision control, more experiments should be performed to find out the determinants for the hysteresis in the cutting process and to find out a much more accurate hysteresis model.

2. Robust adaptive control schemes are proposed in the thesis, and through simulations they prove to be successful in chatter suppression. Owing to the complexity of metal cutting, more intelligent control methods may be employed for chatter suppression, including fuzzy control, neuro-networks, etc

3. Chatter suppression is discussed mostly in the one dimensional system, with focus on the offset chip thickness variation, which directly reflects the chatter marks on the workpiece. This work is extended to the two dimensional system in Chapter 6, though with simplicity. Furthermore, the modeling and controller design can be extended to three dimensional turning system in the future research.

4. Linear cutting system dynamics are considered in this thesis, however, there are a lot of references [for example, Lee et al (1995), Tarng et al (1994)] indicating that one of the most important chatter mechanisms is the process damping force which has a great influence on the cutting process stabilization. The complex and highly nonlinear process damping force in chatter vibration should be given more attention in the future system modeling.

References

Albrecht, P., "New Development in the Theory of the Metal-Cutting Process, Part I. The Ploughing Process in Metal Cutting", *Trans. ASME,* Vol. 82, 348-358, 1960

Albrecht, P., "New Development in the Theory of the Metal-Cutting Process, Part II. The Theory of Chip Formation", *Trans. ASME,* Vol. 83, 557-571, 1961

Albrecht, P., "Dynamics of the Metal-Cutting Process," *Trans. ASME, Journal of Engineering for Industry*, Vol. 87, 429-441, 1965

Altintas, I. Y., *Principles of Metal Cutting and Machine Tool Automation,* 1997

Arnold, R. N., "The Mechanism of Tool Vibration in the Cutting of Steel", *Proceedings Institution of Mechanical Engineers,* Vol. 154, 261-284, 1946

Asibu, K. E. Jr., "A Transport-Diffusion Equation in Metal Cutting and its Application to Analysis of the Rate of Flank Wear", *Trans. ASME, Journal of Engineering for Industry*, Vol. 82, 324-332, 1960

Bhatacharyya, A. and Ham, I., "Analysis of Tool Wear, Part I: Theoretical Models of Flank Wear", *Trans. ASME, Journal of Engineering for Industry*, Vol. 91, 790-798, 1969

Chandrasekaran, H. and Nagarajan, R., "Influence of Flank Wear on the Stresses in a Cutting Tool", *Trans. ASME, Journal of Engineering for Industry*, Vol. 99, 566-577, 1977

Chen, B.-S. and Chang, Y.-F., "Robust PI Controller Design for a Constant Turning Force System", *International Journal of Machine Tools Manufacture*, Vol.31, 257-272, 1991

Chiou, R. Y. and Liang, S. Y., "Chatter Stability of A Slender Cutting Tool in Turning with Tool Wear Effect", *International Journal of Machine Tools Manufacturing*, Vol. 38, 315-327, 1998

Chiou, R. Y. and Liang, S. Y., "Chatter Frequency in Turning Considering Tool Compliance and Wearland", *Journal of Manufacturing Science and Engineering*, Vol. 121, 307-311, 1999

Chiriacescu, S. T., *Stability in the Dynamics of Metal Cutting*, 1990

Cuttino, J.F., Miller, A.C., Jr, Schinstock D.E., "Performance Optimization of a Fast Tool Servo for Single-Point Diamond Turning Machines", *IEEE/ASME Trans Mechatronics*, Vol. 4, 169-178, 1999

Danai, K. and Ulsoy, A. G., "A dynamic State Model for On-Line Tool Wear Estimation in Turning", *Trans. ASME, Journal of Engineering for Industry*, Vol. 109, 396-399, 1987

Doi, S. and Kato, S., "Chatter Vibration of Lathe Tools", *Trans. ASME*, Vol.78, 1127-1134, 1956

Elanayar, S. and Shin, Y. C., "Modeling of Tool Forces for Worn Tools: Flank Wear Effects", *Trans. ASME, Journal of Manufacturing Science and Engineering*, Vol.118, 359-366, 1996

Elbestawi, M.A., Ismail F., Du, R., Ullagaddi, B.C., "Modelling Machining Dynamics Including Damping in the Tool Workpiece Interface", *Trans. ASME, Journal of Engineering for Industry*, Vol.116, 435-439, 1994

Fabris, N. S. and D'Souza, A. F., "Nonlinear Stability Analysis of Chatter in Metal Cutting", *Trans. ASME, Journal of Engineering for Industry*, Vol.96, 670-675, 1974

Fawcett, S.C., "Small Amplitude Vibration Compensation for Precision Diamond Turning," *Precision Eng.*, Vol.12, no.2, 1990

Fripp, M. and Hagood, N., "Comparison of Electrostrictive and Piezoceramic Actuation for Vibration Suppression", *SPIE,* Vol. 2443, pp.334-348, 1995

Fu, J., Yuan, Z. and Yao, Y., "A unified System Model of Cutting Chatter and Its Transformation Function", *International Journal of Machine Tools Manufacture*, Vol.29, 601-609, 1989

Gasparetto, A. "A System theory Approach to Mode Coupling Chatter in Machining", *Trans. ASME, Journal of Manufacturing Science and Engineering,* Vol.120, 545-547, 1998

Ge, P. and Jouaneh, M., "Tracking Control of a Piezoceramic Actuator", *Trans. on Control Systems Technology*, vol.4, No.3, 209-216, 1996

Gorbet, R.B., Morris, K.A., and Wang, D.W.L., "Passivity-Based Stability and Control of Hysteresis in Smart Actuators", *IEEE Trans. on control Systems Technology,* Vol. 9, No.1, 5-16, 2001

Hanna, N. H. and Tobias, S. A., "The Nonlinear Dynamic Behavior of a Machine Tool Structure," *International Journal of Machine Tools & Manufacture*, Vol.9, 293-307, 1969

Hanna, N. H. and Tobias, S. A., "A Theory of Nonlinear Regenerative Chatter", *Trans. ASME, Journal of Manufacturing Science and Engineering,* Vol.96, 247-255, 1974

Hwang, H.-Y., Oh, J.-H. and Kim, K.-J., "Modeling and adaptive Pole Assignment Control in Turning", *International Journal of Machine Tools Manufacture*, Vol.29, 275-285, 1989

Hwang, C.L., "Adaptive Turning Force Control With Optimal Robustness and Constrained Feed Rate", *International Journal of Machine Tools Manufacture*, Vol.33, 483-493, 1993

Jemielniak, K. and Widota, A., "Numerical Simulation of Non-Linear Chatter Vibration in Turning", *International Journal of Machine Tools & Manufacture*, Vol.29, 239-247, 1989

Kaneko, T., Sato, H., Tani, Y., O-hori, M., "Self-Excited Chatter and its Marks in Turning", *Trans. ASME, Journal of Engineering for Industry*, Vol.106, 222-228, 1984

Kato, S. and Marui, E., "On the Cause of Regenerative Chatter Due to Workpiece Deflection", *Trans. ASME, Journal of Engineering for Industry*, Vol. 96, 179-186, 1974

Kegg, R. L., "Cutting Dynamics in Machine Tool Chatter, Contribution to Machine-Tool Chatter Research—3", *Trans. ASME, Journal of Engineering for industry*, Vol.87, 464-470, 1965

Kobayashi, S., and Thomsen, E. G., "The Role of Friction in Metal Cutting," *Trans. ASME, Journal of Engineering for Industry*, Vol. 107, 81-89, 1985

Koenigsberger, F. and Tlusty, J., "Machine Tool Structure", 1970, Pergamon Press

Kondo, Y., Kawano, O., Sato, H., "Behavior of Self-Excited Chatter Due to Multiple Regenerative Effect", *Trans. ASME, Journal of Engineering for Industry*, Vol. 103, 324-329, 1981

Kondo, E., Ota, H., Kawai, T., "A New Method to Detect Regenerative Chatter Using Spectral Analysis, Part 1: Basic Study on Criteria for Detection of Chatter", *Trans. ASME, Journal of Manufacturing Science and Engineering*, Vol. 119, 461-466, 1997

Koren, Y. and Lenz, E., "Mathematical Model of the Flank-Wear while turning Steel with Carbide Tools", *CIRP, Proceedings of Manufacturing Systems,* Vol. 1, No. 2, 1972

Koren, Y., "Flank Wear Model of Cutting Tools Using Control Theory", *Trans. ASME, Journal of Engineering for Industry*, Vol. 100, 103-109, 1978

Koren, Y., "Control of Machine Tools", Journal of Manufacturing Science and Engineering, Vol. 119, 749-755, 1997

Lee, Y. –S., "Theoretical Model of Crater Wear", *Trans. ASME, Journal of Engineering for Industry*, Vol.93, 1051-1056, 1971

Lee, B.Y., Tarng, Y.S. and Ma, S.C., "Modeling of the Process Damping Force in Chatter Vibration", *International Journal of Machine Tools Manufacture*, Vol.35, 951-962, 1995

Lin, J.S. and Weng, C.I., "A Nonlinear Dynamic Model of Cutting", *International Journal of Machine Tools Manufacture*, Vol.30, 53-64, 1990

Liu, D., Sutherland, J.W., Moon, K.S., Sturos, T.J. and Kashani, A.R., "Surface Texture Improvement in the turning Process Via Application of a Magnetostrictively Actuated Tool Holder", *Journal of Dynamic Systems, Measurement, and Control*, Vol. 120, 193-199, 1998

Long, G. W. and Lemon, J. R., "Structural Dynamics in Machine-Tool Chatter, Contribution to Machine-Tool Chatter Research—2", *Trans. ASME, Journal of Engineering for industry*, Vol.87, 455-463, 1965

Marui, E., Ema, S. and Kato, S., "Chatter Vibration of Lathe Tools. Part 1: General Characteristics of Chatter Vibration", *Trans. ASME, Journal of Engineering for Industry*, Vol. 105, 100-106, 1983

Marui, E., Ema, S. and Kato, S., "Chatter Vibration of Lathe Tools. Part 2: On the Mechanism of Exciting Energy Supply", *Trans. ASME, Journal of Engineering for Industry*, Vol. 105, 107-113, 1983

Marui, E., Kato, S. Hashimoto, M., Yamada, T., "The Mechanism of Chatter Vibration in a Spindle-Workpiece System: Part 2 – Characteristics of Dynamic Cutting Force and Vibration Energy", *Trans. ASME, Journal of Engineering for Industry*, Vol.110, 242-247, 1988

Marui, E., Hashimoto, M. and Kato, S., "Regenerative Chatter Vibration Occurring in Turning with Different Side Cutting Edge Angles", Journal of Engineering for Industry, Vol.117, 551-558, 1995

Merchant, M. E., "Mechanics of the Metal Cutting Process I. Orthogonal Cutting and a Type 2 Chip", *Journal of Applied Physics*, Vol. 16, 267-275, 1945

Merchant, M. E., "Mechanics of the Metal Cutting Process, II. Plasticity Conditions in Orthogonal Cutting", *Journal of Applied Physics*, Vol. 16, 318-324, 1945

Merritt, H. E., "Theory of Self-Excited Machine-Tool Chatter, Contribution to Machine-Tool Chatter Research—1", *Trans. ASME, Journal of Engineering for industry*, Vol. 87, 447-454, 1965

Minis, I. And Tembo, A., "Experimental Verification of a Stability Theory for Periodic Cutting Operations", *Trans. ASME, Journal of Engineering for industry*, Vol. 115, 9-14, 1993

Ota, H. and Kono, K., "On Chatter Vibrations of Machine Tool on Work Due to Regenerative Effect and Time Lag", *Trans. ASME, Journal of Engineering for industry*, Vol. 96, 1337-1346, 1974

Pandit, S. M., Subramanian, T. L., Wu, S. M., "Modeling Machine Tool Chatter by Time Series", *Trans ASME, Journal of Engineering for Industry*, Vol. 97, 211-215, 1975

Pandit, S. M., Subramanian, T. L. and Wu, S. M., "Stability of Random Vibration with Special Reference to Machine Tool Chatter", *Trans ASME, Journal of Engineering for Industry*, Vol. 97, 216-219, 1975

Rao, B. C. and Shin, Y. C., "A Comprehensive Dynamic Cutting Force Model for Chatter Prediction in Turning", *International Journal of Machine Tools & Manufacture*, Vol. 39, 1631-1654, 1999

Rasmussen, J.D., Tsao, T.-C., Hanson R.D. and kapoor, S.G., "Dynamic Variable Depth of Cut Machining Using Piezoelectric Actuators", *International Journal of Machine Tools Manufacture*, Vol.34, 379-392, 1994

Rubenstein, C., "An Analysis of Tool Life Based on Flank-Face Wear, Part I: Theory", *Trans. ASME, Journal of Engineering for industry*, Vol. 98, 221-226, 1976

Rubenstein, C., "An Analysis of Tool Life Based on Flank-Face Wear, Part 2: Comparison of Theory With Experimental Observations", *Trans. ASME, Journal of Engineering for industry*, Vol. 98, 227-232, 1976

Sarnicola, J. F. and Boothroyel, G., "Machine Tool Chatter: Effect of Surface Slope on Machining Forces During Wave Removing", *Trans. ASME, Journal of Engineering for industry*, Vol.96, 1202-1206, 1974

Shaw, M. C. and DeSalvo, G. J., "On the Plastic Flow Beneath a Blunt Axis Symmetric Indenter", *Trans. ASME, Journal of Engineering for industry*, Vol.92, 480-494, 1970

Shi, H. and Tobias, S., "Theory of Finite Amplitude Machine Tool Instability", *International Jounal of Machine Tool Design and Research*, Vol.24, No.1, 45-69, 1984

Shiraishi, M., Yamanaka, K. and Fujita, H., "Optimal Control of Chatter in Turning", *International Journal of Machine Tools Manufacture*, Vol.31, 31-43, 1991

Shumsheruddin, A. A., Dynamic Orthogonal Metal Cutting, University of Birmingham, Ph. D. Thesis (1964)

Sisson, T. R., and Kegg, R. L., "An Explanation of Low-Speed Chatter Effects", *Trans. ASME, Journal of Engineering for Industry,* Vol. 91, 951-958, 1969

Smith, J. D. and Tobias, S. A., M. T. D. R., Vol. 1 (4), 1961

Su, C.-Y., Stepanenko, Y., Svoboda, J., and Leung, T. P., "Adaptive Control of a Class of Nonlinear Systems Preceded by an Unknown Backlash-Like Hysteresis", *IEEE Trans. on Automat. Contr.* Vol. 45, 2427-2431, 2000

Szakovits, R. J. and D'Souza, A. F., "Metal cutting Dynamics with Reference to Primary Chatter", *Trans. ASME, Journal of Engineering for Industry,* Vol.98, 258-264, 1976

Tao, G. and Kokotovic, P.V., "Adaptive Control of Plants with Unknown Hystereses", *IEEE Trans. on Automatic Control*, Vol. 40, No.2, 200-212, 1995

Tao, G. and Kokotovic, P.V., "Adaptive Control of Systems with Unknown Output Backlash", *IEEE Trans. on Automatic Control*, Vol. 40, No.2, 326-330, 1995

Tao, G. and Kokotovic, P.V., "Continuous-Time Adaptive Control of Systems with Unknown Backlash", *IEEE Trans. on Automatic Control*, Vol. 40, No.6, 1083-1087, 1995

Tarng, Y.S. and Wang, Y.S., "An Adaptive Fuzzy Control System for Turning Operations", *International Journal of Machine Tools Manufacture*, Vol.33, 761-771, 1993

Tarng, Y. S. Young, H. T. and Lee, B. Y., "An Analytical Model of Chatter Vibration in Metal Cutting", *International Journal of Machine Tools Manufacture*, Vol.34, 183-197, 1994

Thomsen, E. G., MacDonald, A. G., and Kobayashi, S., "Flank Friction Studies with Carbide Tools Reveal Sub-layer Plastic Flow", *Trans. ASME, Journal of Engineering for Industry*, Vol.84, 53-64, 1962

Tlusty, J. and Ismail, F., "Basic Non-Linearity in Machining Chatter", *C.I.R.P.*, Vol.30, 299-304, 1981

Tobias, S. A., *Machine Tool Vibration*, 1965, London, Blackie.

Tobias, S. A. and Fishwick, W., "The Chatter of Lathe Tools Under Orthogonal Cutting Conditions", *Trans. ASME, Journal of Engineering for industry*, Vol. 80, 1079-1088, 1958

Usui, E. Shirakashi, T., and Kitagawa, T., "Analytical Prediction of Three Dimensional Cutting Process—Part 3: Cutting Temperature and Crater Wear of Carbide Tool," *Trans. ASME, Journal of Engineering for Industry,* Vol. 100, 236-243, 1978

Wu, D.W. and Liu, C.R., "An Analytical Model of Cutting Dynamics. Part 1: Model Building", *Trans. ASME, Journal of Engineering for industry*, Vol. 107, 107-111, 1985

Wu, D.W. and Liu, C.R., "An Analytical Model of Cutting Dynamics. Part 2: Verification", *Trans. ASME, Journal of Engineering for industry*, Vol. 107, 112-118, 1985

Wu, D. W., 1989, "A New Approach of Formulating the Transfer Function for Dynamic Cutting Processes," *Trans. ASME, Journal of Engineering for industry*, Vol. 111, 37-47, 1989

Yen, D. W. and Wright, P. K., "Adaptive Control in Machining—A New Approach Based on the Physical Constraints of Tool Wear Mechanisms", *Trans. ASME, Journal of Engineering for industry*, Vol. 105, 31-38, 1983

Publications Relevant to This Thesis

Conferences

[1] "Active Control for Chatter in Metal Cutting via Piezoactuator", to appear in the 2001 International Symposium on Adaptive and Intelligent Systems and Control, Virginia, USA (with C-Y. Su);

[2] "Modeling and Chatter Suppression with Ultra-Precision in Dynamic Turning Metal Cutting Process", to appear in ASME International 2001 Design Engineering Technical Conference, (with C-Y. Su);

[3] "Modeling and Robust Adaptive Control of Metal Cutting Mechanical Systems", to appear in American Control Conference 2001, (with C-Y. Su and Y. Stepanenko);

Submissions

[4] Xinkai Chen and Chun-Yi Su, "Modeling and Chatter Suppression with Ultra-Precision in Dynamic Turning Metal Cutting> Process", submitted to *IEEE Trans. on Mechatronics,* (with X. Chen and C.-Y. Su);

[5] "Chatter Suppression with Adaptive Control in Turning Metal Cutting via Application of Piezoacutator", submitted to *40th IEEE Conferences on Decision and Control, 2001,* (with C.-Y. Su).